HELLENIC REPUBLIC
National and Kapodistrian University of Athens

INTERDEPARTMENTAL POSTGRADUATE PROGRAM:
OCEANOGRAPHY AND MANAGEMENT OF THE MARINE ENVIRONMENT

"RECONSTRUCTION OF THE SUBMERGED LANDSCAPE OF VATIKA BAY (SE PELOPONNESE, GREECE)"

MASTER THESIS

MARILIA PAVLIDI-PALLA

Athens, 2018

INTERDEPARTMENTAL POSTGRADUATE PROGRAM:
OCEANOGRAPHY AND MANAGEMENT OF THE MARINE ENVIRONMENT

"RECONSTRUCTION OF THE SUBMERGED LANDSCAPE OF VATIKA BAY, S.E. PELOPONNESE, GREECE"

MASTER THESIS

MARILIA PAVLIDI-PALLA

Advisory and Evaluation Commitee:

Prof. Poulos Serafeim, Department of Geography & Climatology, Faculty of Geology and Geoenvironment, NKUA

Dr. Sakellariou Dimitris, Research Director, Hellenic Center of Marine Research

Dr. Rousakis Grigoris, Senior Researcher, Hellenic Center of Marine Research

Athens, 2018

ACKNOWLEDGEMENTS

I would like to thank my supervisor Dr. Poulos Serafeim, Professor in Oceanography and Physical geography and Head of the Section of Geography and Climatology, to whom I am grateful for his support and collaboration. I express my sincere gratitude to Dr. Dimitris Sakellariou, Research Director in Institute of Oceanography of HCMR (Hellenic Center of Marine Research), for his essential guidance and continuous support. His valuable contribution throughout the elaboration of this thesis was crucial for its completion. Moreover, I would like to express a special acknowledgement to Dr. Rousakis Grigoris, Senior Researcher of HCMR, for his collaboration. Finally, I own many thanks to my family and friends, who have been encouraging and supportive.

ABSTRACT

Vatika Bay is located in SE Peloponnese and belongs to Laconia peninsula. The area is seismically active because it is part of the Hellenic Arc and is characterized by long term uplift, also postulated by a sequence of uplifted Late Quaternary marine terraces. This fact contrasts with the subsidence by about 3-4 m bellow the present sea level of the prehistoric city of Pavlopetri, located at Punta beach, Viglafia, in the strait of Elaphonisos. That is what is called the “Laconia Paradox”: a submerged archaeological site within a long term uplifting area. Thus, the aim of this thesis is to reconstruct the submerged prehistoric landscapes and provide understanding of the geological processes and sea-level fluctuation, which led to the present geomorphological configuration.

A marine geological survey, carried out in 2015 aboard the 14m long RV Alkyon of HCMR and positioned with GPS and differential GPS, allowed to obtain complete high resolution swath bathymetry coverage of the area. Both Multi Beam 200/400 kHz and Single Beam echosounders have been used. Bathymetric data were integrated with the acquisition of high-resolution seismic profiling data, such as Chirp, Pinger and Boomer and side scan sonar data.

The bay displays valley-like morphology. High resolution seismic profiles across the western steep slope of the Bay provide evidence that relative subsiding and uplifting areas are controlled by active faulting. The eastern slope of the Bay displays marked differences: it dips smoothly westwards, while the observed submarine terraces do not match with the ones mapped along the western slope. Holocene sediment deposition is fairly limited across the bay. A series of submerged paleo-channels occurs running off the northern shore of the Bay and buried below the recent sediments. Evidence on morphological terraces has been found at several depths ranging roughly between 40 m and 104 m bsl.

Active faulting separates the long-term uplifting parts of the surveyed area from the relative subsiding seafloor of Vatika Bay. The occurrence of three beachrock bands at different depths indicates rapid, incremental subsidence due to tectonic activity in historical times. The submerged ancient city of Pavlopetri is located on the subsiding, hanging wall of the dominant fault. Differential vertical tectonics has led to the occurrence of low sea-level terraces at different depths across the Vatika Bay.

ΠΕΡΙΛΗΨΗ

ΑΝΑΠΑΡΑΣΤΑΣΗ ΤΟΥ ΠΑΛΑΙΟΑΝΑΓΛΥΦΟΥ ΣΤΟΝ ΚΟΛΠΟ ΤΩΝ ΒΑΤΙΚΩΝ, ΝΑ ΠΕΛΟΠΟΝΝΗΣΟΣ, ΕΛΛΑΔΑ.

Ο κόλπος των Βατίκων, στη ΝΑ Πελοπόννησο, ανήκει στο Ελληνικό Τόξο και χαρακτηρίζεται από έντονες ενεργές τεκτονικές κινήσεις και σεισμικότητα. Η παρουσία αλλεπάλληλων ανυψωμένων θαλάσσιων αναβαθμίδων του Ανώτερου Τεταρτογενούς ιδιαίτερα στην δυτική πλευρά του Κόλπου και την Ελαφόνησο αποτελεί μαρτυρία μακροπρόθεσμης τεκτονικής ανύψωσης της περιοχής. Σε αυτό το τεκτονικό καθεστώς, η παρουσία της βυθισμένης προϊστορικής πόλης του Παυλοπετρίου, η οποία βρίσκεται σε βάθος μέχρι στα 3-4 μέτρα στην παραλία Πούντα, στα Βιγκλάφια, αποτελεί ένα παράδοξο που δεν έχει εξηγηθεί επαρκώς μέχρι σήμερα Σκοπός αυτής της εργασίας είναι η κατανόηση των γεωλογικών-τεκτονικών διεργασιών σε συνδυασμό με τις διακυμάνσεις της στάθμης της θάλασσας στο Ανώτερο Πλειστόκαινο και Ολόκαινο με στόχο την αναπαράσταση της εξέλιξης του βυθισμένου προϊστορικού ανάγλυφου και την ερμηνεία της σημερινής γεωμορφολογικής διάταξης.

Στην παρούσα εργασία χρησιμοποιήθηκαν δεδομένα πολυδιαυλικής βυθομετρίας, τομογράφου υποδομής πυθμένα και ηχοβολιστή πλευρικής σάρωσης, που συλλέχθηκαν σε δύο ερευνητικούς πλόες του σκάφους ΑΛΚΥΩΝ του ΕΛΚΕΘΕ το 2010 και το 2015.

Ο κόλπος των Βατίκων παρουσιάζει μορφολογία κοιλάδας. Σεισμικά προφίλ υψηλής ανάλυσης κατά μήκος του δυτικού απότομου υποθαλάσσιου πρανούς δείχνουν ότι σχετικές βυθιζόμενες και ανυψωμένες περιοχές ελέγχονται από ενεργά ρήγματα. Το ανατολικό πρανές του κόλπου εμφανίζει σημαντικές διαφορές: κλίνει ομαλά προς τα δυτικά, ενώ οι υποθαλάσσιες αναβαθμίδες που ανήκουν σε αυτό το τμήμα δε συμπίπτουν με αυτές που χαρτογραφήθηκαν στο δυτικό πρανές. Οι μορφολογικές αναβαθμίδες που χαρτογραφήθηκαν βρίσκονται σε διάφορα βάθη, από 40 έως 104 μέτρα. Ο ρυθμός ιζηματογένεσης κατά το Ολόκαινο είναι πολύ μικρός. Στη βόρεια ακτή του κόλπου παρατηρούνται πολλαπλά παλαιο-κανάλια, θαμμένα κάτω από πρόσφατα, Ολοκαινικά ιζήματα.

Τα μακροπρόθεσμα ανυψωμένα τμήματα της περιοχής μελέτης διαχωρίζονται από το σχετικά βυθιζόμενο πυθμένα του κόλπου των Βατίκων μέσω ενεργών ρηγμάτων. Τα τρία beachrock σε διαφορετικά βάθη κατά μήκος της βόρειας ακτής υποδεικνύουν σταδιακά γρήγορη βύθιση λόγω τεκτονικών κινήσεων σε ιστορικό χρόνο. Η βυθισμένη αρχαία πόλη του Παυλοπετρίου βρίσκεται στο βυθιζόμενο τμήμα του κυρίαρχου ρήγματος. Διαφορικές κάθετες τεκτονικές κινήσεις δημιούργησαν μορφολογικές αναβαθμίδες χαμηλής στάθμης σε διάφορα βάθη κατά μήκος του κόλπου των Βατίκων.

CONTENTS

1. INTRODUCTION

1.1. Scope of the Thesis

The present MSc thesis refers to the processing and interpretation of marine geological-geophysical data from the Vatika Bay, southeast Peloponnese aiming at the reconstruction of the palaeo-geographical evolution of Vatika Bay. The data sets used for the thesis include bathymetric and sub-bottom profiling data acquired during two marine geological - oceanographic surveys of the Hellenic Center of Marine Research (HCMR) in June 2010 and in May 2015. The main objectives of the thesis were (i) to identify and map palaeo-sea-level indicators (terraces, shorelines), (ii) to study and understand the seismic stratigraphy of the substrate, (iii) to map and characterize the main faults at the area and understand tectonic movements and (iv) to reconstruct the submerged landscape and palaeo-geographic evolution of the Vatika Bay.

1.2. Geodynamics of the Aegean

Greece is located in the Eastern Mediterranean Sea which is characterized by active geodynamic processes involving plate tectonic movements of larger and smaller plates and crustal blocks, ongoing complicate geological processes and formation of new relief. The oceanic crust bellow the Ionian and Levantine Seas is the last remnant of the Tethys Ocean, which disappeared due to the convergent motion between the Eurasian and African continents. The collision of these two continental plates gave birth to some of the highest mountain ranges on earth. The Aegean region belongs to the Alpine orogenic belt, a mountain chain which starts from the Pyrenees and the Alps in the west and continues over the Balkan Peninsula, Anatolia and the Caucasus Mountains, to the Himalayas and further east. In the context of Africa – Eurasia N-S convergence, the Aegean region represents a piece of continental lithosphere undergoing widespread N-S extension behind the Hellenic Subduction zone, above the northward plunging, relict oceanic lithosphere of the African plate *(e.g. Le Pichon and Angelier, 1979; Meulenkamp and Hilgen, 1986; Mascle & Martin, 1990; Taymaz et al., 1991)*.

In a larger scale, the following are the most important geodynamic processes in the Eastern Mediterranean Sea (Fig.1.1):

- The northward movement of the Arabian peninsula along the Dead Sea Fault.
- The westward movement of Anatolia along the North Anatolian Fault.
- The NNE-ward subduction of the oceanic crust of Tethys underneath the Aegean lithosphere.
- The N-S to NNE-SSW directed extension of the Aegean.
- The collision of the Aegean "microplate" with the Apulia, north of the Kefalonia Fault.
- The incipient collision of the Aegean with the Libyan promontory south of Crete.

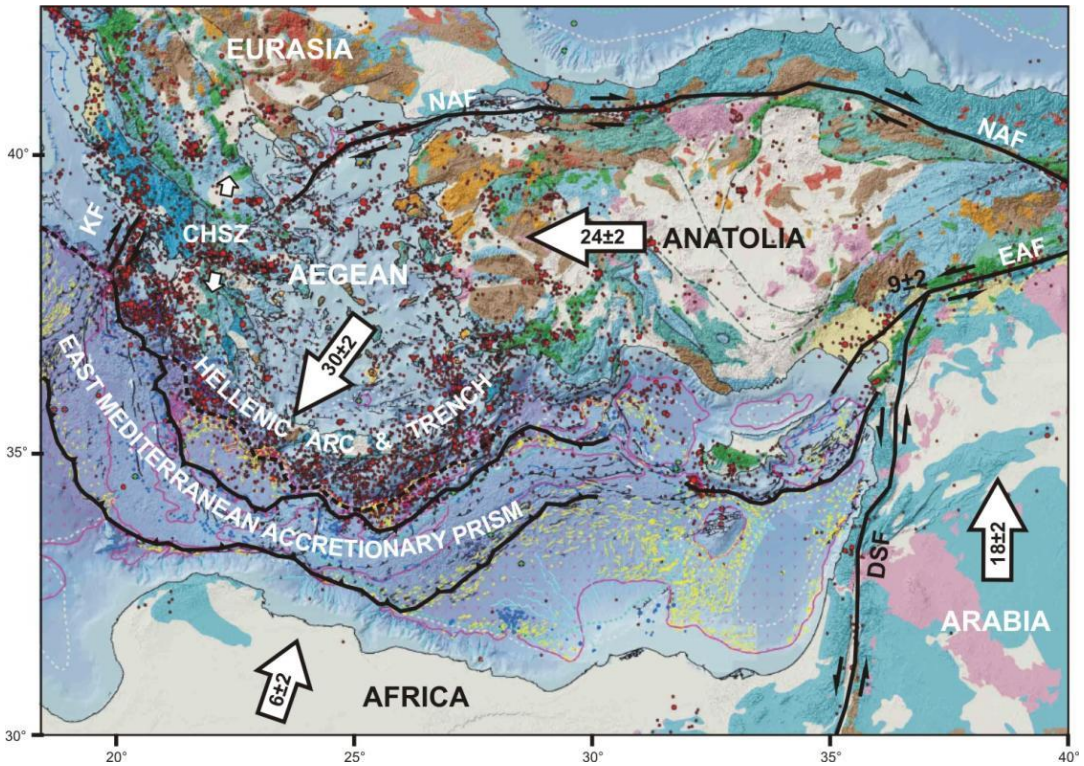

Fig.1.1: Morpho- tectonic Map of the Eastern Mediterranean with main tectonic structural features and the major tectonic boundaries of the actively deforming Aegean region (*Mascle & Mascle, 2012*). Mean GPS horizontal velocities after *McClusky et al 2000*. DSF: Dead Sea Fault, EAF: East Anatolian Fault, NAF: North Anatolian Fault, KF: Kefalonia Fault, CHSZ: Central Hellenic Shear Zone.

1.3. The Hellenic Arc and Trench

The Hellenic Arc and Trench had been initially interpreted as a consuming plate boundary between the subducting African plate and the overriding Aegean lithosphere *(Ryan, 1970; Ryan et al., 1970; Le Pichon and Angelier, 1979)*. It was only after the Mediterranean Ridge was recognized as an accretionary prism (Chaumillon & Mascle, 1995; Chaumillon et al., 1996; Chaumillon & Mascle, 1997) when it became evident that the Hellenic Trench has developed on the forearc of the Aegean microplate and does not mark the boundary between the latter and the African plate. The last remnant of Tethys Ocean is being consumed by the fast (5 mm/year) Africa-Eurasia convergence and associated north-northeastward subduction beneath the Hellenic Arc. The active subduction and the subsequent deformation of the overriding Aegean microplate have led to the formation of a complicate geodynamic structure. Convergence between the African plate and the Hellenic forearc is nearly perpendicular along western Crete and highly oblique (30˚) in the eastern Hellenic forearc as far as Rhodes (Fig.1.2) (*Ten Veen and Kleinspehn, 2002*).

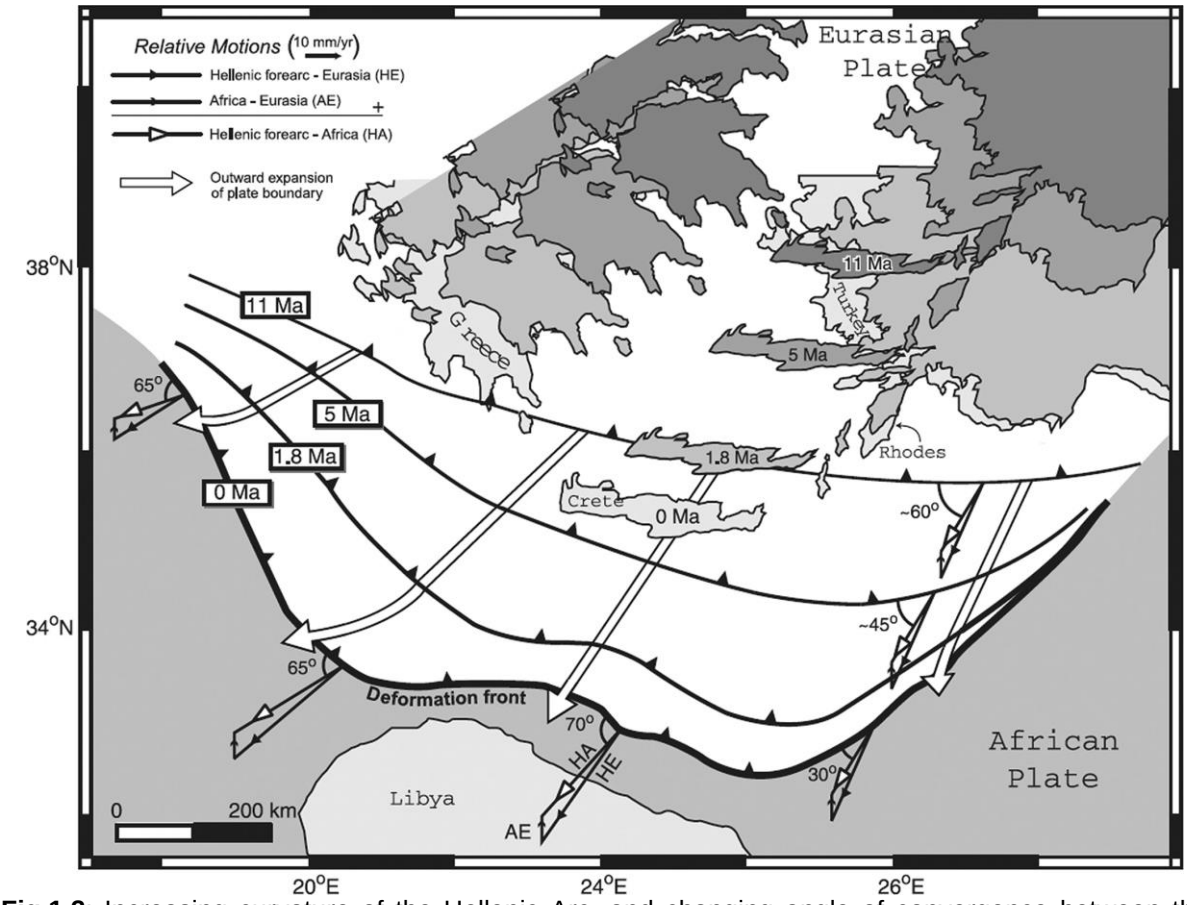

Fig.1.2: Increasing curvature of the Hellenic Arc, and changing angle of convergence between the African and Eurasian continents along the Hellenic fore-arc since 11 Ma (Late Miocene), together with reconstructed paleogeography of the Aegean region using a Mercator projection of modern coastlines *(Ten Veen and Kleinspehn, 2002)*.

The Hellenic Arc, extending from the Ionian Islands to the north-west through the south Peloponnese and Crete to Karpathos and Rhodes to the south-east, has developed above the north-northeastward subduction of the East Mediterranean crust and is one of the most active geological structures worldwide. It separates the 3 km deep Mediterranean basin filled with up to 10 km of sediments to the south from the Hellenic mountain belt to the north *(Biju-Duval et al., 1974; Le Pichon and Angelier, 1979).* The curvature of the Hellenic Arc (Fig.1.2) and consequent obliquity of convergence has increased systematically since the Middle/Late Miocene. This has been associated with several processes including rollback of the subduction interface induced by the slab-pull force of the downgoing African slab (*Le Pichon & Angelier 1979; Angelier et al., 1982; Le Pichon 1982; Meulenkamp et al., 1988*), gravitational body forces associated with over-thickened Alpine crust (*e.g. Le Pichon et al. 1995; Jolivet 2001*) and westward extrusion of the Anatolian block along the North Anatolian Fault (*Taymaz et al., 1991; Le Pichon et al., 1995*).

The subduction of the African plate beneath the Aegean varies significantly along the Hellenic Arc, with head-on convergence and incipient collision at the south of western Crete *(Mascle et al., 1999; Huguen et al., 2006)*. Late Cenozoic oblique convergence has been associated with rapid exhumation of basement units in the forearc region, where Crete, Gavdos, and Karpathos Islands are located *(Le Pichon et al., 2002)*. The eastern sector of the Hellenic Arc separates the forearc region to the south, which is deformed by major, NE-SW trending sinistral strike-slip fault-zones, from the back-arc region to the north where

transtensional deformation prevails, accommodated by diffuse strike-slip and oblique-slip normal faulting (Fig.1.3). The western (Ionian) sector of the Hellenic Arc is characterized by dextral oblique-slip along NW-SE trending fault zones *(Papazachos et al., 2000; Bohnhoff et al., 2005; Shaw and Jackson, 2010)*.

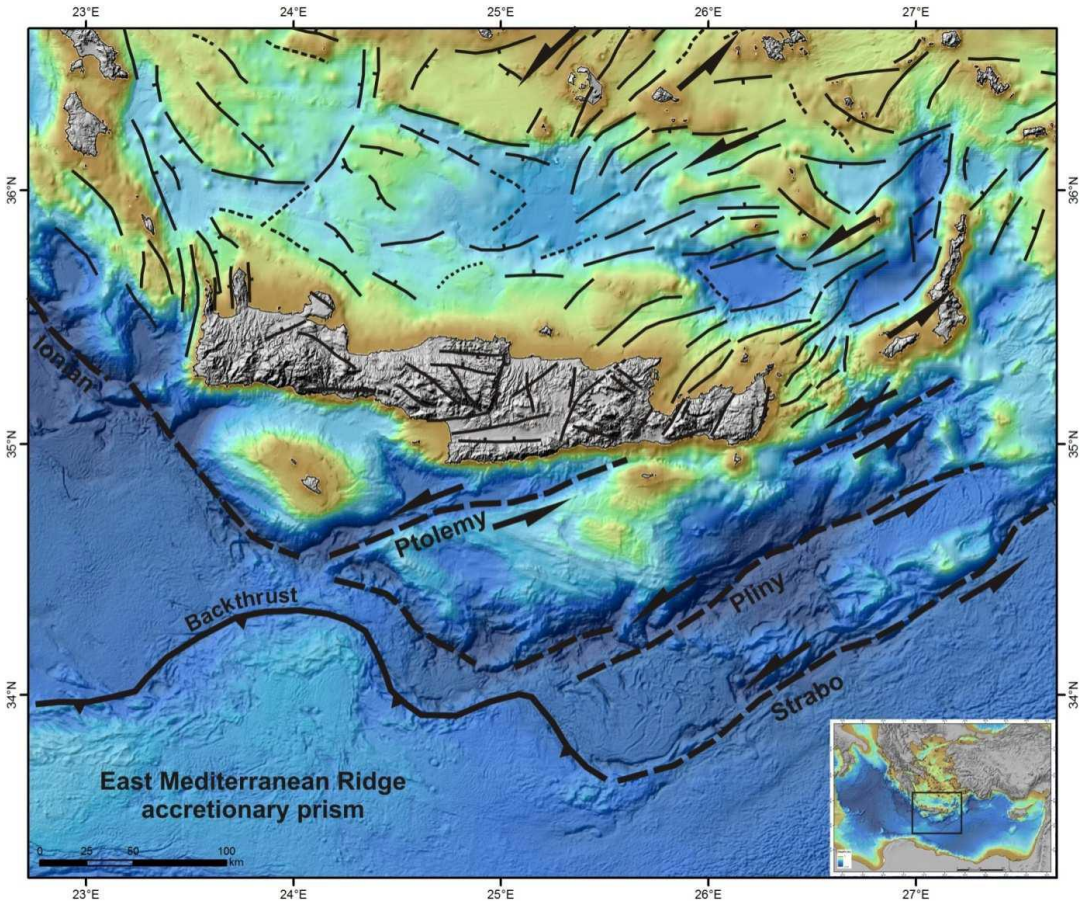

Fig.1.3: Relief map of the central part of the Hellenic Arc. Seafloor: DEM, 250m grid (EMODNET Hydrography, HCMR processing). Land relief: SRTM90. Major faults on Crete after *Kokkinou et al (2012)* and references therein. South Aegean fault network after *Sakellariou & Tsampouraki-Kraounaki (2016)* and references therein. Structural pattern south of Crete after *Leite and Mascle., (1982)*, *Ten Veen and Postma (1999), Le Pichon et al., (2002) and Mascle et al., (1999)*.

Frequent large earthquakes nucleated on major active faults of the crust, as well as long-term tectonic movements, create a puzzle of uplifting or subsiding tectonic blocks. Vertical tectonic movements along the Hellenic Arc and in other areas of the Aegean region significantly modify the relative coastal effect of Quaternary sea-level fluctuations.

Within the southwestern Hellenic Arc, Peloponnese and Crete are connected by a 100 km long NNW-SSE ridge in the southwestern Aegean area. This narrow segment of the Hellenic arc is bounded by major scarps on both sides, and it separates the 3000-5000 m deep Hellenic Trench to the west from the 1000-2000 m deep Cretan Sea basin to the east *(Lyberis et al., 1982)* (Fig.1.4).

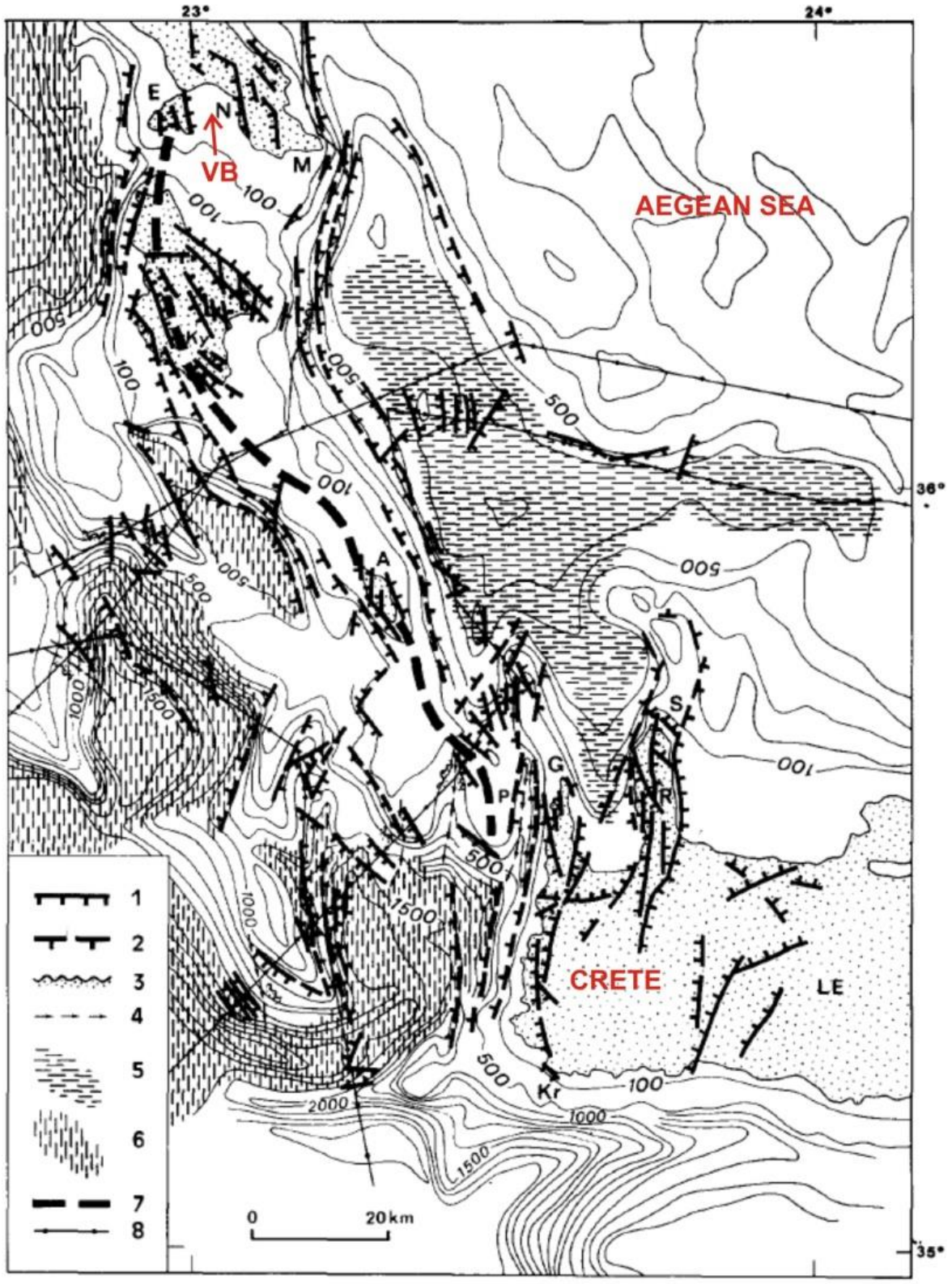

Fig.1.4: Neotectonic structure of the Kythira strait area after *Lyberis et al. (1982)*. VB: Vatika Bay; E: Elafonissos; N: Neapolis; M: Cape Maleas; Ky: Kythera; A: Antikythera; P: Pontikonissi; G: Cape Gramvoussa; R: Rhodopou peninsula; S: Cape Spatha; Kr: Cape Krios; LE: Lefka Ori, VB: Vatika Bay. 1: normal fault scarp; 2: probable normal fault scarp; 3: erosional morphologies; 4: submarine canyon; 5: deep Cretan Sea Basin; 6: deep sedimentary basins of the Hellenic margin; 7: morphological axis of the Kythira-Antikythira ridge; 8: ship-track lines. Depth contours in fathoms

The West Cretan Strait separates the island of Crete from SE Peloponnese. The area is known for very high seismic potential and long-term vertical tectonic movements. Uplifted Late Pleistocene marine terraces and Holocene shorelines *(Pirazzoli et al., 1982)* are evident along the coastline of the south-eastern Peloponnese indicating continuous tectonic uplift during the Quaternary as a response to the ongoing subduction of the Ionian lithosphere underneath the overriding Aegean microplate and the deformation of the latter *(Sakellariou et al., 2017)*.

Evidence of long-term tectonic uplift is obvious in the Laconia peninsula, in the SE Peloponnese, mainland Greece. The area belongs to the seismically active Hellenic Arc and displays long term uplift, as postulated by the uplifted Late Quaternary marine terraces, and a short-term (historic) subsidence, as indicated by the submerged cities of Pavlopetri and Plytra.

1.4. Geology and Geomorphology of Vatika Bay

Vatika Bay is located in southeastern Peloponnese and is part of the Laconia peninsula. Concerning the geological sequences of the broader area, the alpine basement of Neapolis-Maleas Peninsula is mainly composed of Tripolis unit limestones and metamorphics of the Arna unit. Thin- to thick-bedded Jurassic limestones and thick bedded, Upper Triassic limestones to dolomites form the mountainous parts of the peninsula (Fig.1.5) *(Gerolymatos, 1999)*.

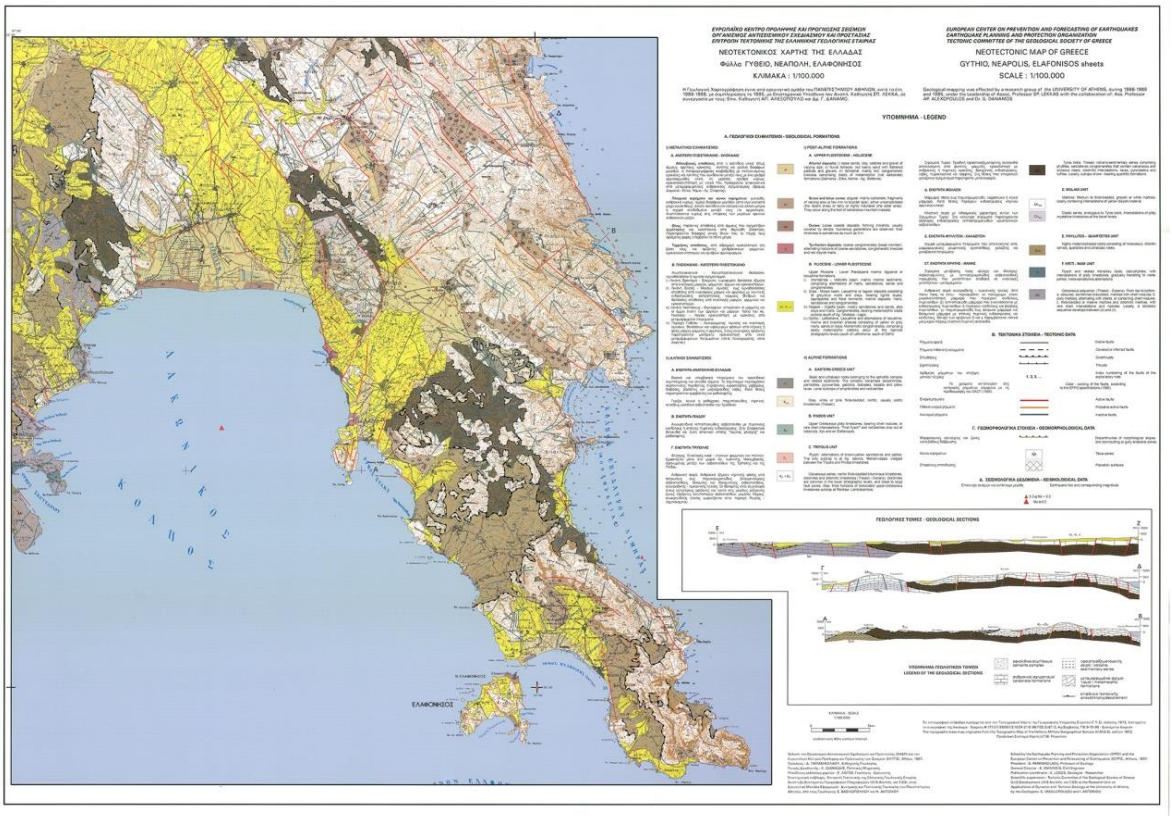

Fig.1.5: Geological and neotectonic map of Gythio, Neapoli, Elafonisos. (Lekkas et al., 1995)

They tectonically overlay clastic, carbonate and volcanic rocks of the Tyros beds and the metamorphic rocks (metaclastites, thin marbles and metavolcanites) of Phyllites-Quartzites

(Arna) unit (Gerolymatos, 1999). Upper Pliocene(?)– Lower Pleistocene fluvio-terrestrial deposits as well as marine and lacustrine pelites, sandstones, conglomerates and carbonate rocks occur in the morphologically lower and the coastal parts of the peninsula. The Quaternary deposits may be as thick as 250-300 m and cover unconformably the alpine basement. They alternate rapidly, both horizontally and vertically and commonly contain layers of terrestrial origin *(Gerolymatos, 1999)*.

Vatika Bay is a region of particular interest for several reasons. Evidence of long-term tectonic uplift has been observed in the area. A sequence of Pleistocene elevated marine terraces in the area of Neapolis- Elaphonisos ranging from a few meters to a few hundreds of meters above sea level, indicate that the region undergoes tectonic uplift during the Quaternary (Fig.1.6). This fact contrasts with the subsidence by about 3-4 m bellow the present sea-level of the prehistoric city of Pavlopetri, located at Punta beach, Viglafia, in the strait of Elaphonisos, and the roman city of Plytra in the bay of Plytra. That is what is called the “Laconia Paradox”: submerged city within a long term uplifting area.

Fig.1.6: Uplifted marine terraces at Vatika Bay: The northwestern flanks of Elaphonisos (left) and the mountain slopes behind Viglafia (right).

Along the Lakonian coast, the island of Elaphonisos protects the Bay of Neapolis from the open Mediterranean Sea to the west. Elaphonisos is separated from the mainland by a 1 km wide, 2.5 m deep channel of water (Fig.1.6) *(Scheffers et al., 2008)*

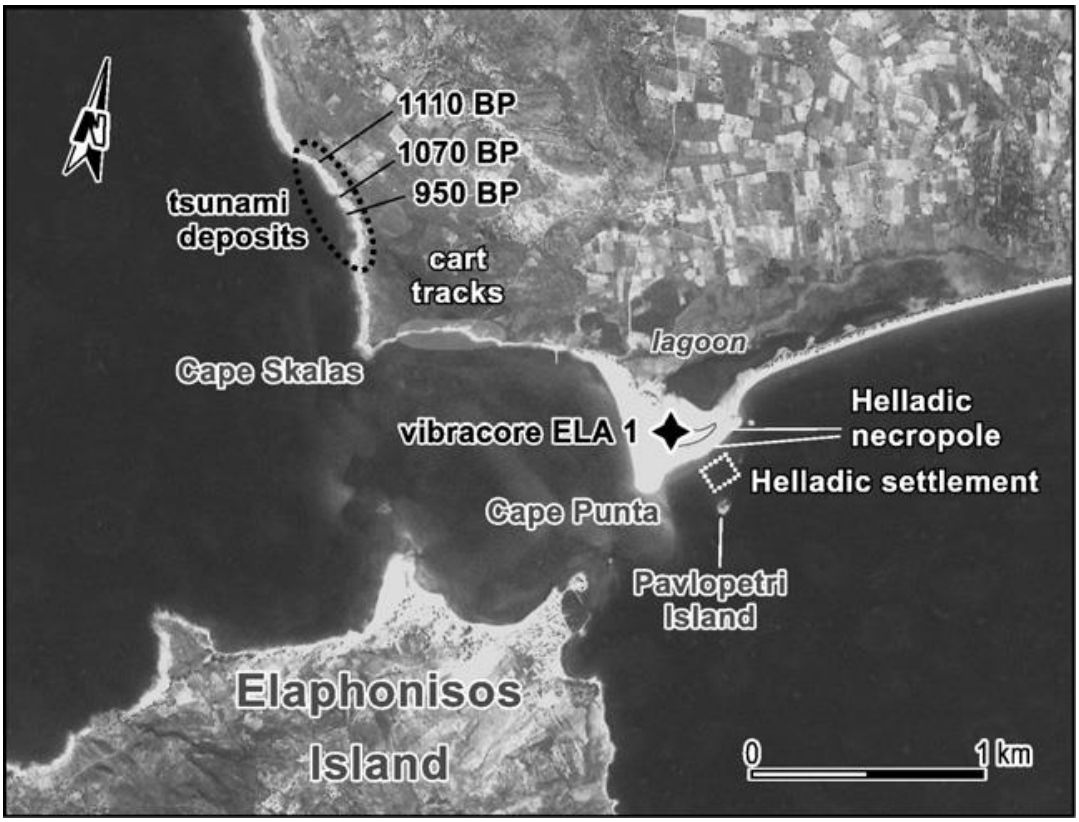

Fig.1.7: Aerial photo of the Elaphonisos channel and the archeological and tsunami sites nearby. Dislocated blocks and tsunamogenic sand sheets, almost 2 km thick, provide geomorphological and sedimentological evidence of strong tsunami impact on the area. *(Scheffers et al., 2008)*

Scheffers et al., 2008 found tsunami indicators west of Cape Skalas, where the mainland coast opens to the west and southwest (i.e. to the Hellenic Trench) and is no longer in the wave shadow of Elaphonisos Island for waves from the SW and WSW. Large boulders - some found more than 150 m inland and up to +14 m a.s.l. provide the most important proof of a tsunami impact along this shallow water coast.

Furthermore, in 2009 submerged strips of beachrock have been identified and drawn by divers in Vatika Bay within 200 m of the northeastern edge of the submerged city of Pavlopetri, approximately 150 m from shore, extending several km parallel to the shore, at a depth of 3–4 meters (Fig.1.7). Satellite imagery indicated two or more parallel dark strips on the seabed in the same location *(Henderson et al., 2011; Pizzaro et al., 2012)*. These strips of beach-rock provide the potential to measure the position and depth of the shoreline at precise dates *(Henderson et al., 2011)*.

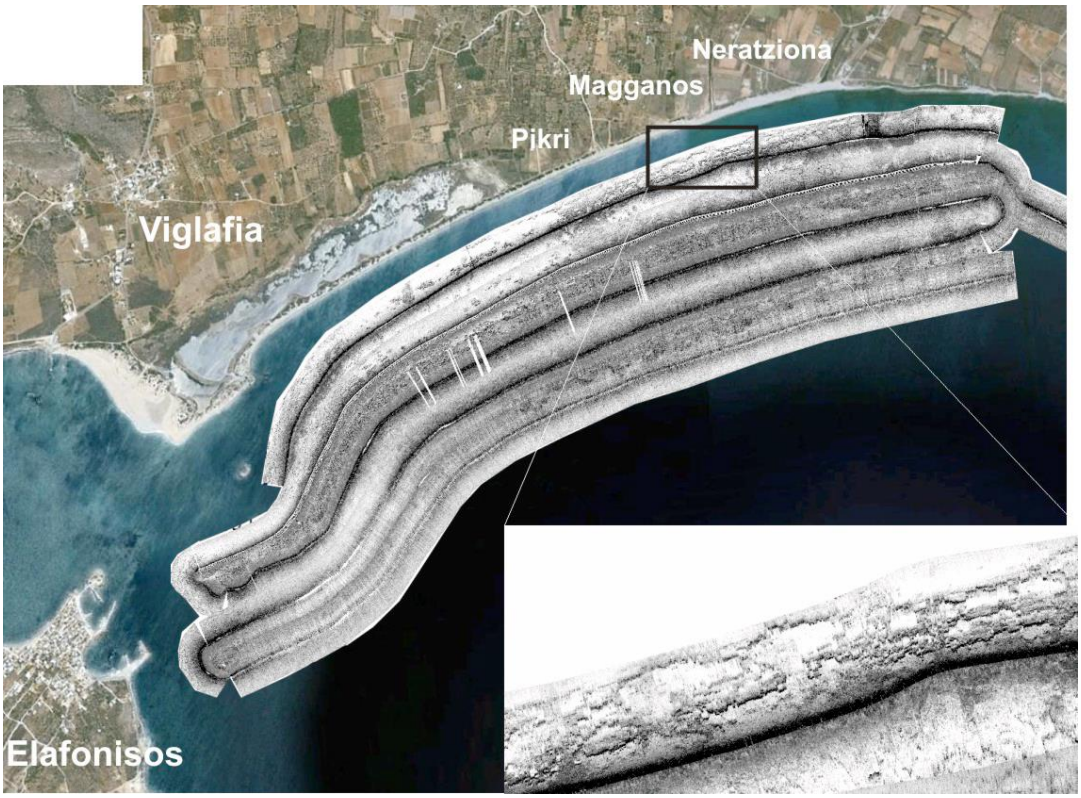

Fig.1.8: Side Scan Sonar survey overlaid on satellite imagery of Vatika Bay. The inset shows the acoustic returns consistent with beachrock formations. These run roughly parallel to the beach for a large part of the bay *(Sakellariou et al., 2011; Pizzaro et al., 2012)*.

Beachrocks are formed at sea level, at about +/- 0.5m and can be dated by extracting shells and the aragonite cement from the matrix, and conducting radiocarbon 14 C dating. Thus, it is provided robust evidence for the local relative sea-level at three different dates, right next to the ancient town. For each sea level the ancient shoreline can then be reconstructed, so that the beginning of the submergence of the city can be defined.

After radiocarbon analysis, the intermediate band (2.6-3.5 m bsl) yielded conventional radiocarbon age of 1320±30 BP and calibrated age of AD 1030 to 1160 which is consistently younger than the age of the deeper band. The shallowest beachrock band (2.5-3.0 m bsl) yielded ages which do not comply with their stratigraphic position as they are older than the ages obtained for the deeper bands. These datings point to an incremental subsidence of the coastal area around Pavlopetri, probably associated with two or three earthquake events with a drop of 0.5-1.0 m on each occasion *(Pizzaro et al., 2012)*.

1.5. Archeological setting

Along the northwestern coast of Vatika Bay, there have been encountered remains of a settlement from Helladic times (about 5000–3000 BP) near the small rocky island of Pavlopetri. The submerged Neolithic-Bronze Age town of Pavlopetri has sunk by at least 4.0-5.0 m since its foundation in the 4th millennium BC, based on the depth of the lowest structures discovered so far and the storm waves which they would have to survive (Pizzaro et al., 2012). The archeological site of Plytra, 26 km to the north of Pavlopetri, is also submerged by several meters *(Flemming, 1973; Hadjidaki et al., 1985)*.

Submerged archeological remains were first identified in 1904 by the geologist Fokion Negris (1904: 362-363) but the importance was not widely recognized at the time The remains were re-discovered in 1967 by Nicolas Flemming, who identified and confirmed the existence of a prehistoric town at the location *(Flemming,1968a., 1968b; Henderson et al., 2011)*.

The first survey took place in 1968 by a team from the University of Cambridge. A fixed grid system and hand tapes have been used *(Harding et al., 1969; Harding., 1970).* The small amount of surface founds from the seabed, suggested a date range from the Early to the Late Bronze Age (c. 2800-1180 BC) *(Harding et al., 1969).* The submerged buildings of Pavlopetri were considered to date mainly from the Mycenaean Period (1650-1180 BC) *(Harding et al., 1969)*. The occurrence of a fair quantity of later pottery, shed light for the later occupation of the Hellenistic, Roman and the late 6th or 7th century AD *(Harding et al., 1969)*.

Another survey, carried out in 2009 (Fig.1.9), from a joint Greek and British team of archeological divers and archeologists employing cutting- edge methods of underwater survey (Fig.1.10) *(Henderson et al. 2011).* There have been found newly discovered remains that consist of an area of at least 25 conjoined square and rectilinear rooms, together with a 40 m long street. The new discoveries, combined with the data from the 1968 survey, suggest that the town is of great importance and its size is greater than previously thought *(Henderson et al. 2011)*.

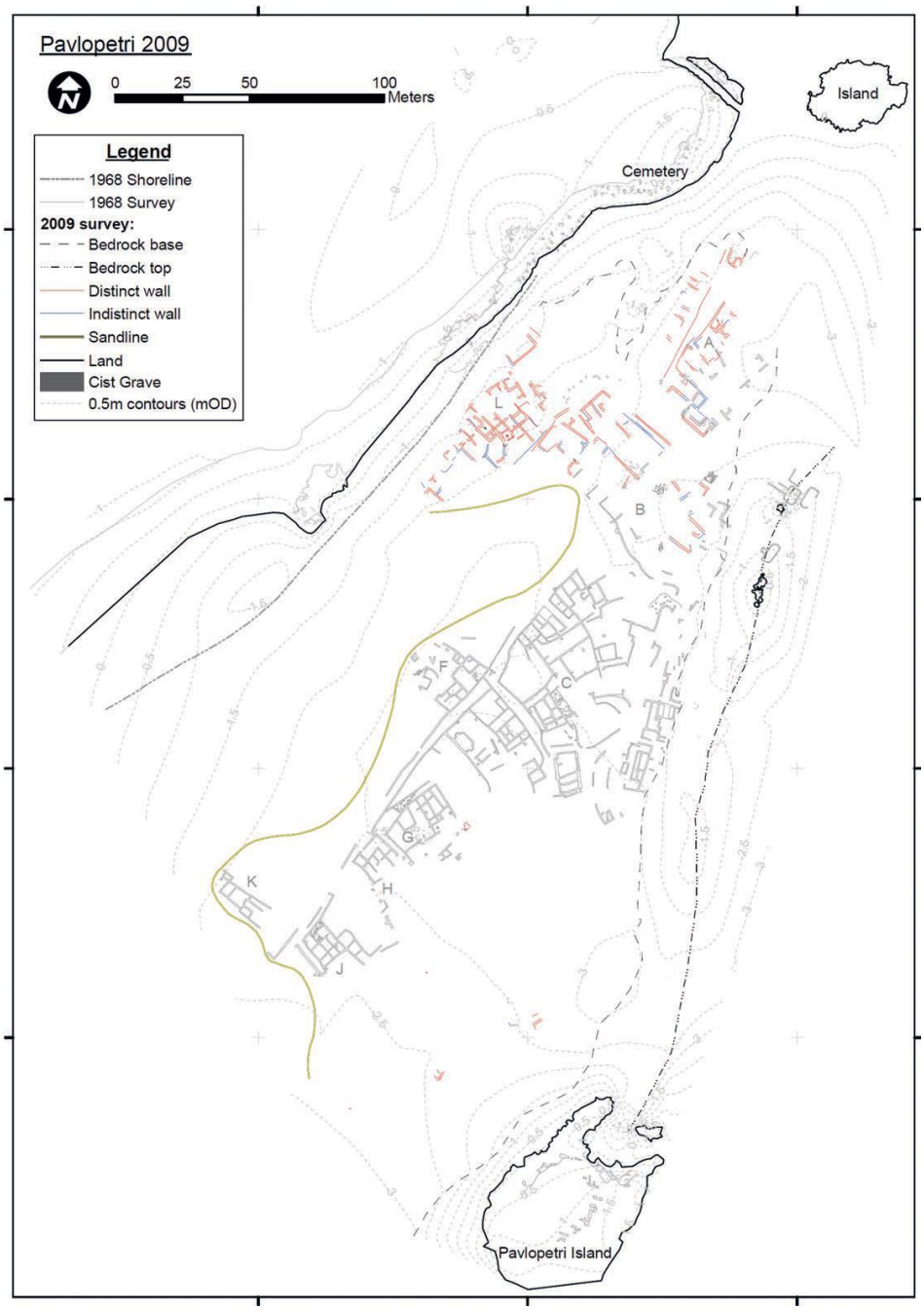

Fig.1.9: 2009 total station contour survey of Pavlopetri *(Henderson et al., 2011).*

The submerged city of Pavlopetri is one of the oldest submerged cities in the world. Its remains are dating from the Final Neolithic, through to the Roman/ Byzantine Period. The remains of the city are traced over 8 hectares, submerged by 3 to 4 m of water and consist of intact domestic buildings, large public structures, countryards, streets, graves and rock-cut tombs (Fig.1.9) *(Henderson et al., 2011)*. Beyond the Pavlopetri Islet and the eastern rocky ridge the sea is deeper and no artificial constructions have been traced. Nothing to indicate the existence of artificial harbor constructions or jetties could be identified *(Henderson et al., 2011)*. Also, the existence of the rocky ridge has protected the remains from the wave action, over the years. There were also found remains of the associated necropolis as well, being partly submerged. Houses and cist graves were excavated by the Helladic people out of

Pleistocene eolianite which partly lies under the Holocene dunes of the mainland spit (Cape Punta) opposite Elaphonisos *(Mentis, 2007)*.

Revisiting the site in future years and at different seasons may reveal further parts of the Bronze Age town, which are at present under thick beds of sand. The reason is that changes in sand cover could be related to changes in the position and shape of the shoreline over time, caused by variability in wave action *(Galili and Rosen, 2011)* and sedimentation rate. Historical reports of *Thoukidides*, indicate that Elaphonisos was connected to the mainland during the Peloponesian war in the 5th century BC. Portolans of the 16th and 17th century AD show Elaphonisos *(Cervus)* as an island. A sequence of Pleistocene elevated marine terraces in the area of Neapolis- Elaphonisos ranging from a few meters to a few hundreds of meters above sea level, indicate that the region undergoes tectonic uplift during the Quaternary. This is what is called the “Lakonia Paradox”: a submerged city within a long term uplifting area. The hypothesis is that the submergence of Pavlopetri is due largely to tectonic factors, associated with the plate convergence and subduction of the Hellenic Arc and the related local and regional faulting.

1.6. Sea level changes

During the Pleistocene, extended periods of glaciation, characterized by extended ice sheets covering the polar and sub-polar regions of the earth, were separated by warmer intervals, called interglacials with decreasing ice sheets and higher sea levels. The last 500 ka of the abovementioned geological epoch, with a dominant scale of approximately 125 ka, sea level fluctuated by over 100 m. Relative sea level change depends on eustatic change and vertical movements of the crust. Vertical movements include both tectonic movements and isostatic movements, associated with changes in the mass of ice and water surface. Thus, eustacy, isostasy and tectonics are the three factors which control the relative sea level changes.

Past sea level is measured with respect to its present position and contains information on both land movement and changes in ocean volume. During glacial cycles of $\sim 10^5$ year, the most important contribution with a global signature is the exchange of mass between the ice sheets and oceans, with tectonic vertical land movements being important mainly on local and regional scales.

The major cause of sea-level change during ice ages is the exchange of water between ice and ocean and the planet’s dynamic response to the changing surface load (Lambeck et al., 2014). Ocean volume changes related to the glaciation have an impact on ocean’s oxygen isotope composition. This led to the reconstruction of sea-level curves related to past climate changes (Fig.1.11). The precision of the curves is reduced by three basic factors. The first is the effect of ambient temperature on the isotopic composition of planktonic and benthic foraminifera *(Shackleton, 1987)*. Secondly, variation in the isotopic composition of ice sheets with size and latitude *(Mix and Ruddiman, 1984)* and the effect of bioturbation in degrading the resolution of the isotopic record *(Bard et al., 1989)*. Moreover, sea level with use of a terrestrial datum may vary essentially in tectonically active areas on account of tectonism and glacio-isostatic effects.

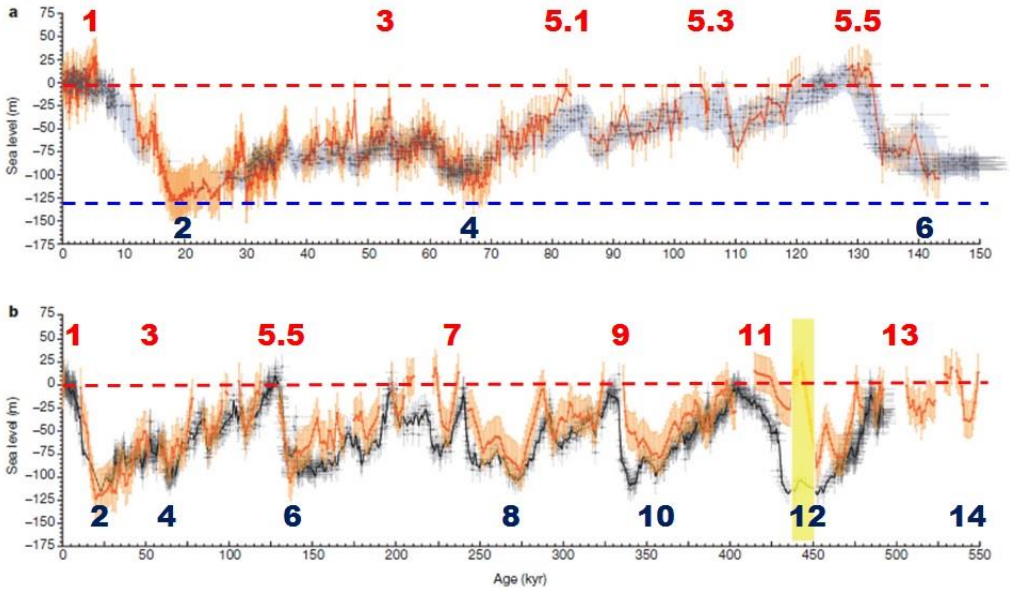

Fig.1.10: The global sea level during the last 500 ka oscillated between 120-130 m below present sea level and 5-10m above present sea level. Numbers indicate marine isotope stages (MIS): glacial (down = heavy ^{18}O values) and interglacial (up = light ^{18}O values) intervals *(Rohling et al., 2014).*

The sea-level signal from the glacial cycle exhibits significant spatial variability from its globally averaged value because of the combined deformation and gravitational response of the Earth and ocean to the changing ice-water load. During ice-sheet decay, the crust rebounds beneath the ice sheets and subsides beneath the meltwater loaded ocean basins; the gravitational potential and ocean surface are modified by the deformation and changing surface load; and the planet's inertia tensor and rotation changes, further modifying equipotential surfaces. Together, this response of the earth-ocean system to glacial cycles is referred to as the glacial isostatic adjustment (GIA) (Fig.1.11) *(Lambeck et al., 2014)*.

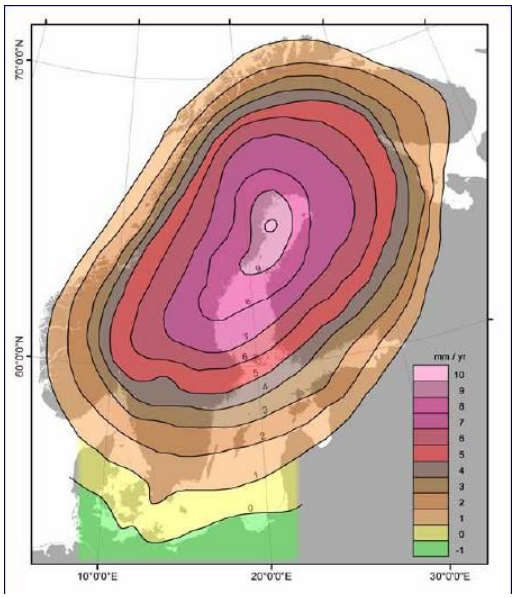

Fig 1.11: Glacial isostatic adjustment or rebound effect: an example. Elimination of ice sheets let to the reduction of pressure, resulting in the uplift of Scandinavia (pink color is for the most uplifting areas). In the same time, at the edge of the ice cover subsidence has occurred *(Harff and Meyer, 2005)*.

In a smaller scale, major sea level changes have occurred during glacial cycles in the Mediterranean basin and there is evidence in geological and archeological records throughout the last glacial cycle *(Lambeck and Purcell, 2005)*. In the latest Pleistocene sea-level was about 120 m lower than the present (Fig.1.13) and it started rising rapidly since the Last Glacial Maximum (LGM), 18 ka BP *(Shackleton, 1987; Fairbanks, 1989; Bard et al., 1990)*. Former to the sea-level rise, large areas of land were exposed and occupied by terrestrial vegetation, animals, and early human.

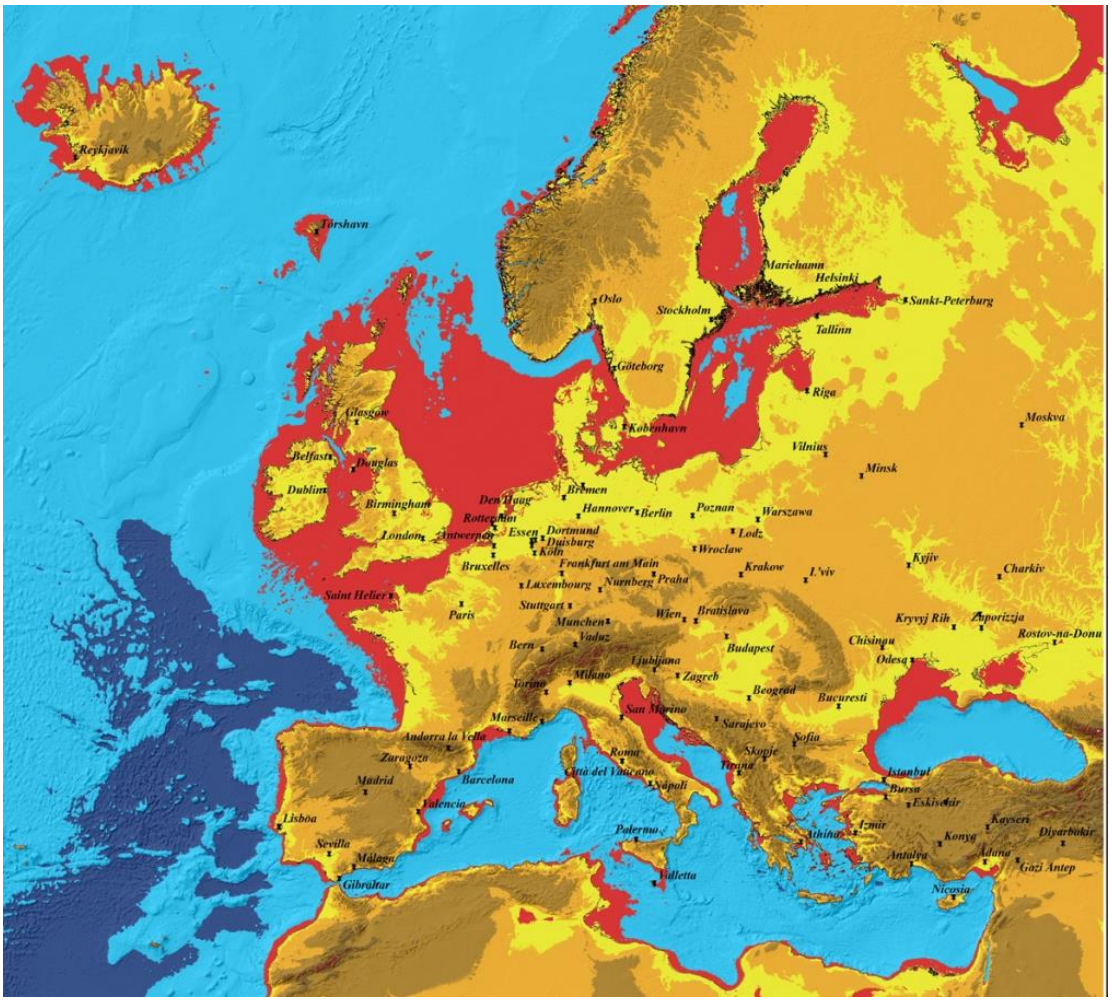

Fig.1.12: During the last glacial period (20-18 kyrs BP) sea level has been by about 120m lower than the present one. The drawing highlights in red color the continental shelf of Europe between the present shoreline and the 120m depth-contour, which represents roughly the presently submerged LGM landscape (HCMR courtesy).

The geo-archaeological setting of Vatika Bay indicates that, since the mid-Holocene, the relative sea level has obviously never been higher than the modern one *(Henderson et al., 2011)*. Undated cart tracks between Cape Punta and Cape Skalas, disappearing under water and leading to Elaphonisos Island support this scenario *(Sheffers et al., 2008)*. It is also strongly supported by the fact that the eustatic sea level rise after the Last Glacial Maximum terminated at c. 6800-5700 cal BP *(Flemming, 1978; Lambeck and Chappel, 2001; Lambeck, 2004; Lambeck et al., 2004)* and regional sea level in the Mediterranean has fluctuated by less than 0.5-1 m since that date *(Flemming and Webb, 1986; Morhange et al., 2006; Marriner and Morhange, 2007)*.

2. TECHNIQUES AND METHODOLOGY

2.1. TECHNIQUES

The marine geophysical data presented in this MSc thesis were acquired during two systematic geological-geophysical surveys of the Institute of Oceanography of HCMR, one in June 2010, and a second one in May 2015. The surveys were conducted aboard the 14 m long Research Vessel “Alkyon” of the Hellenic Center for Marine Research (Fig. 2.1), equipped with GPS and differential GPS, allowed to obtain high resolution swath bathymetry of the area. The survey in 2010 has been carried out in the frame of the research project for the submerged prehistoric city of Pavlopetri. The 2015 survey has been conducted in the context of the project *“Environmental impact of ship anchoring on the seafloor of Vatika Bay”*, funded by the Prefecture of Peloponnese.

Fig.2.1: RV Alkyon in Vatika Bay.

During the research cruises, both Multi Beam 200/400 kHz and Single Beam Echo Sounders have been used. Bathymetric data were integrated with the acquisition of high-resolution sub-bottom profiles and side scan sonar imaging of the seafloor. Three different types of sub-bottom profilers have been used during the two survey campaigns: Pinger (3,5 kHz), Chirp (2-7 kHz) and Boomer (1-2 kHz).

2.1.1. Multi Beam Echo Sounder

Multi Beam Echo Sounder (MBES) systems aim to simultaneously collect seafloor bathymetry and backscatter information over a swath of seafloor. MBES allow the sounding along a swath, on both sides of the route of the ship, whose extend depends on the current depth. They tend to be fairly complex systems requiring sophisticated motion reference units in order to rectify vessel pitch, roll and heave when positioning the data relative to the seafloor *(Le Bas and Huvenne, 2009)*.

The variation of the backscatter strength with the angle of incidence is an intrinsic property of the seafloor, which can be used as a robust method for acoustic seafloor characterization. Furthermore, in a comparable way to Side Scan Sonar, continuous coverage data of the seafloor can be collected by running parallel survey tracks at appropriate line spacing for the system

For the detailed bathymetric mapping of the seafloor of the surveyed area, a high resolution multi-beam echo sounder (200/400 kHz) RESON Sea Bat 7125 has been used, which is installed in the hull of the research vessel Alkyon (Fig.2.2).

Fig.2.2: The monitors of the deck unit of the RESON Sea Bat 7125 multibeam system onboard RV Alkyon.

This high-resolution multi beam system provides horizontal scan width on the bottom up to 4-5 times the current depth, while the error of the measurements is only within a few centimeters for shallow water depths. The high frequencies of the system in combination with the small shape of the hydrophone ensure both large coverage and narrow beam width scanning.

Reson SeaBat 7125 is able to record up to 512 points of depth (400 kHz mode) or 256 points of depth (200 kHz mode) across the ship' track on every emitted acoustic pulse (ping).

For the determination of the measured depths, RTK GPS system has been used and provides accuracy of 0.02 m. The sound velocity in the water column has been regularly measured with the use of a CTD (Conductivity, Temperature, Depth) system. The sound velocity profiles were imported into the multi beam measurements, enabling maximum accuracy of the measured depths.

Multi Beam operational control, as well as collection of the data and real time processing has been done via software 7k Control Center and PDS2000 respectively. After the processing of the acquired data, the grid of the corrected depths stored in asci file format, have been the basis for the construction of the bathymetric map, using ArcGIS software, Fledermaus and PDS2000.

2.1.2. Single Beam Bathymetry

Bathymetric mapping was integrated, especially in the deeper parts of the Bay, with the single beam echo sounder Humminbird 998c Sl Combo (Fig.2.3). This particular digital sonar operates in two frequencies, 200 kHz and 83 kHz. Higher frequency provides beam emission range 20°, while lower frequency 60°, thus extending the scanning area at the seafloor in the width equal to the current depth. Besides, this particular echo sounder, features embedded GPS which allows positioning of the vessel and depth per 2 seconds.

Fig.2.3: Single Beam Echosounder Humminbird 988c SI Combo.

Measurements with the single beam echo-sounder have also been performed at the shallower parts of Vatika Bay in order to complement the data obtained with the multi beam echo-sounder in the deeper parts of the surveyed area.

2.1.3. Sub-Bottom Profilers

A large range of sub-bottom profilers are designed to provide data from below the seafloor. They can be divided on the basis of the wavelengths and strengths of the emitted sound into “sparkers”, “chirps”, “pingers”, “boomers” and “air guns”. Sub bottom profilers can be either towed behind the survey vessel, hull or pole mounted, and provide a two-dimensional profile of the seismic stratigraphy below the seafloor. A major role of the sub-bottom profilers when used in parallel with seabed mapping techniques, like multi beams and

side scan sonars, is to provide data on the nature of shallow sub-seafloor stratigraphy and contribute towards a more precise interpretation of the seafloor data and sonographs.

In the present MSc thesis, three different data sets obtained with the use of three different, high-resolution sub-bottom profiling systems have been used: Chirp, Boomer and Pinger sub-bottom profilers.

2.1.3.1. Chirp Sub-Bottom Profiler

Chirp systems can be operated from small vessels while chirp transducers have also been designed for remotely operated vehicles (ROVs).

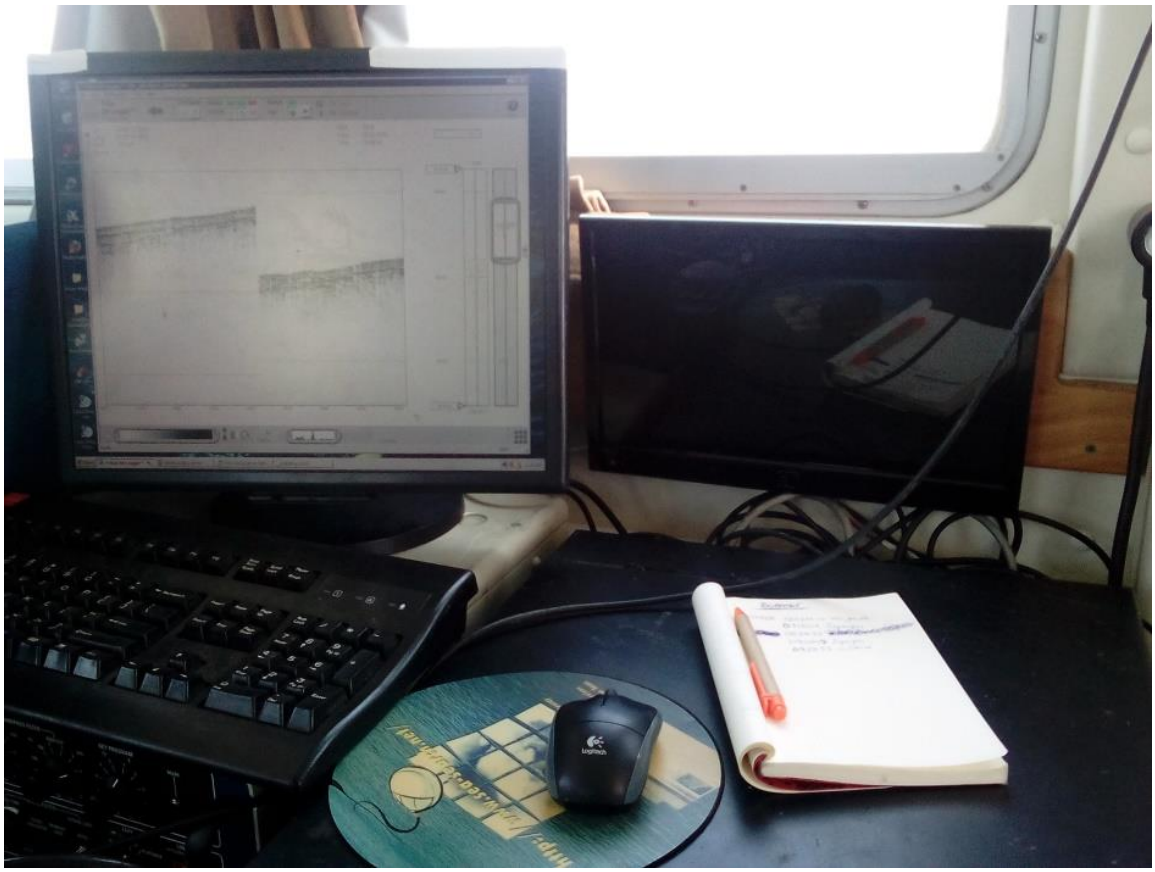

Fig.2.4: The monitor of the chirp system on board RV Alkyon during the acquisition of sub-bottom profiling data.

In general, chirp systems employ wideband frequency modulated (FM) “Chirp” technology. The system transmits a linearly swept, wide band FM pulse into the water (the “chirp” pulse). This technique provides penetration that is comparable to low frequency narrow band systems with resolution comparable to high frequency narrow band systems. Depending on the used frequency window and the nature of the sediments, penetration depth may reach 50 m or more below the seafloor with vertical resolution of about 10 cm.

A hull-mounted, chirp system (Geoacoustics LTD) has been used during the 2015 survey in the Vatika Bay with the R/V Alkyon. The system is set to produce sound frequency ranging between 2 and 7 kHz. The vertical resolution provided by the profiles was estimated at about 20-40 cm.

2.1.3.2. Pinger (3,5 kHz) Sub-Bottom Profiler

Conventional echo sounders (pingers) emit narrow bandwidth signal commonly within the range 3-10 kHz, centered on a main frequency. The most commonly used conventional echo-sounder is the 3.5 kHz sub-bottom profiler, also used in the case of Vatika Bay. Vertical resolution is typically 20-50 cm, with a maximum penetration between 30 and 60 m depending on the nature of the sub-seafloor. The transducer is also used as receiver allowing higher positioning precision of the observed features. The tow-fish (transducer) is normally attached to the side of the ship or towed and the seismic acquisition system on board.

2.1.3.3. Boomer Sub-Bottom Profiler

Boomer is an electromagnetically triggered sound source and consists of:

- A controlled seismic source of energy (Fig.2.5 left).
- A boomer type sound source (Fig.2.5 right)
- A streamer of 48 hydrophones, towed on the sea surface.
- A data acquisition system.

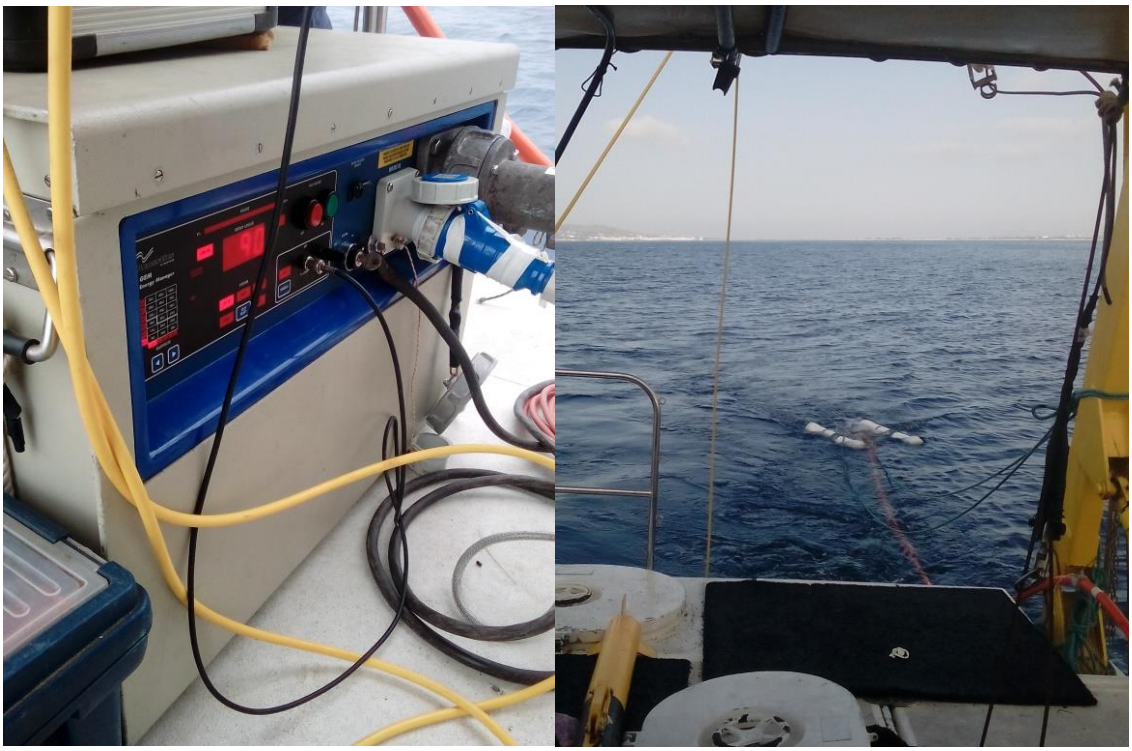

Fig.2.5: Left: Source of energy of Boomer. Right: Sound source of Boomer on a towed catamaran.

The sound source has been mounted on a towed catamaran (Fig.2.5) while a hydrophone array (streamer) is used for to receive the reflected signal. This construction allows data acquisition in shallow coastal water areas. Conventional boomers operate typically at

frequencies of 0.5-15 kHz at 90- 175 Joule and pulse length of 100-200 μs. During the field work in Vatika Bay frequency range was set between 0.7-3 kHz at 120 Joule.

Vertical resolution ranges theoretically between 25 and 50 cm, but practically boomers allow lower resolution than the 3.5 kHz profilers. Since they operate at sound frequencies lower than the pingers, they offer higher penetration in coarse grain (sandy) sediments. Penetration may reach 100 m or even deeper in very soft sediments.

2.2. METHODOLOGY

During the field surveys in 2010 and 2015 in Vatika Bay, with the RV Alkyon, bathymetric mapping has been held out mainly in the western and central part of the Bay, with a total area of approximately 25 km^2 (Fig. 3.1). Swath bathymetry has been integrated with the acquisition of high resolution seismic data, such as Chirp, Boomer and 3,5 kHz Pinger (Fig.3.1). The total length of the seismic profiles was about 70 km for Chirp (38 nautical miles), about 80 km for Boomer (43 nautical miles) and 176 km for 3.5 kHz Pinger (95 nautical miles). Chirp profiles were acquired at constant speed of 5 knots, boomer and 3.5 kHz profiles at 3-3.5 knots.

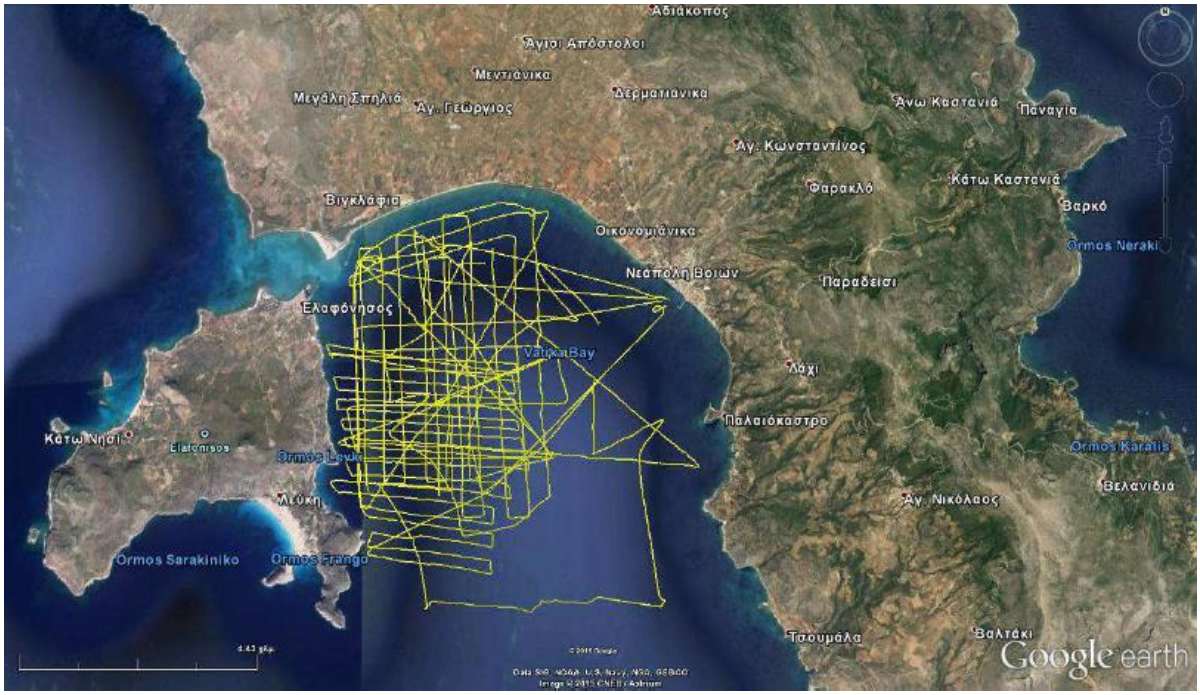

Fig.2.6.: Bathymetry and seismic tracks at Landstat satellite imagery of Vatika Bay (Google Earth).

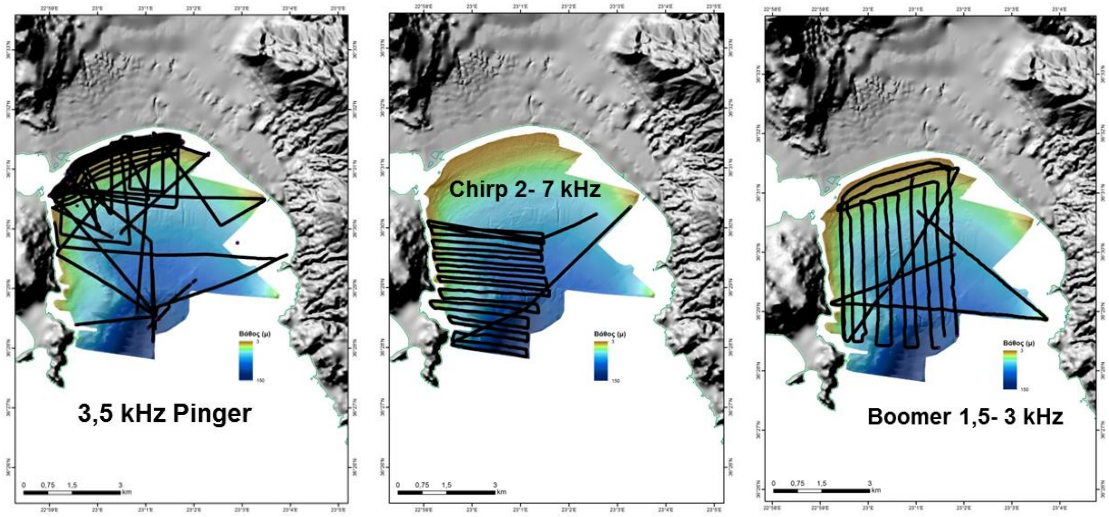

Fig.2.7: Seismic grid of the study area.

"TRITON SB INTEPRETER" software has been used for the processing and interpretation of the high-resolution seismic profiles. The graphical presentation of the seismic data and the line-drawing of the resolved stratigraphy have been done with the use of "Corel DRAW X3". During the interpretation of the seismic profiles, the main reflectors were identified and the main acoustic units were determined on the basis of their geometrical relationship with the overlying and underlying layers and their acoustic character.

3. RESULTS

3.1. Seafloor morphology

The bathymetric map of the largest part of the Vatika Bay presented in Fig. 3.1 is a composite map resulted from the integration of swath bathymetric and single beam echo sounding data.

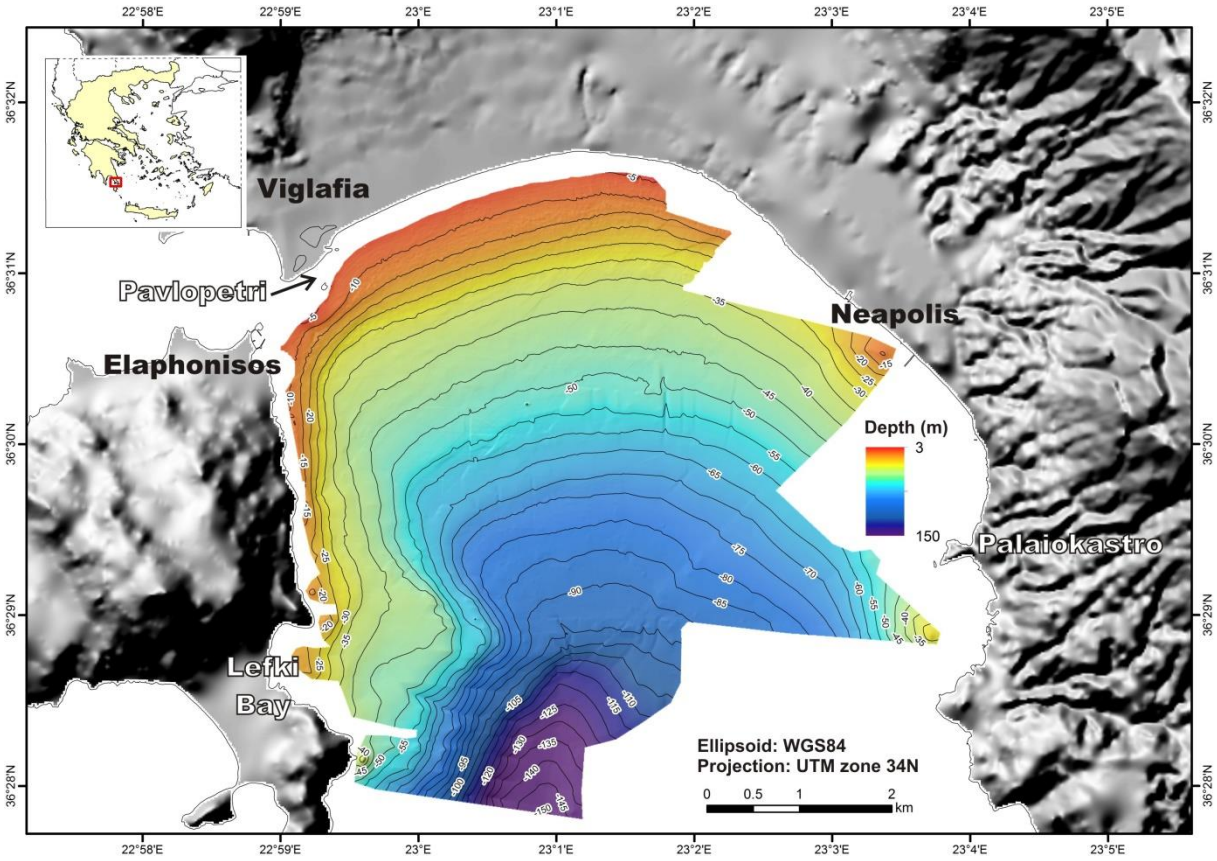

Fig.3.1: Bathymetric map of the study area revealed a valley-like morphology with smooth relief in the northern and eastern part of Vatika Bay, while the western part close to Elafonisos Island is characterized by steep slopes.

The northern, shallow part of the Bay displays the morphology of a wide, slightly asymmetric valley deepening gently towards SE with 1-1,5^{o} up to depth of 90-95 m. The western slope, towards Elaphonisos is considerably steeper than the eastern one, towards Neapolis.

At the latitude of Lefki Bay and beyond 95-100 m depth the axis of the valley turns to NNE-SSW direction and becomes narrower, with steeper slopes.

The steepest slopes are observed off the southeastern coast of Elafonisos island, in particular between depths of 50 m and 130 m. The maximum depth measured during the two survey campaigns (chapter 2.2) reaches 150 m.

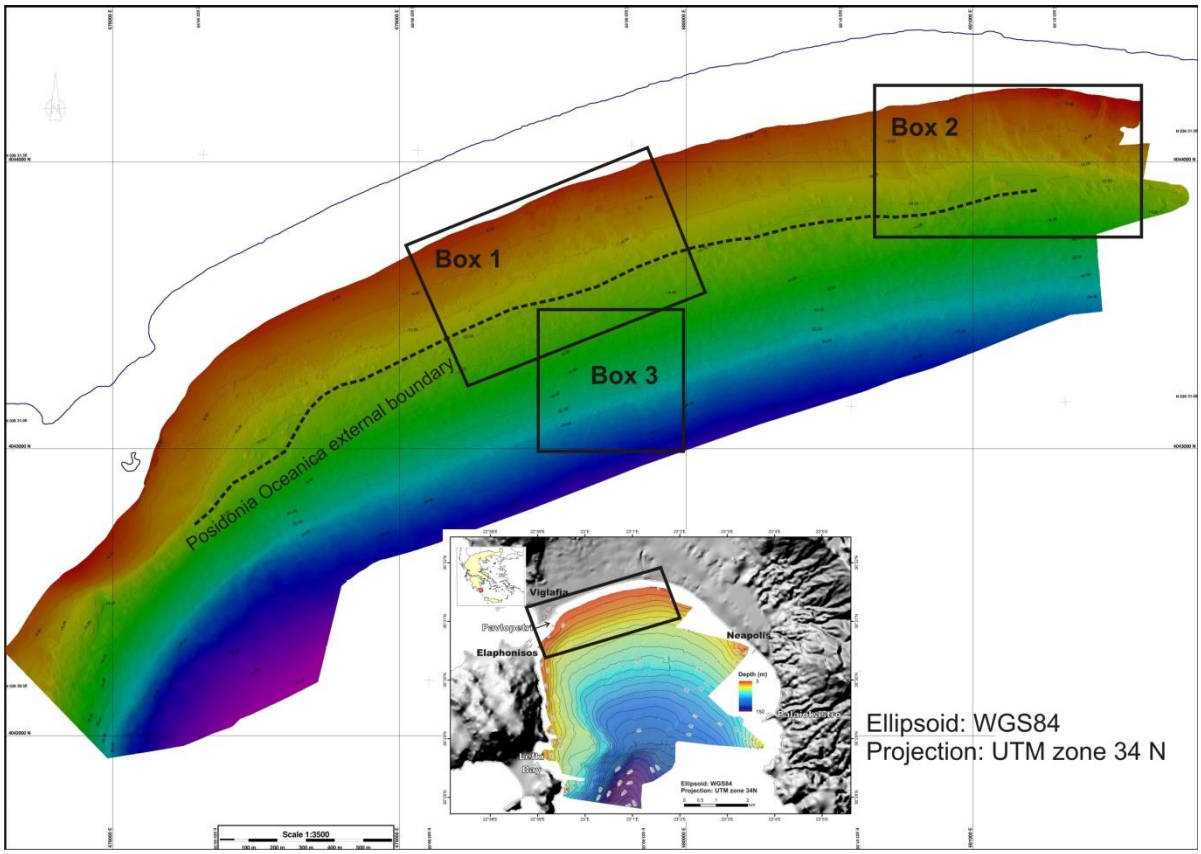

Fig.3.2: High resolution bathymetric map (1m grid cell) of the northern shallow part of Vatika Bay. The dashed line represents the Posidonia Oceanica external boundary.

Characteristic features have been observed at the seafloor of Vatika Bay, especially at the northern shallow part (Fig 3.2). Seafloor channels, beachrocks, Posidonia Oceanica meadows and trawling and anchoring marks patterns will be analyzed in the following chapters.

3.1.1. Seafloor channels

At the shallow northeastern part of Vatika Bay numerous channels have been observed on the seafloor (Fig. 3.3). Their general direction is NW-SE and they occur up to the boundary of 12 m depth. The channels have developped a triangular shape on the seafloor contours.

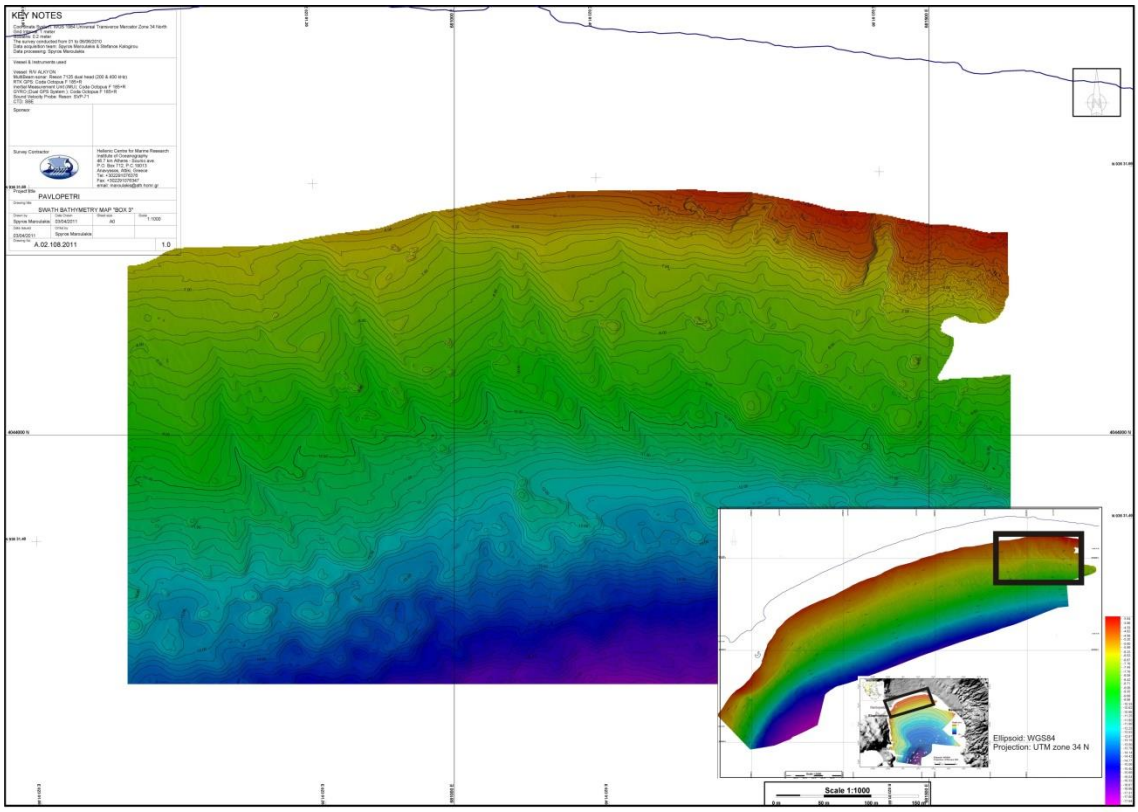

Fig. 3.3: Seafloor channels at the northeastern shallow part of Vatika Bay.

3.1.2. Beachrocks

At the shallow northern part of Vatika Bay multiple, dinsict bands of submerged beachrock can be observed from shore and satellite imagery (Fig. 3.4). The nearest bands are 150 m from shore, in depths of 3-4 m. Diving research on the site, conducted in June 2011 by Pizzaro et al. 2012, combined with aerial photography, shows that there are three bands of submerged fossil “beachrock” extending several km parallel to the shore north-east from the submerged prehistoric town (chapter 1.4) (Fig. 3.4).

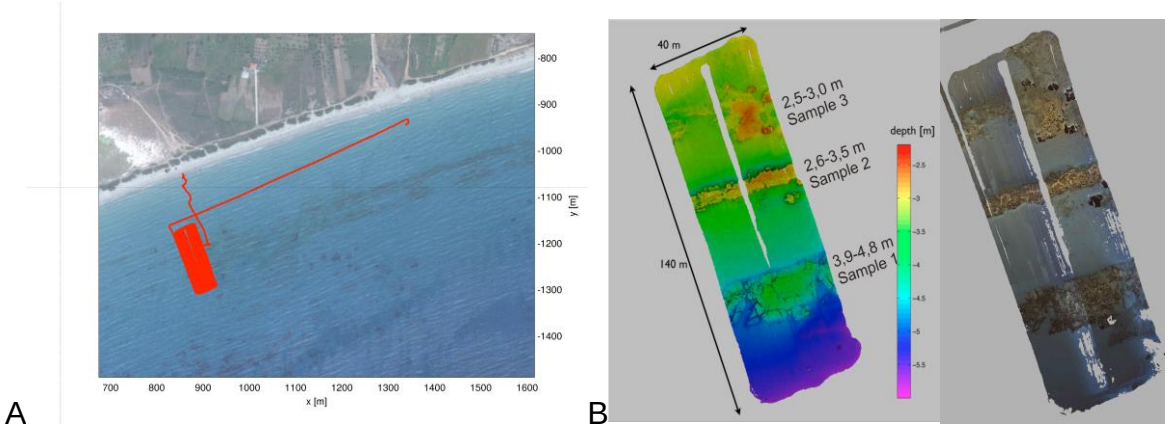

Fig.3.4: A) Satellite imagery showing the beachrock formations in shallow water. AUV survey path colored in red. B) Two views of the 3D reconstruction from optical imagery. 3D structure shaded by depth (above left) and with the optical images projected back onto the 3D surface (above right) to form a 3D mosaic. The bands of beachrock are clearly visible. Core samples depths indicated (above left) *(Pizzaro et al.2012)*.

3.1.3. Posidonia Oceanica meadows

The occurence of Posidonia Oceanica Meadows in the area is very limited. The boundaries are marked by dashed lines in Fig. 3.2 and Fig. 3.5. The external boundary (Fig. 3.2) does not exceed 12-14 m depth. The internal one is about 5-7 m depth.

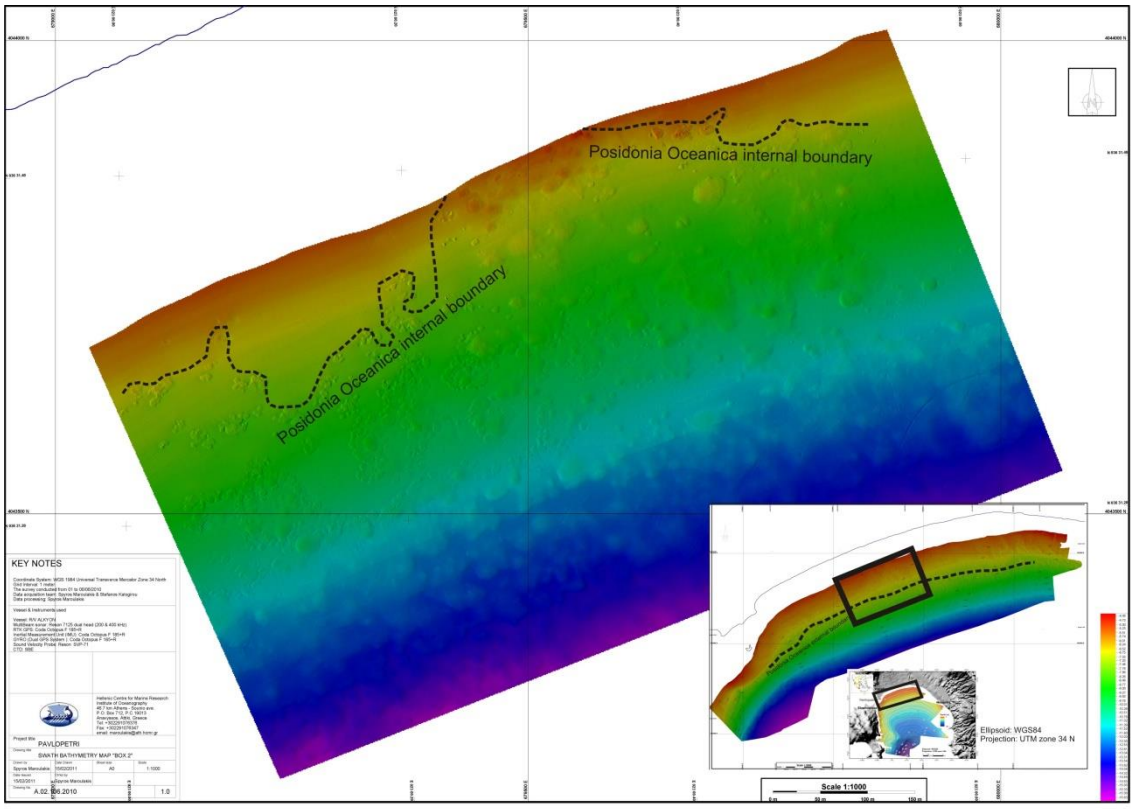

Fig.3.5: Posidonia oceanica meadows on the seafloor of Vatika Bay. The dashed line represents the Posidonia Oceanica internal boundary.

Fig. 3.5 is a zoom in the Fig. 3.2 in the area enclosed by the square 1. Scattered meadows of Posidonia Oceanica are clearly visible at the seafloor of Vatika Bay at depths of about 10-12 m. Normally they are pottentialy expected to be seen at depths of up to 28 m. Their dimensions are of the order of a few meters to a few tens of meters and their occurences are degradeted.

3.1.4. Trawling and anchoring marks

Multiple trawler marks have been observed at the sea bottom of Vatika Bay. An example of an area with strong trawler marks at the shallow part of the bottom of the bay is presented at the Fig .3.7, which is a zoom in the Fig. 3.2 in the area enclosed by the square 3. The seafloor of Vatika Bay has suffered mechanical disturbance, which has affected the vegetation that grows on it.

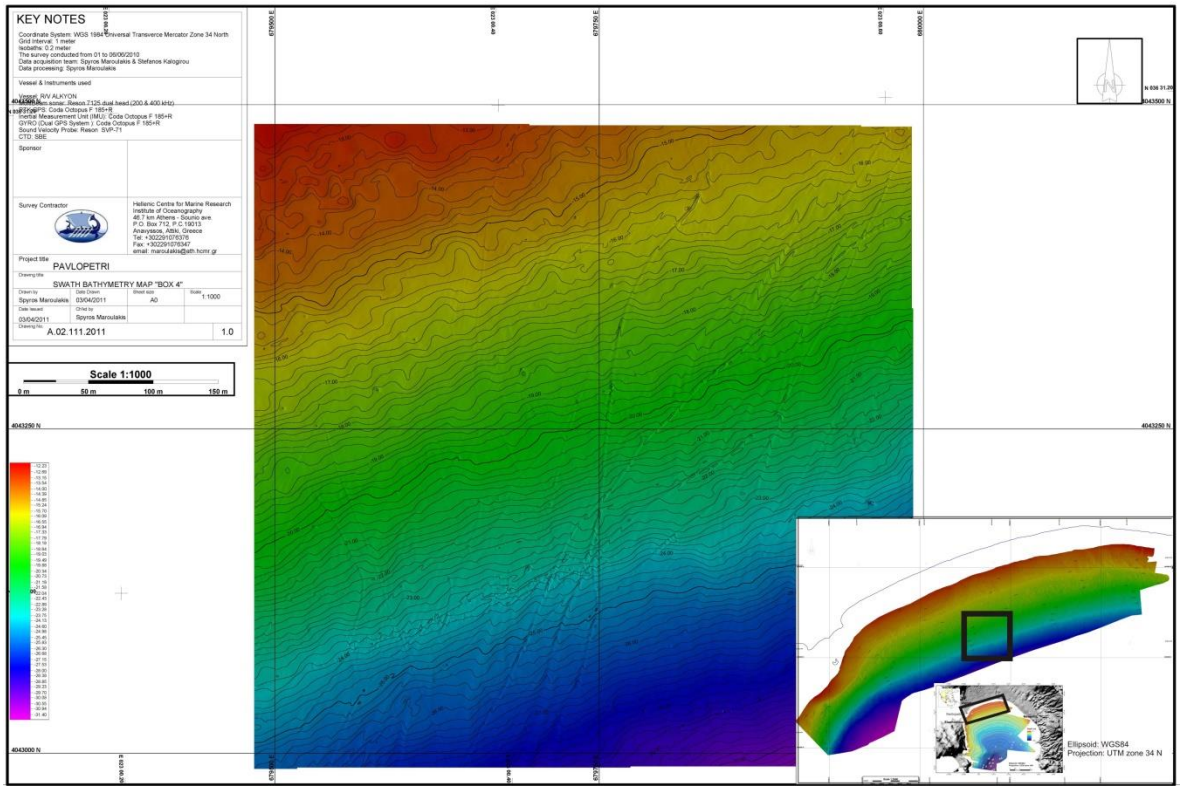

Fig.3.7: Trawler marks at the bottom of the shallow part of Vatika Bay in a high resolution bathymetric image (grid cell: 1m, ellipsoid: WGS- 84, coordinate reference system: UTM34N).

The shape, the continuity and the length of the marks are leading to the conclusion that they result from human activity. It seems that they have altered the occurrence of Posidonia Oceanica meadows. More precisely, the dragging of the ships chains anchoring for decades within the bay has resulted into the elimination of the meadows. Furthermore, another factor is the dragging of fishing equipment of trawl nets at the coastal zone of the bay at depths of less than 15-20 m.

3.2. Seismic Stratigraphy

The main acoustic reflectors have been mapped during the interpretation of the Boomer seismic profiles, in order to understand and determine the factors that affect the relief of the present seafloor. Concerning the detailed exploration of the recent sedimentary deposits and marine terraces occurrence, Chirp and 3,5 kHz seismic profiles have been used.

3.2.1. The northern shallow part of Vatika Bay (Chirp & 3.5 kHz profiles)

3.2.1.1. Profiles across the northern part of the Bay

Profile 27 (Fig.3.10) trending SW-NE, displays a cross-section of the northern shallower part of the bay. A valley-like morphology is revealed with smooth relief in the eastern part while the western part is characterized by steep slopes. In the uppermost part of the profile a transparent layer occurs. Within it, there is a chaotic package marked out by a strong irregular reflection of step-like morphology, colored in green. It represents transgressive deposits (TST). The transparent layer is separated from the acoustic basement with a reflector colored in yellow. The latter reflector is characterized by strong reflectivity and irregular morphology. The geometry along with its reflectivity indicates a landscape surface and represents the base of the Holocene. Holocene sedimentation varies across the profile with thicker (8 ms) deposits at the NE part and very thin deposits in the central-SW part. At the NE and SW part of the profile, inside the transparent layer, two reflectors of low reflectivity and amplitude occur (marked with light blue and purple lines). They indicate recent sediment deposition related to the present littoral wedge of the eastern slope (Fig.3.10). A paleo-channel occurs at the NE part as seen in the Fig.3.10. It is V shaped, about 50 m wide and 3 m deep.

Profile 57 (Fig.3.11) displays a cross section of the shallower part of the bay. The seismic stratigraphy observed here is similar to the one observed on the profile 27, Fig. 3.10. The transparent layer seen in the uppermost part represents Holocene sedimentation. . The thickness of the Holocene sediments across the profile is more or less 4-5 ms and reaches 10 ms at the central part of it.. Three V shaped paleo-channels occur at the NE part of the profile. From SW to NE, the first one is about 80 m wide and 2.5 m deep, the second is about 15 m wide and 1 m deep and the last one is about 40 m wide and 1.5 m deep.

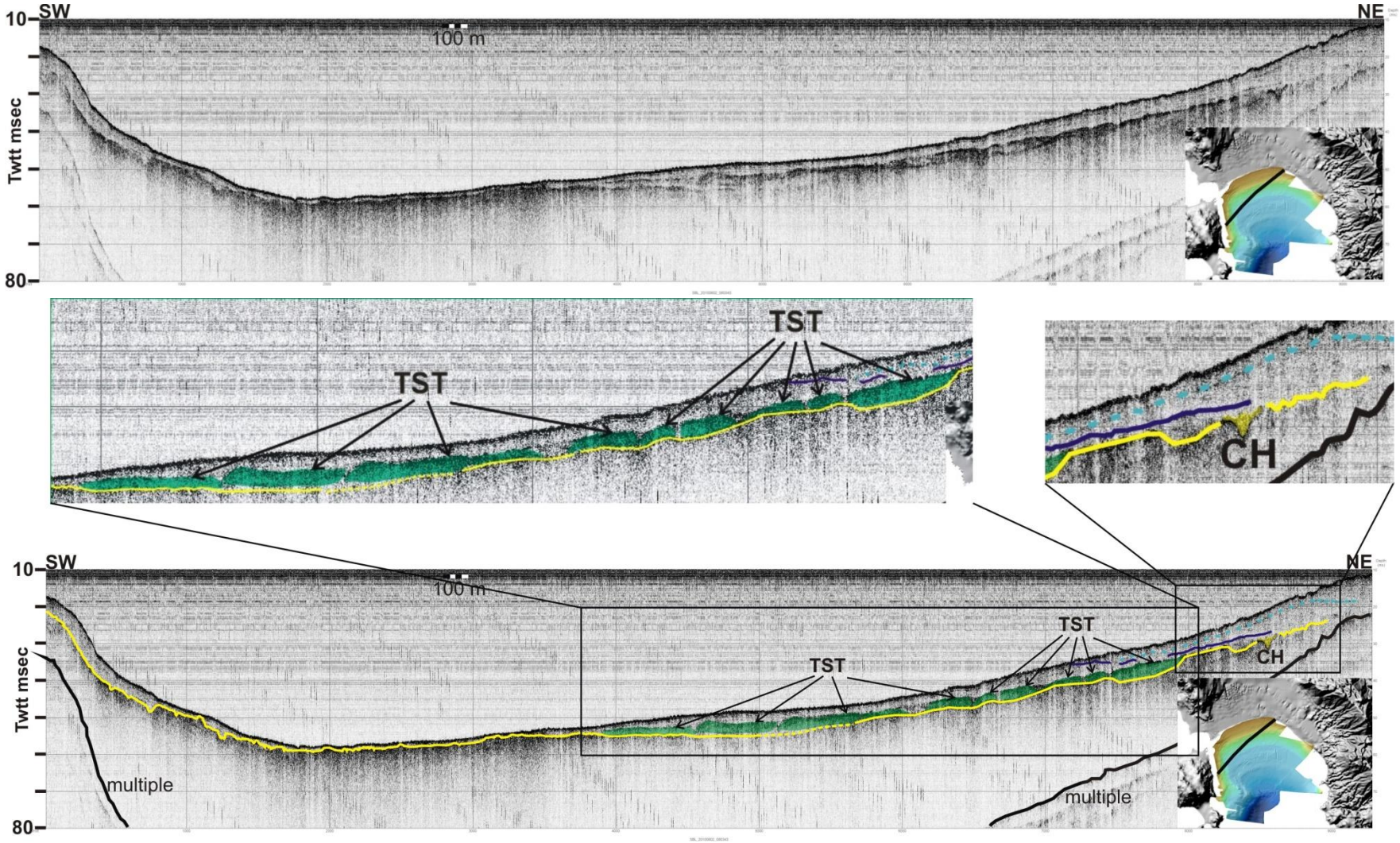

Fig.3.10: Profile 27, Pinger (3.5 kHz). TST= Transgressive system track. CH= Paleo-channel.

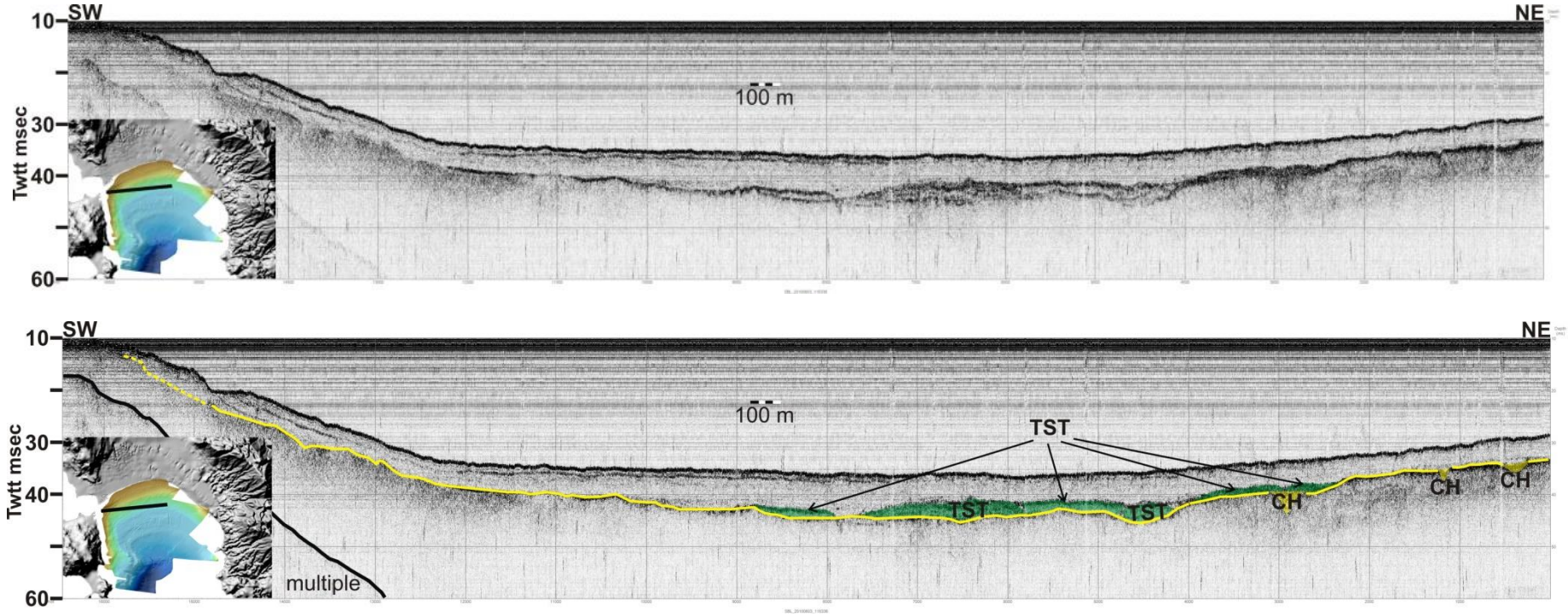

Fig.3.11: Profile 57, Pinger (3.5 kHz).TST=Transgressive system track. CH= Paleo-channels.

3.2.1.2. Profiles parallel to the northern shore of the Bay

Profile 9 (Fig.3.12) displays a transparent layer in the uppermost part. Bellow there is a reflector of strong reflectivity and irregular morphology colored in yellow. It marks the base of the Holocene sediments and the top of the acoustic basement and therefore, it represents the now submerged, paleo-landscape of the area before the post-LGM sea-level rise. Holocene sediment thickness is 5 ms. At the NE part of the profile, five V shaped paleo-channels occur (C, B, A, F. L). C is about 200 m wide and 4 m deep. B is about 180 m wide and 6 m deep. A is about 120 m wide and 5 m deep. F is about 60 m wide and 1.5 m deep and L is about 45 m wide and 2.5 m deep. They occur at the base of the Holocene, so they have probably been shaped before the post-LGM sea level rise during the erosion of running water. The seafloor has a hummocky morphology. The hummocks possibly represent the patches of the Posidonia Oceanica meadows.

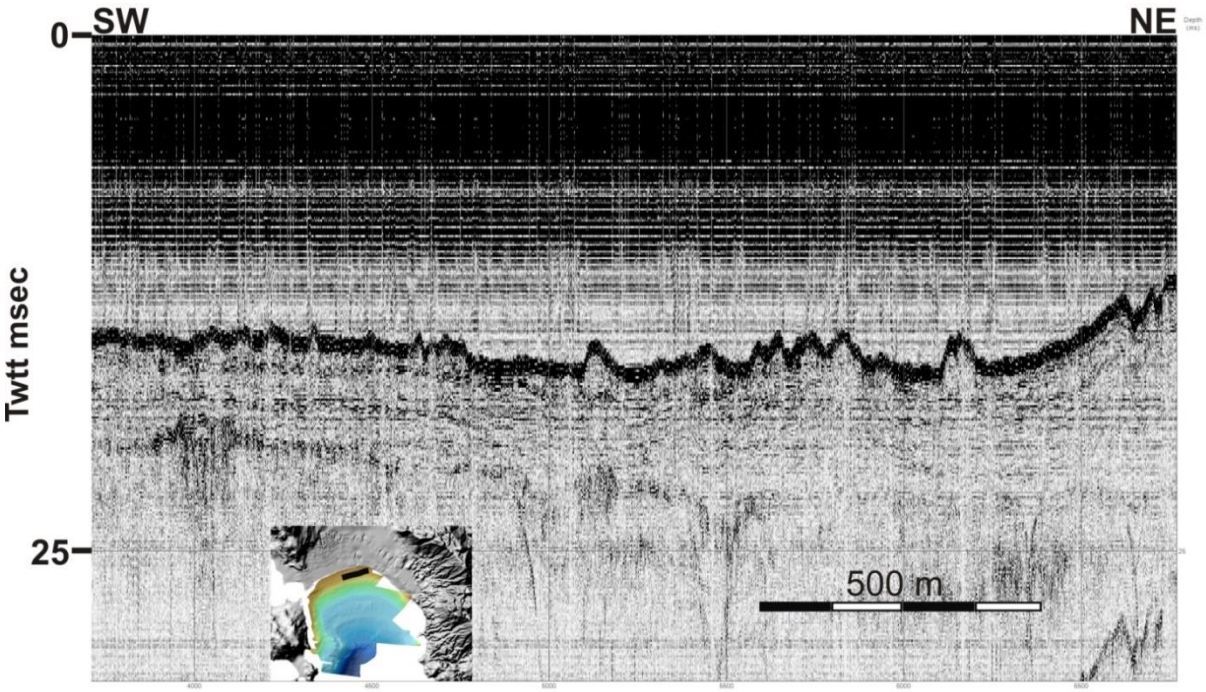

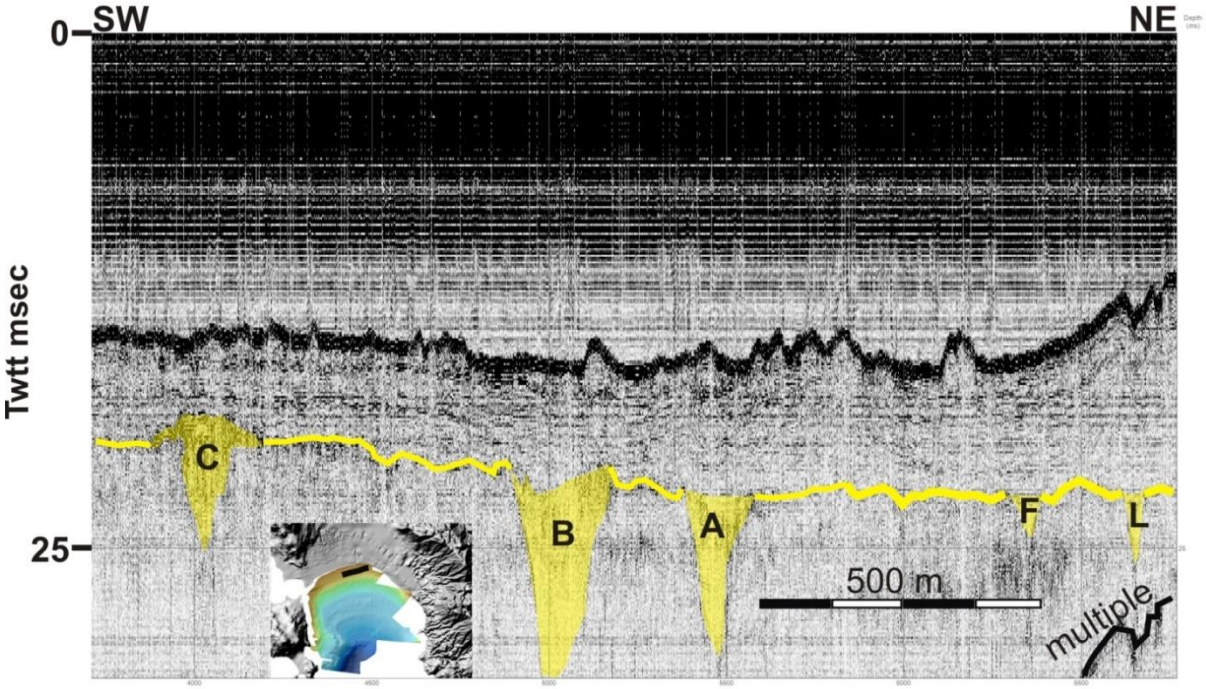

Fig.3.12: Profile 9, Pinger (3.5 kHz). C, B, A, F, L are paleo-channels.

Profile 11 (Fig.3.13) runs parallel to the profile 9, is located to the south of it and displays similar seismic stratigraphy. Holocene sediment thickness is 3 ms at the SW part, while at the NE part of the profile is 6 ms. Profile 11 demonstrates three V shaped paleo-channels (M, C, D, B, A, E, F) which occur at the same stratigraphic layer and have been shaped during the erosion of running water. Paleo-channels C, B, A, F are the same that occur at profile 9 and extend also at this profile. M is about 300 m wide and 2 m deep. C is about 200 m wide and 2 m deep. D is about 150 m wide and 4 m deep. B is about 200 m wide and 5 m deep. A is about 90 m wide and 6 m deep. E is about 50 m wide and 1 m deep and F is about 70 m wide and 1.5 m deep. The hummocks at the seafloor possibly represent the patches of the Posidonia Oceanica meadows.

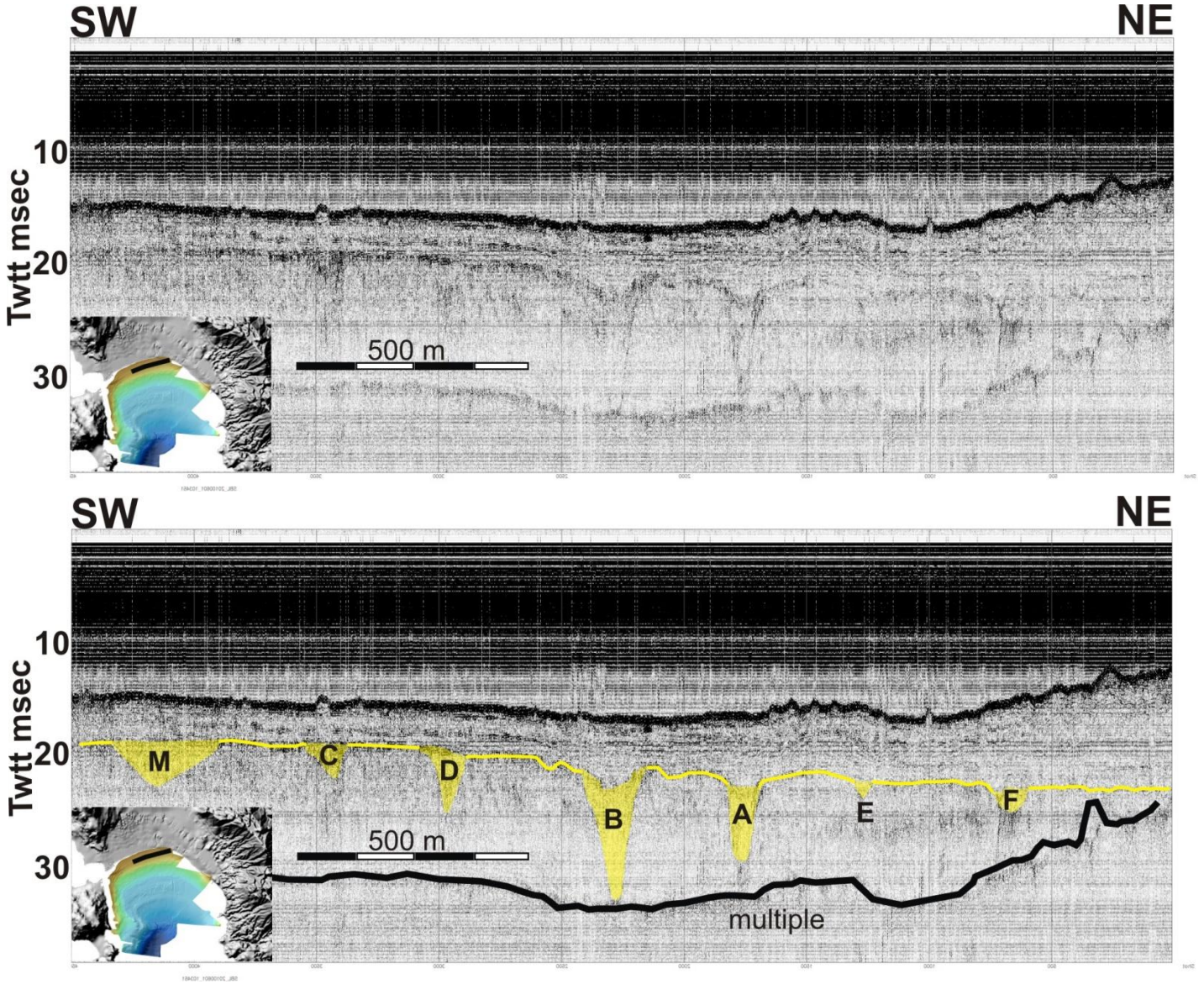

Fig.3.13: Profile 11, Pinger (3.5 kHz). M, C, D, B, A, E, F are paleo-channels.

Profile 14 (Fig.3.14) runs parallel to the profile 11, is located to the south of it and displays similar seismic stratigraphy. The seismically transparent Holocene sediments display thickness of about 3-4 ms at the SW and central part of the profile, while at the NE part they are up to 7 ms thick. Seven paleo-channels (C, D, B, A, Fb, Fa, K) occur along the landscape surface and have possibly the same origin. D and Fb are U shaped, while the rest are V shaped. Paleo-channels C, B, and are the same that occur at the profile 9 and extend also in this profile. D is seen also at the profile 11. C is about 100 m wide and 2 m deep. D is about 200 m wide and 3 m deep. B is about 170 m wide and 7 m deep. A is about 120 m wide and 6.5 m deep. Paleo-channel F, which is observed both at the profiles 9 and 11 is possibly splited into Fa and Fb in this profile. Fb is about 120 m wide and 4 m deep. Fa is about 30 m wide and 1.5 m deep and K is about 60 m wide and 3 m deep. The hummocks at the seafloor possibly represent the patches of the Posidonia Oceanica meadows.

The profiles 16, 20, 29, 49 (Fig.3.15, 3.16, 3.17, 3.18 respectively) run parallel to the previous ones and are successively deeper. Holocene sediment thickness is about 3-5 ms. Profile 49 (Fig.3.18) demonstrates a basin like morphology at the deeper part of the profile. At this part, Holocene sediment thickness is 9-11 ms. Multiple paleo-channels occur buried bellow Holocene sediments (Ga, Gb, M, C, Db, Da, B, A, F, N, O). G is a V shaped paleo-channel and occurs on the profile 16. It is about 200 m wide and 6 m deep.

Profile 20 is split into Ga and Gb, both V shaped. They are 80 m wide and 2 m deep and 130 m wide and 3 m deep, respectively. Paleo-channel M is seen on the profiles 16, 20 and 29 and also on the aforementioned profile 11. It is V shaped, excluding at the profile 20, where it is U shaped. Its width varies from 40 to 200 m, while it is 2-3 m deep. C is V shaped and is seen in all the profiles of this chapter. Its width is about 200 m and its depth 5 m. Paleo-channel B and A are U shaped and also seen in all the profiles of this chapter. B is about 200 m wide and 4-5 m deep. At the profile 20 it is about 100 m wide. A is about 100-150 m wide and 3-4 m deep. F, a V shaped paleo-channel, is about 70-100 m wide and up to 4 m deep. It is seen at the profiles 16 and 20, also at 9 and 11. Finally, N and O are V shaped, seen only at the profile 49. They are both 40-50 m wide and 3 m deep. All the paleo-channels occur along the landscape surface (Holocene base), so they have probably been shaped before the post-LGM sea level rise during the erosion of running water. The hummocks at the seafloor possibly represent the patches of the Posidonia Oceanica meadows.

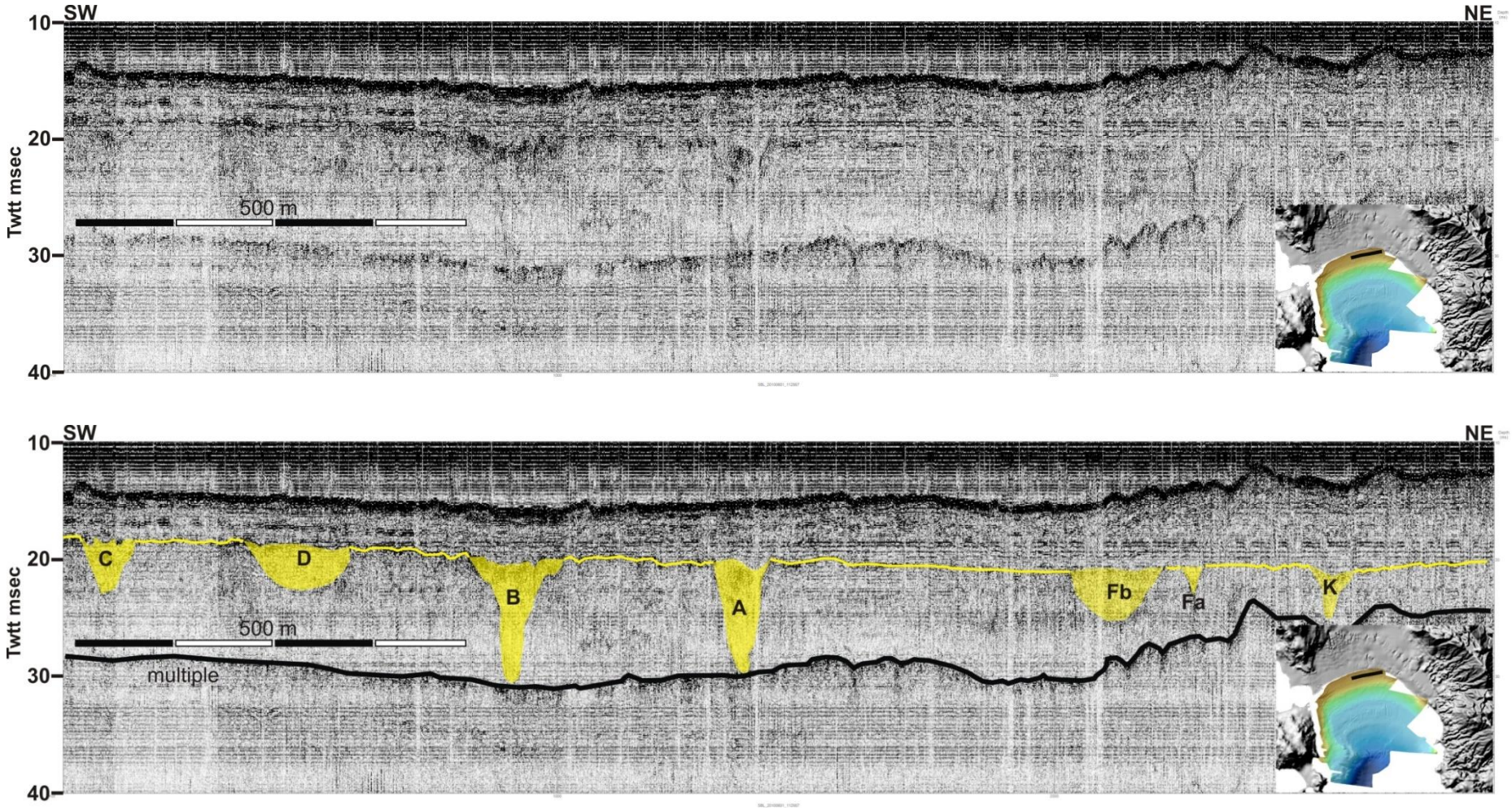

Fig.3.14: Profile 14, Pinger (3.5 kHz). C, D, B, A, Fb, Fa, K are paleo-channels.

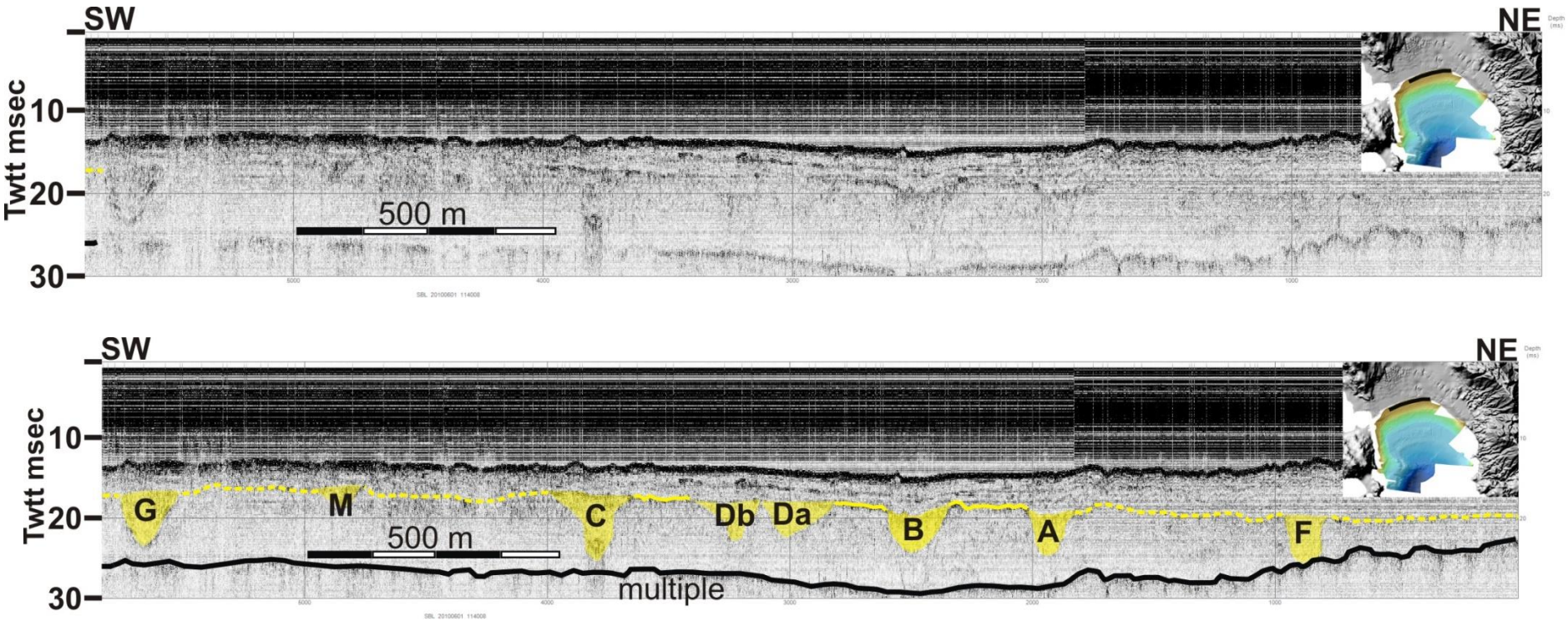

Fig.3.15: Profile 16, Pinger (3.5 kHz). G, M, C, Db, Da, B, A, F are paleo-channels.

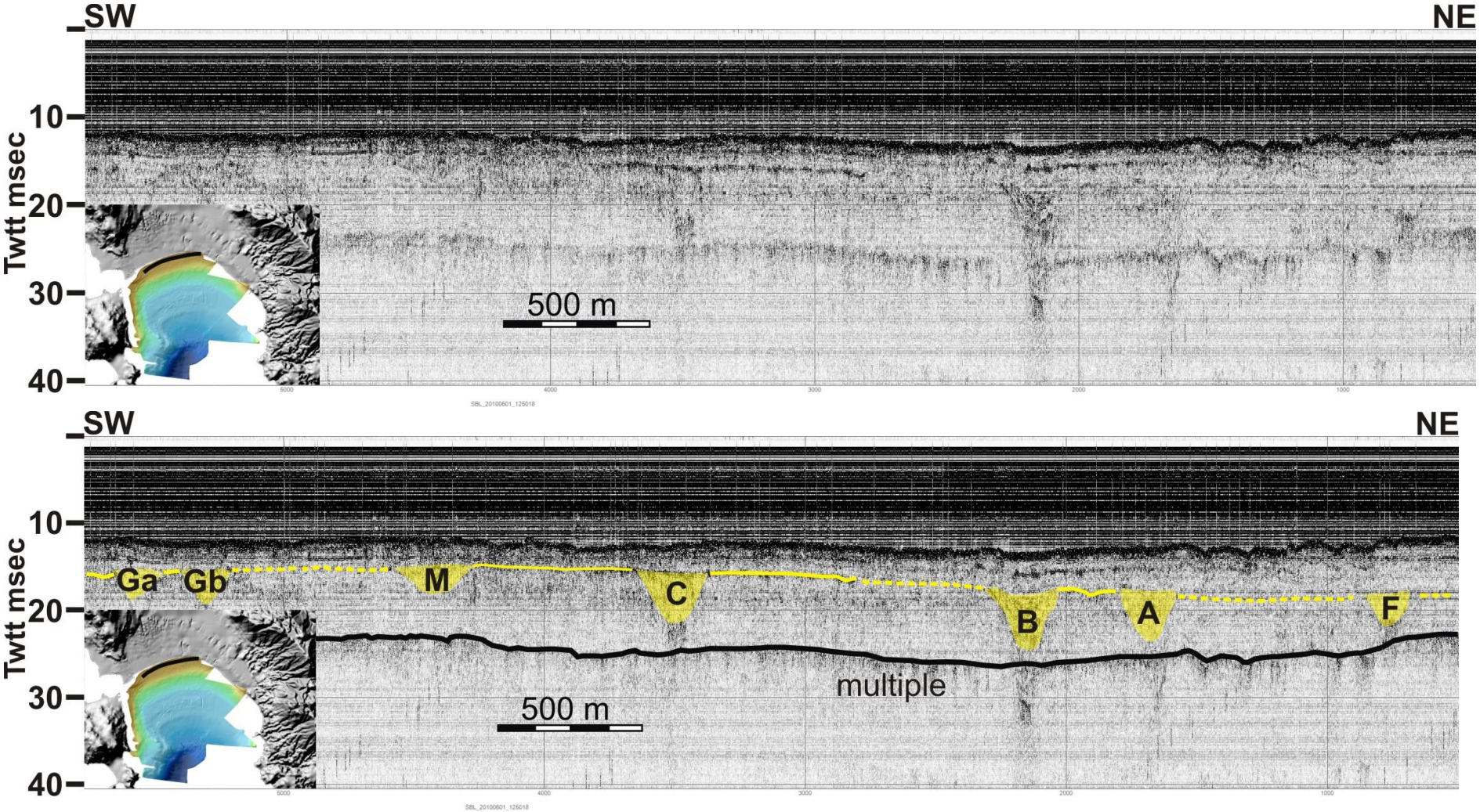

Fig.3.16: Profile 20, Pinger (3.5 kHz). Ga, Gb, M, C, B, A, F are paleo-channels.

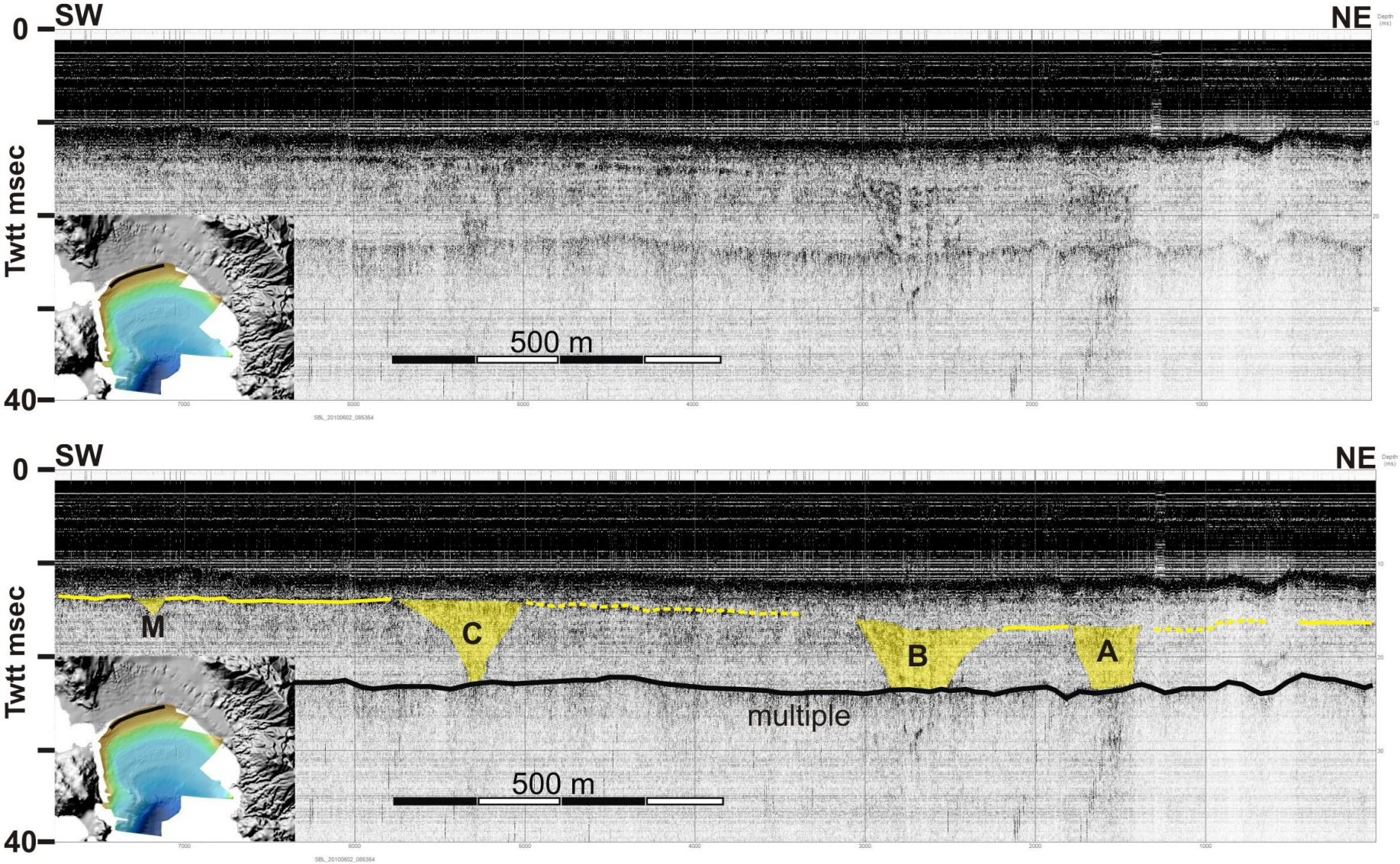

Fig.3.17: Profile 29, Pinger (3.5 kHz). M, C, B, A are paleo-channels.

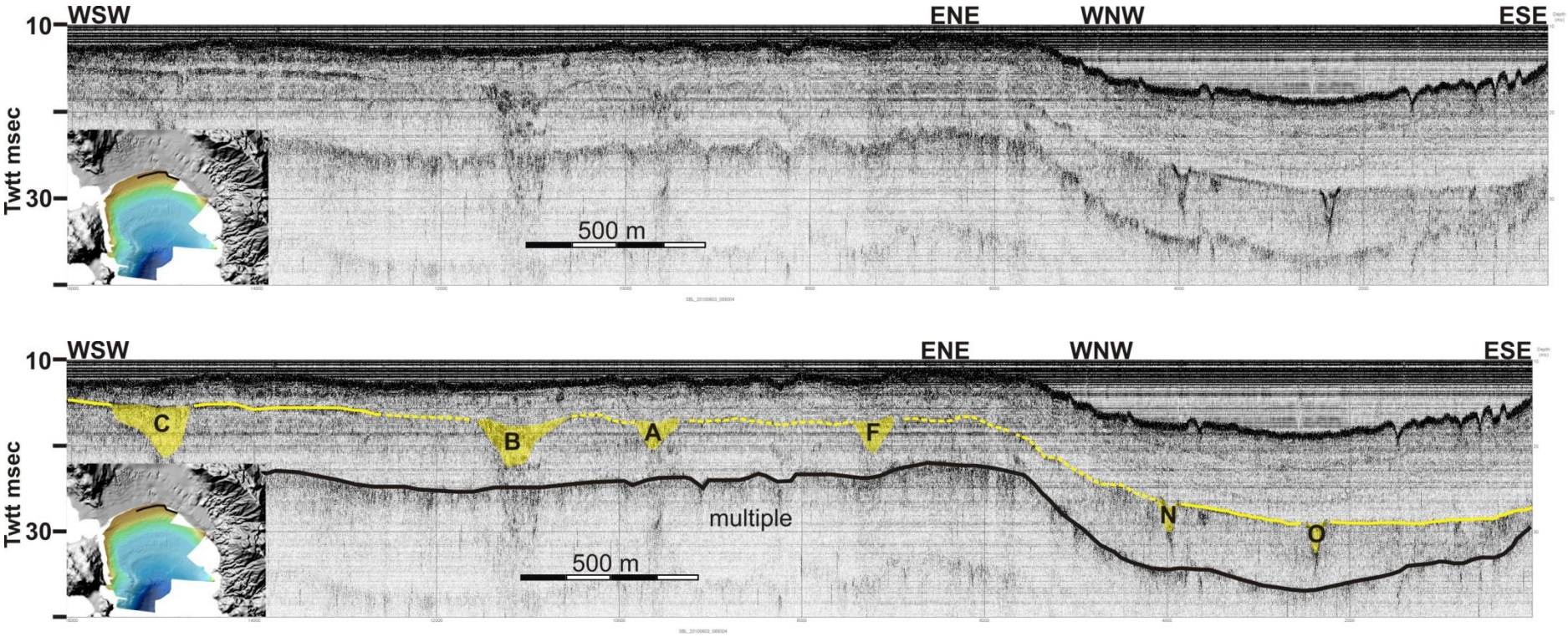

Fig.3.18: Profile 49, Pinger (3.5 kHz). C, B, A, F, N, O are paleo-channels.

Profiles 54, 56 (Fig.3.19 and 3.20) are parallel to the previous ones (Fig.3.12-3.18). In the uppermost part of the profiles, a transparent layer is separated from the acoustic basement with a reflector of strong reflectivity and irregular morphology. The geometry along with the reflectivity of the latter reflector indicates a landscape surface. It represents the base of the Holocene. The uppermost transparent layer indicates sedimentation during Holocene. Its thickness at the deeper part of the profiles is 2-4 ms, while at the rest, it is 6-7 ms. Both profiles 54, and 56, have been acquired a few meters deeper than the abovementioned and demonstrate a basin-like morphology at the SW shallow part of Vatika Bay. Multiple V shaped paleo-channels (G, M, C, D, B, A, F) occur along with the Holocene base (yellow). They have probably been shaped before the post-LGM sea level rise during the erosion of running water. G is 80 m wide at profile 54, while at 56 extends in 140 m. Its depth at both profiles is about 2 m. G is also seen in profile 16. Paleo-channel M, seen in profiles 11, 16, 20, 29, is 80 m wide at profile 54, but extends in profile 56 up to 170 m. Its depth is about 2-3 m. C, B and A is seen in all the profiles parallel to the northern shore. C is about 250 m wide and 5-7 m deep. B is about 200 m wide and 5-6 m deep. A is 100 m wide and 6 m deep at profile 54, while at profile 56 is 160 m wide and 4 m deep. D is also seen in profiles 11, 14 and it is 100 m wide and about 2-3 m deep. F is seen only at profile 54 and it is also seen in 9, 11, 16 and 20. It is 60 m wide and 3 m deep. The hummocks at the seafloor possibly represent the patches of the Posidonia Oceanica meadows.

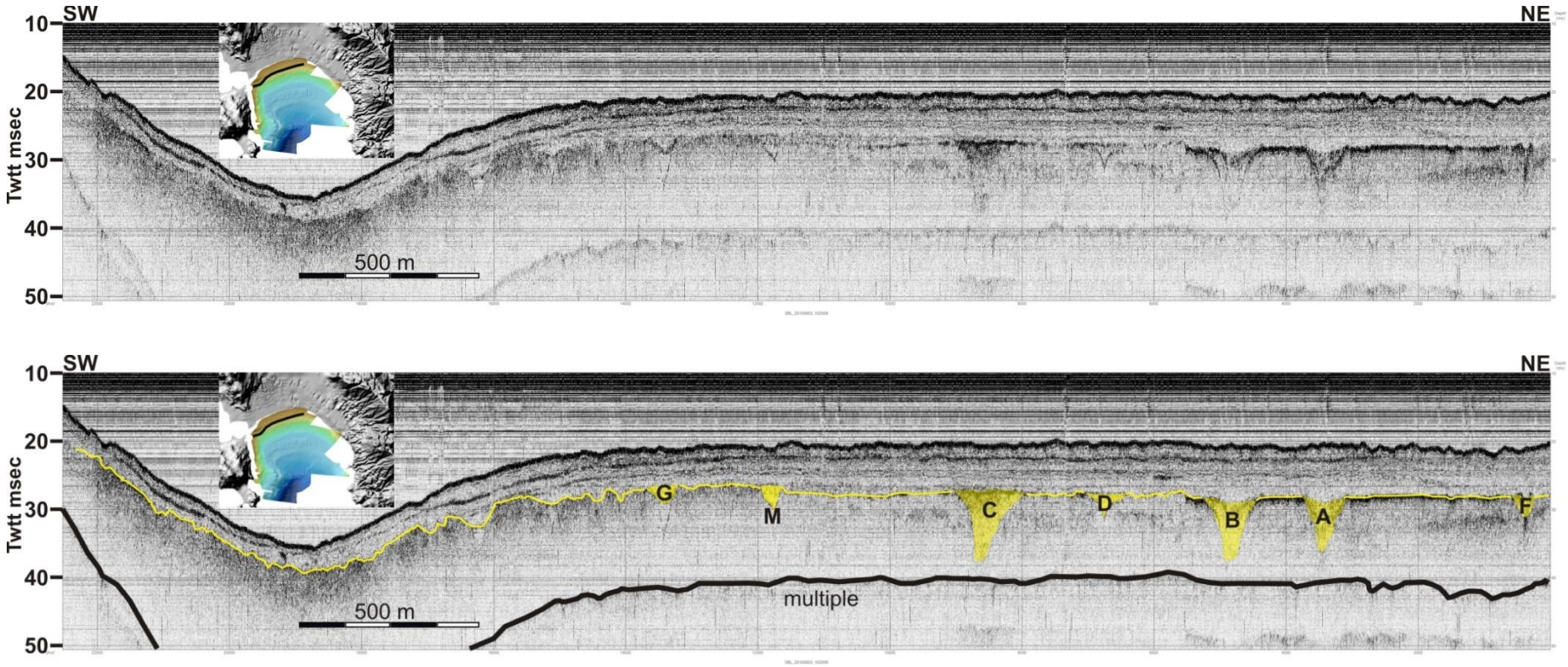

Fig.3.19: Profile 54, Pinger (3.5 kHz). G, M, C, D, B, A, F are paleo-channels

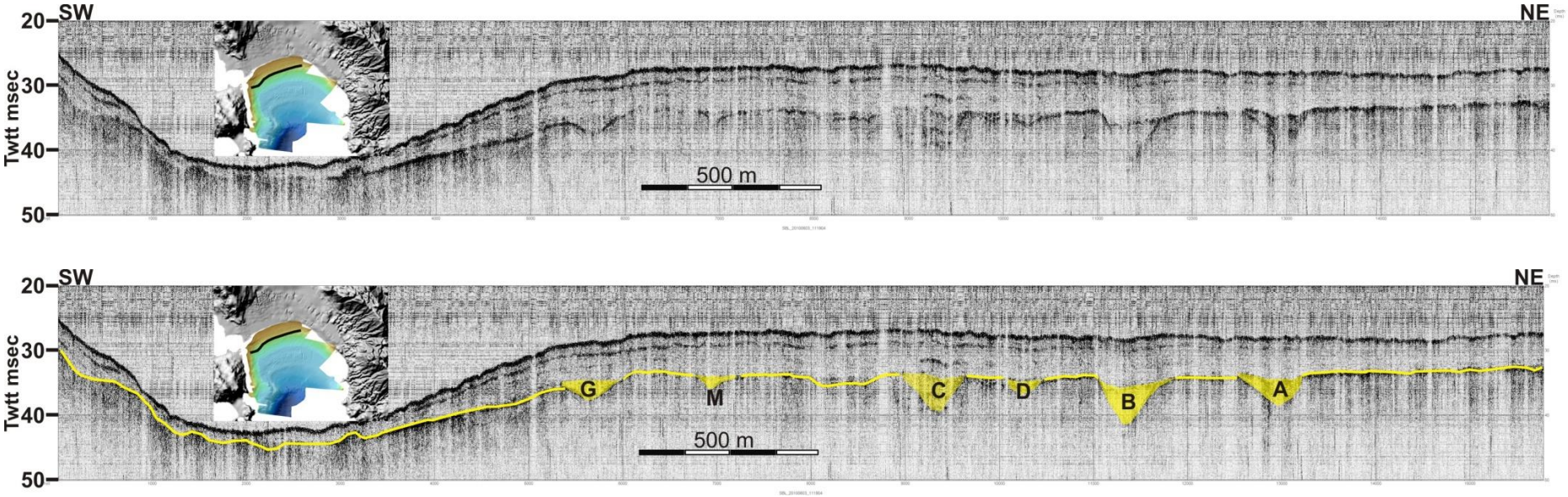

Fig.3.20: Profile 56, Pinger (3.5 kHz). G, M, C, D, B, A are paleo-channels.

3.2.1.3. Profiles perpendicular to the northern shore of the Bay

Profile 7 (Fig.3.21) displays a NW-SE trending cross section of the shallower western part of Vatika Bay. The morphologically irregular yellow reflector separates the upper transparent part from the acoustic basement. It is a landscape surface and represents the base of the Holocene. Sedimentation during Holocene is very limited up to 3 ms. At the NW part of the profile close to the slope it reaches up to 9 ms. At the NW part of the profile inside the transparent body, two reflectors colored in purple and light blue, both locally observed, highlight the sedimentary structure of the present littoral wedge.

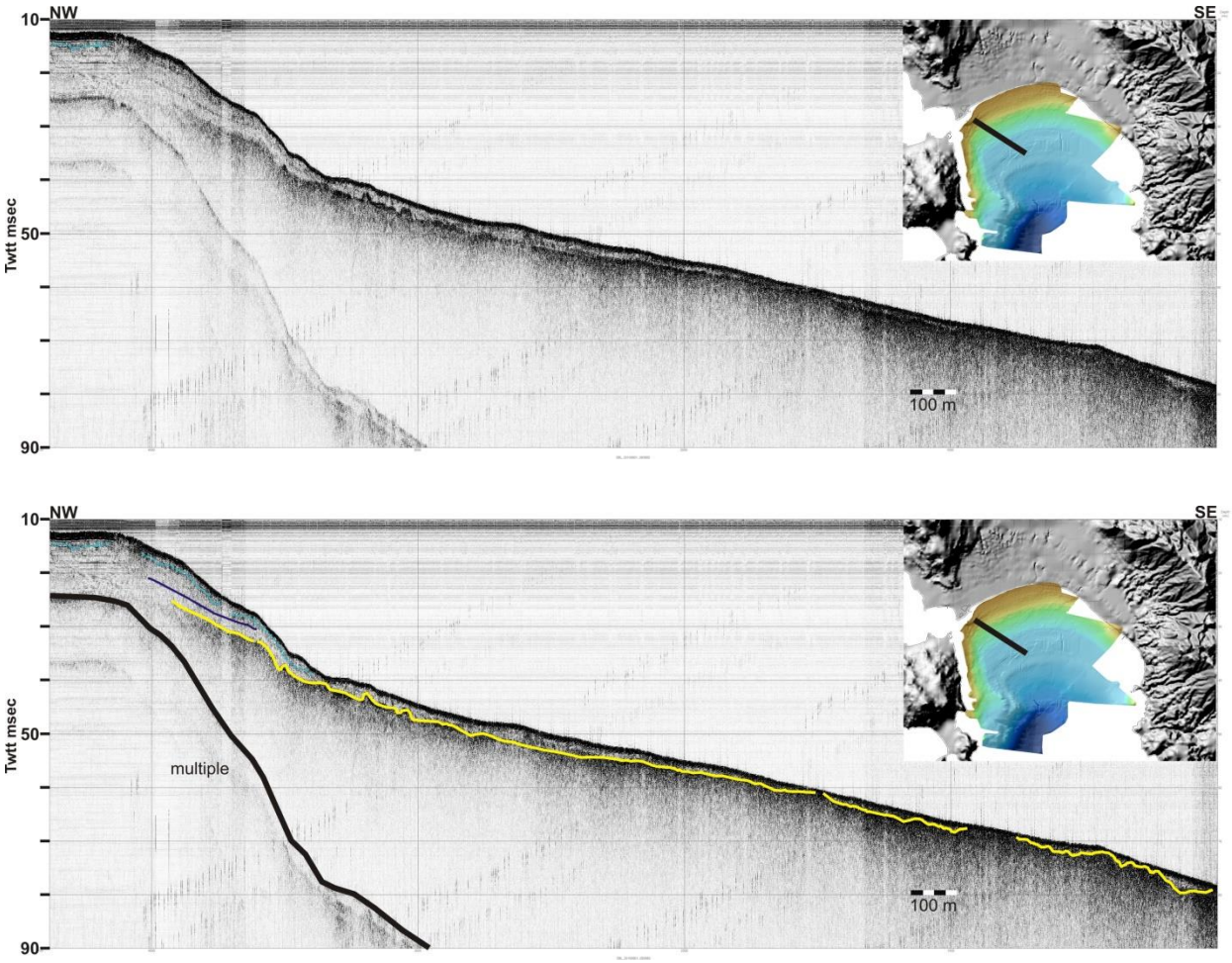

Fig.3.21: Profile 7, Pinger (3.5 kHz).

Profile 65 (Fig.3.22), trending W-E, displays in the uppermost part a transparent layer. It is separated from the acoustic basement with a reflector of irregular morphology and high amplitude. The latter, represents the base of the Holocene, colored in yellow with a very strong acoustic character, as aforementioned. Sedimentation within Holocene is 4 ms thick. Above the acoustic basement, within the transparent layer, a reflector colored in light blue and another one in purple, indicate recent sediment deposition related to the present littoral wedge. The light blue reflector represents continuous sediment deposit within Holocene.

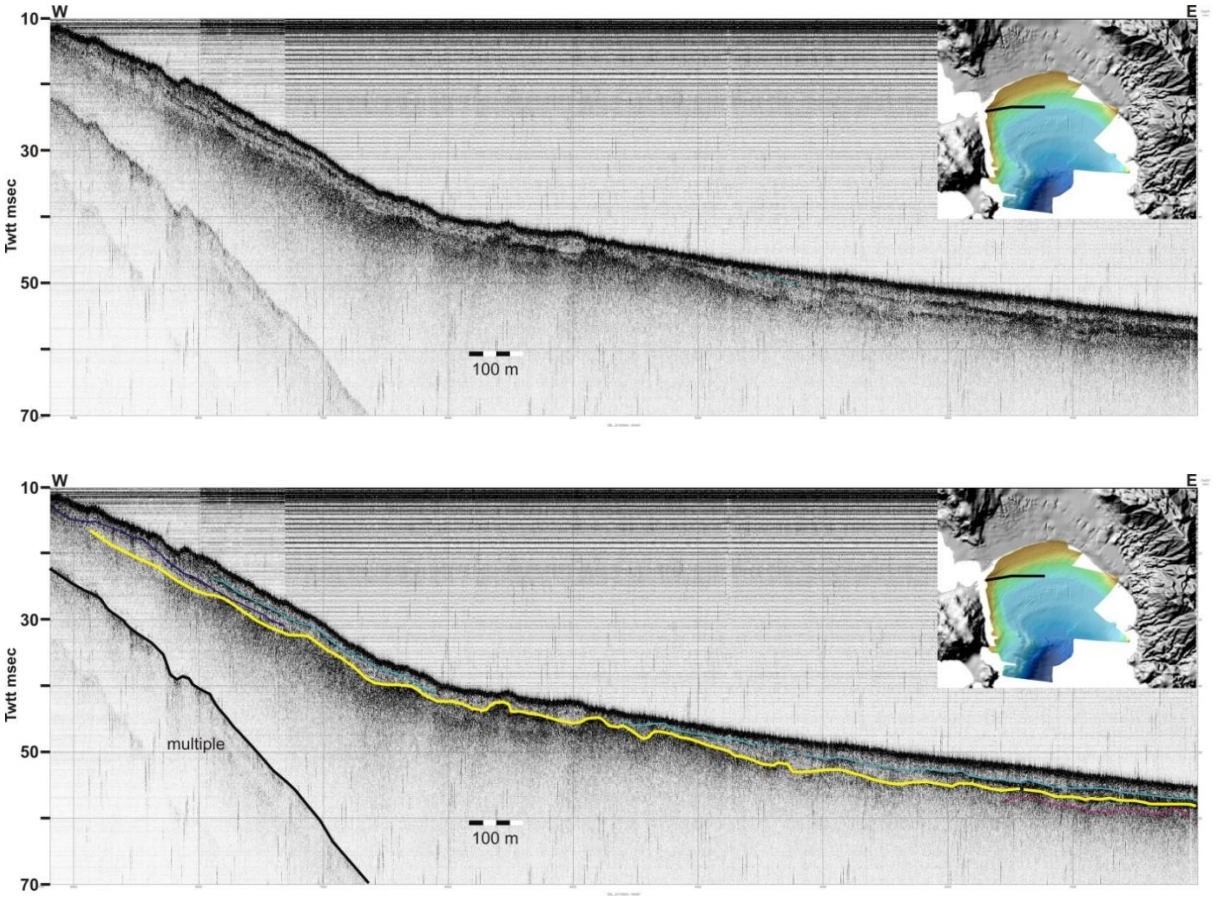

Fig.3.22: Profile 65, Pinger (3.5 kHz)

Profile 6 (Fig.3.23) displays a thin transparent layer in the uppermost part, which is separated from the acoustic basement with a reflector of high amplitude and irregular morphology. It is a landscape reflector and represents the base of the Holocene. Sedimentation during Holocene is very limited (transparent layer above the acoustic basement). It is 2 ms thick, while at the deepest part of the profile it reaches up to 4-5 ms thickness. The profile also displays two terraces at 75 ms (56.2 m) and at 92.8 ms (69.6 m) depth. At the eastern part of the profile, a package colored in yellow has slipped off the acoustic basement.

The NW-SE trending profile 68 (Fig.3.24) provides a cross section of the northern part of the bay. Like on the previous profiles, a thin, seismically transparent layer drapes the strongly reflective top of the acoustic basement. The uppermost transparent layer is thicker close to the northern shore. It reaches up to 7-8 ms where the littoral wedge, occur. The latter is represented by the continuous and high amplitude reflector colored in light blue and also a second discontinuous and low amplitude reflector colored in deep purple. It is separated from the acoustic basement with a reflector colored in yellow, which is continuous and of high amplitude and it is also morphologically irregular. Therefore, it marks the paleo-landscape of the area. . At the central part of the profile, within Holocene sedimentation, a chaotic package marked out by a strong irregular reflection of step-like morphology is locally observed (colored in green). It possibly represents transgressive deposits (TST) (Fig.3.24).

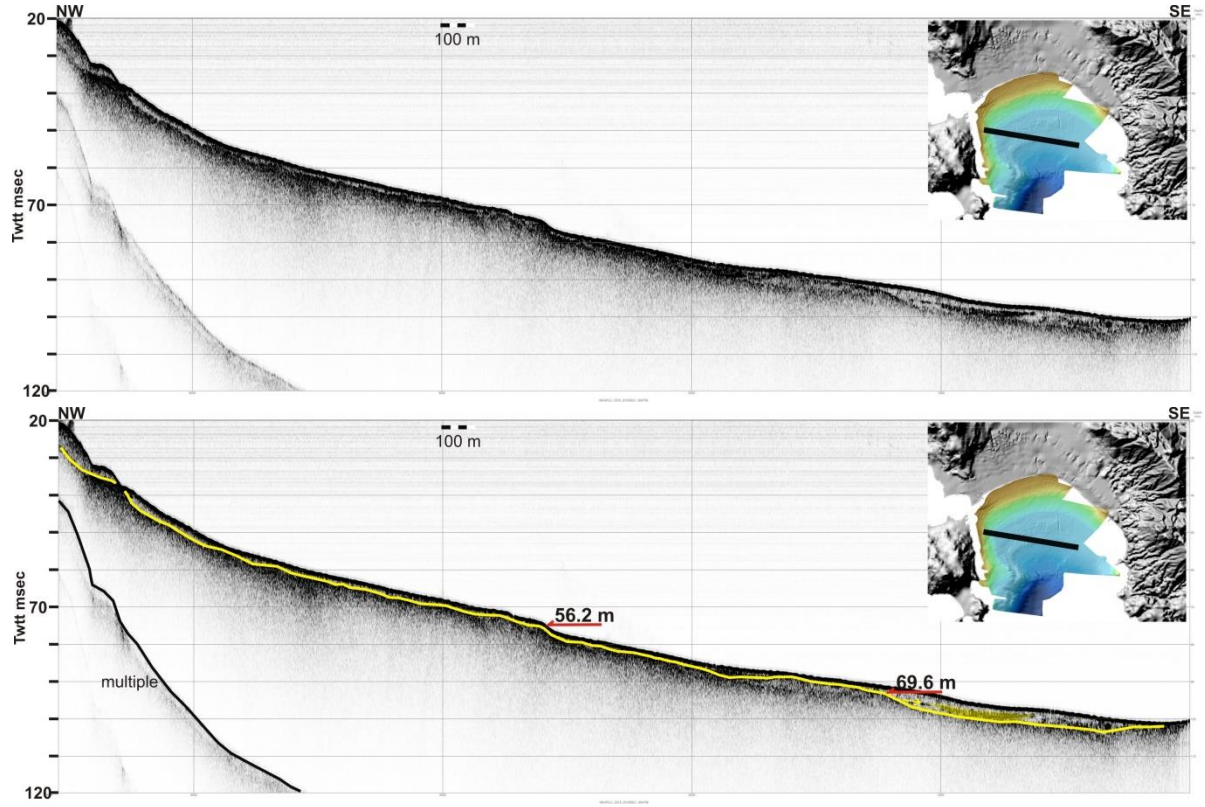

Fig.3.23: Profile 6, Chirp. Red arrows indicate terraces.

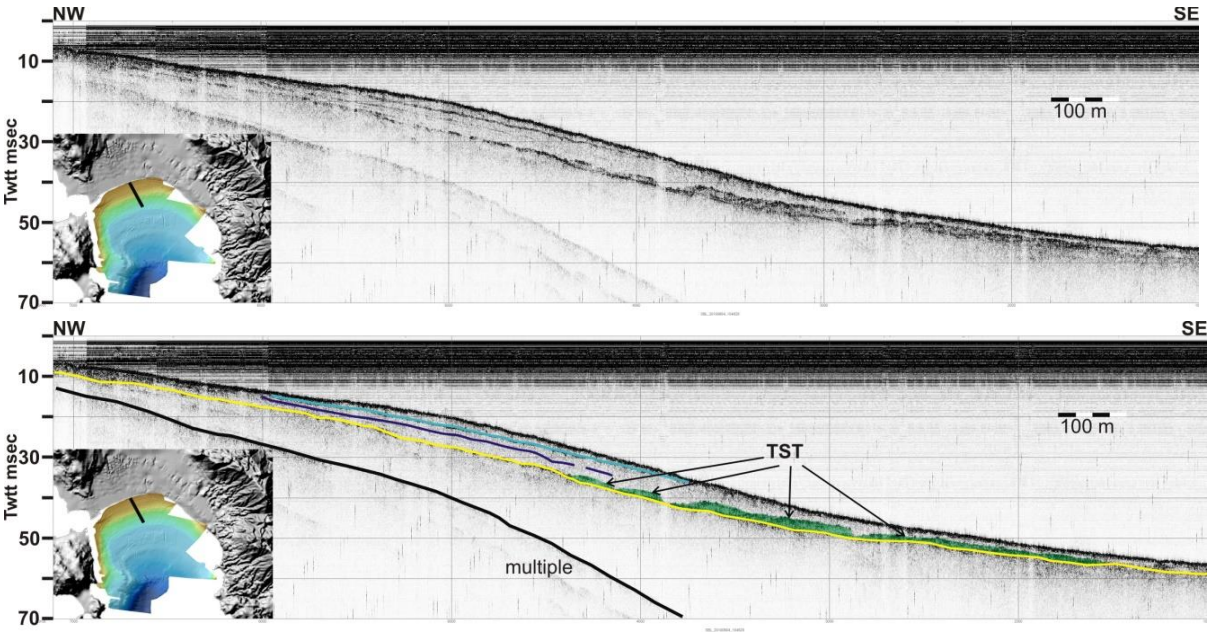

Fig.3.24: Profile 68, Pinger (3.5 kHz). TST=Transgressive System Track.

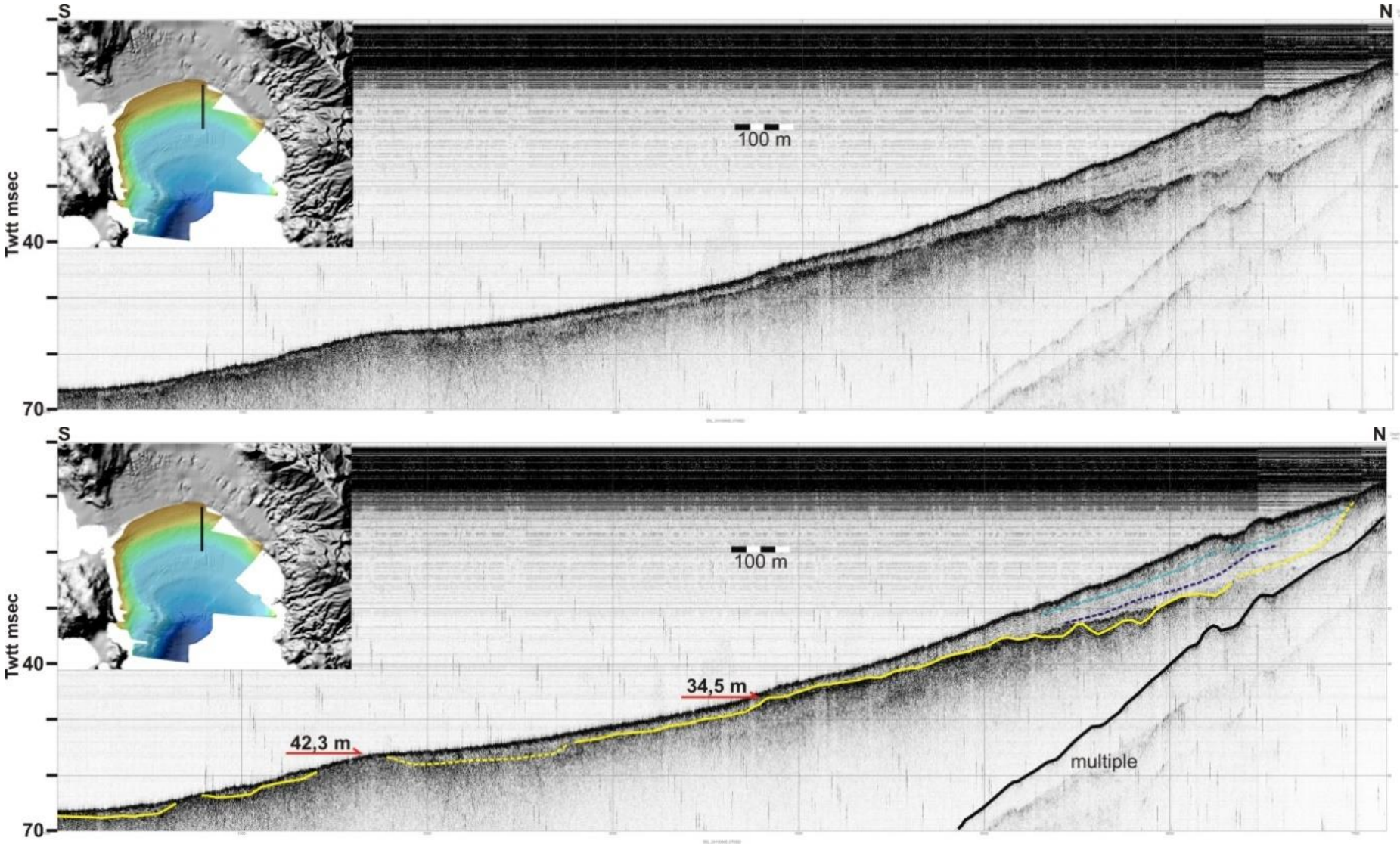

Fig.3.25: Profile 75, Pinger (3.5 kHz).Red arrows indicate terraces.

Profile 75 (Fig.3.25) runs N-S and provides an along-dip cross section below the seafloor of the shallow eastern part of the bay. In the uppermost part, a transparent layer is separated from the acoustic basement by a morphologically irregular, continuous and of high amplitude reflector colored in yellow. The latter reflector is a landscape surface and represents the base of the Holocene. Above, inside the transparent body, two reflectors of lower amplitude, colored in purple and light blue, both locally observed, highlight the sedimentary structure of the present littoral wedge. Holocene sediments reach up to 9.7 ms thickness at the central up to the northern part of the profile, whereas at the rest of the profile they are about 2 ms thick. Two terraces occur at 46.1 ms (34.5 m) and at 56.5 ms (42.3 m) depth.

Profile 81 (Fig.3.26) displays similar seismic stratigraphy as profiles 75 (Fig.3.25) and 68 (Fig.3.24). Inside the transparent uppermost layer, a chaotic package marked out by a strong irregular reflection of step-like morphology is locally observed at the central part of the profile (colored in green). The package possibly represents transgression deposits (TST). This profile is parallel to the profile 75 (Fig.3.25).

Profile 83 (Fig.3.27) is perpendicular to the northern coast of the bay, parallel to profile 68 (Fig.3.24). It displays similar seismic stratigraphy as the aforementioned profiles 68, 75 and 81. A faint discontinuous reflection of low amplitude (marked out by a pink line) is parallel to the landscape surface in a lower stratigraphic position. Furthermore, inside the uppermost transparent layer, another discontinuous but of high amplitude reflector (colored in green) indicates local increase of Holocene sedimentation, which reaches up to 6-7 ms. At the SE part of the profile Holocene sediments are 2-3 ms thick.

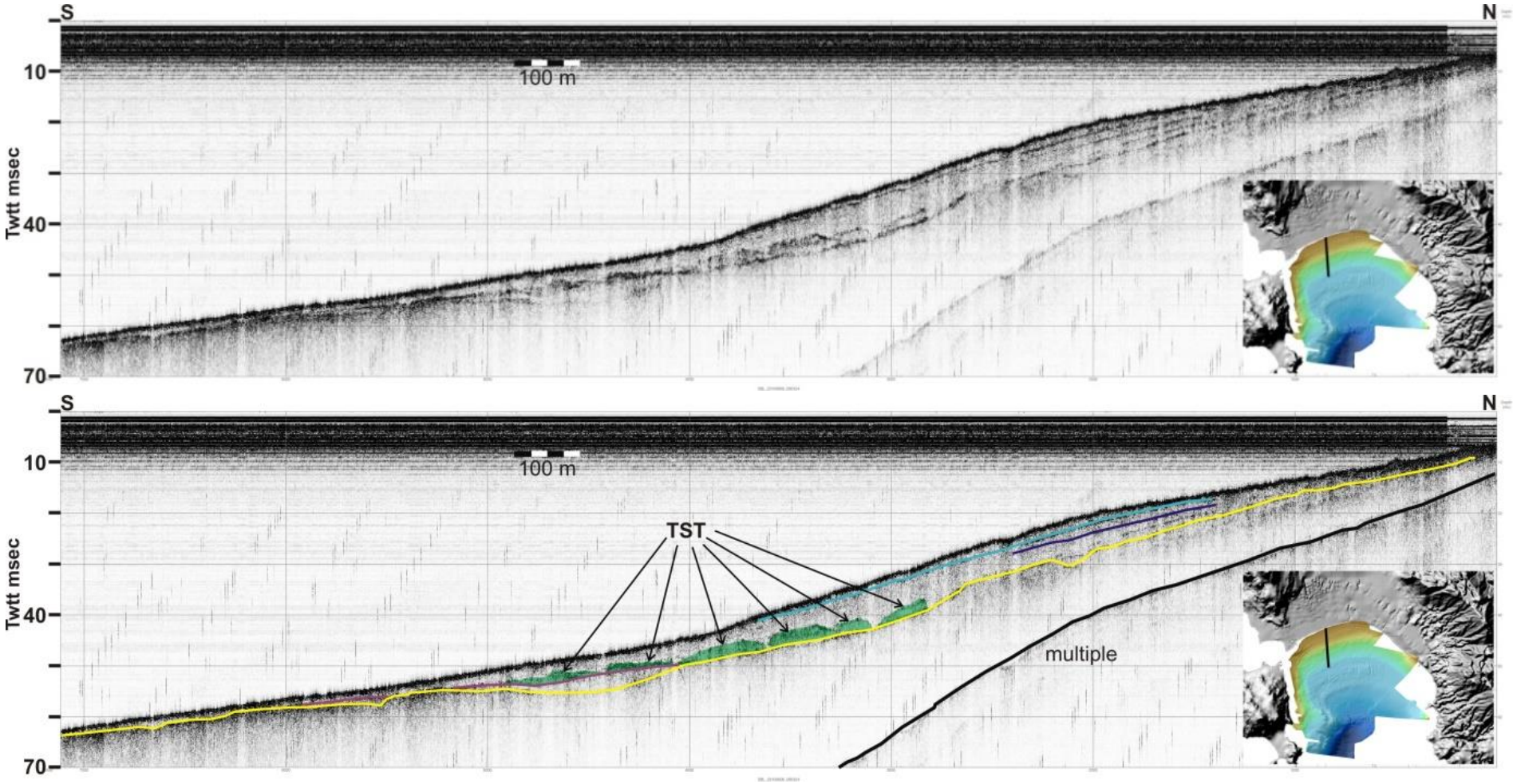

Fig.3.26: Profile 81, Pinger (3.5 kHz).

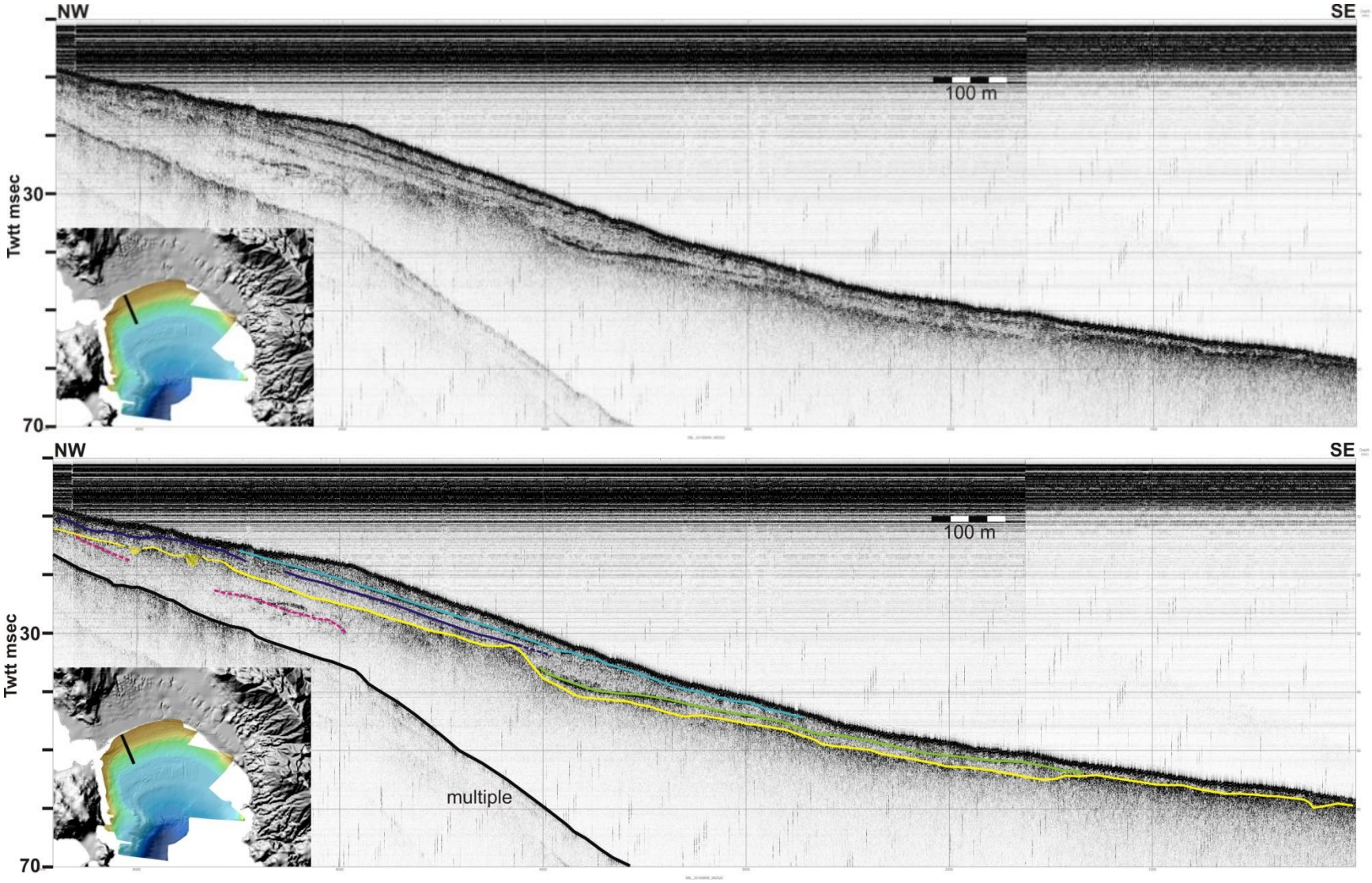

Fig.3.27: Profile 83, Pinger (3.5 kHz).

3.2.2. The western and southern parts of Vatika Bay (Chirp & 3.5 kHz profiles)

Profile 25 (Fig.3.28) is NW-SE directed and runs at a high angle in respect to the mean direction of slope off the eastern coast of Elaphonisos. After a gently dipping upper slope, the seafloor displays steeper, staircase-like morphology. The uppermost, thin, seismically transparent layer occurs locally and covers the strongly reflecting top of the acoustic basement. The latter is marked with a yellow line and displays irregular relief. The transparent layer is interpreted as the marine sediments deposited after the post-LGM sea-level rise. Consequently, the top of the acoustic basement may represent the subaerially exposed landscape during the last low sea-level stage. The thickness of the Holocene deposits is very limited. It reaches about 5 ms on the shallow seafloor at the northwestern end of the profile. The Holocene thickness does not exceed 1-2 ms along most of the slope. Thicker deposits (6-8 ms) are observed only in the central part of the profile, on both sides of the mount-like structure of the basement.

The staircase morphology of the seafloor derives from the presence of multiple terraces developed on the acoustic basement. The most prominent terraces occur at the depths of 57.1 ms (42.8 m), 83 ms (62.2 m), 93.4 ms (70 m), 109.5 ms (82.1 m), 126 ms (94.5 m) and 138 ms (103.5 m) depth and are indicated with red arrows on figure 3.28.

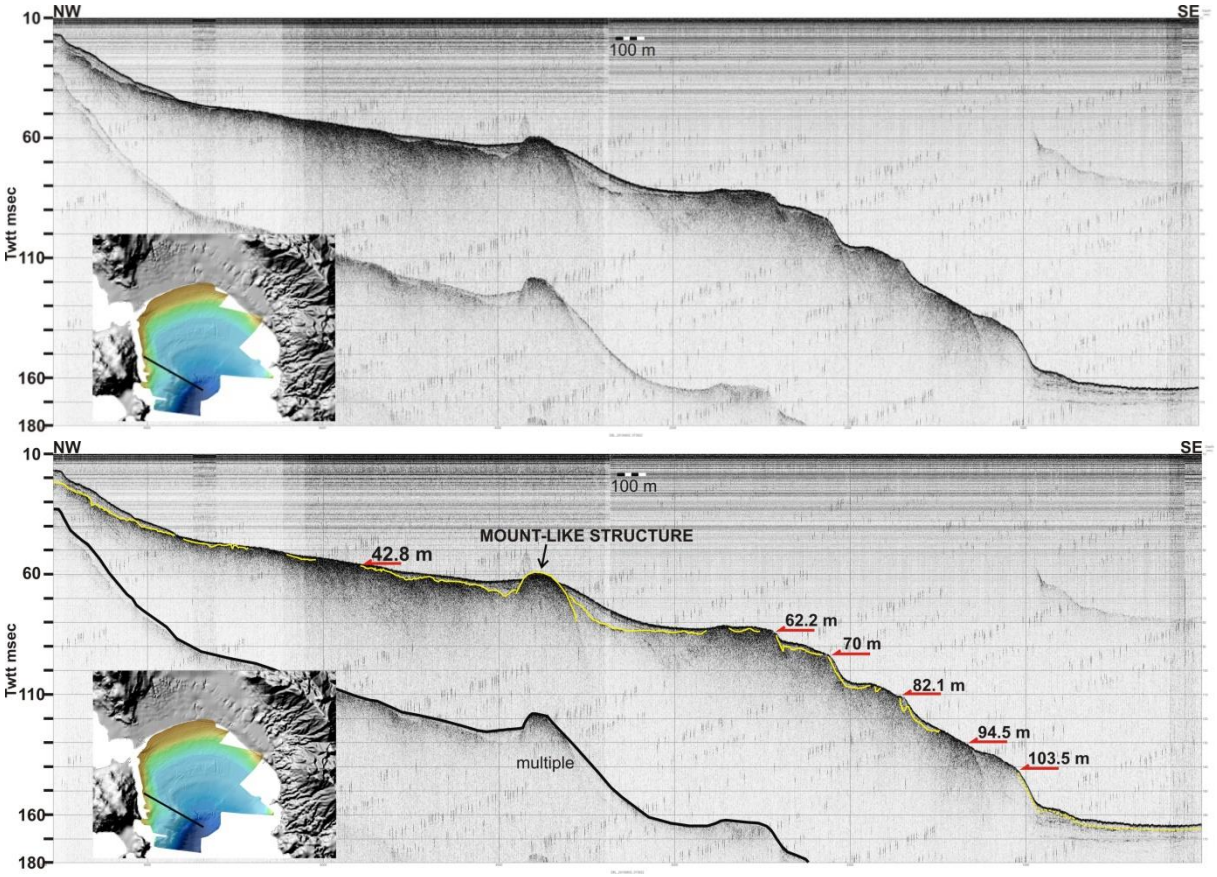

Fig.3.28: Profile 25, Pinger (3.5 kHz). Red arrows indicate terraces.

Profile 45 (Fig.3.29) is trending W-E and runs downslope off the western slope of Vatika Bay, which is characterized by high relief (chapter 3.1). After a steep slope at the western part of the profile, the seafloor displays staircase-like morphology up to the central part of the profile. In the uppermost part, a thin, seismically transparent layer occurs. It is separated from the acoustic basement with a continuous reflector, characterized by strong reflectivity at

the western part up to the center of the profile. At the eastern part the latter reflector is hummocky of medium amplitude, possibly due to coarse grain deposits. It is marked with a yellow line and displays irregular relief. The transparent layer is interpreted as the marine sediments deposited after the post-LGM sea-level rise. Consequently, the top of the acoustic basement may represent the sub-aerially exposed landscape during the last low sea-level stage. Holocene sedimentation does not exceed 2 ms thickness, except from the western and the central part of the profile, where it reaches up to 7 ms. The staircase-like morphology derives from the presence of multiple terraces developed on the acoustic basement. The most prominent occur at 56 ms (42 m), 84 ms (63 m) and 94 ms (70.5 m) depth. At about 40-50 ms (30-38 m) occur two mount-like structures (Fig. 3.29) of significant dimensions. They are about 100 m thick and 3 m long.

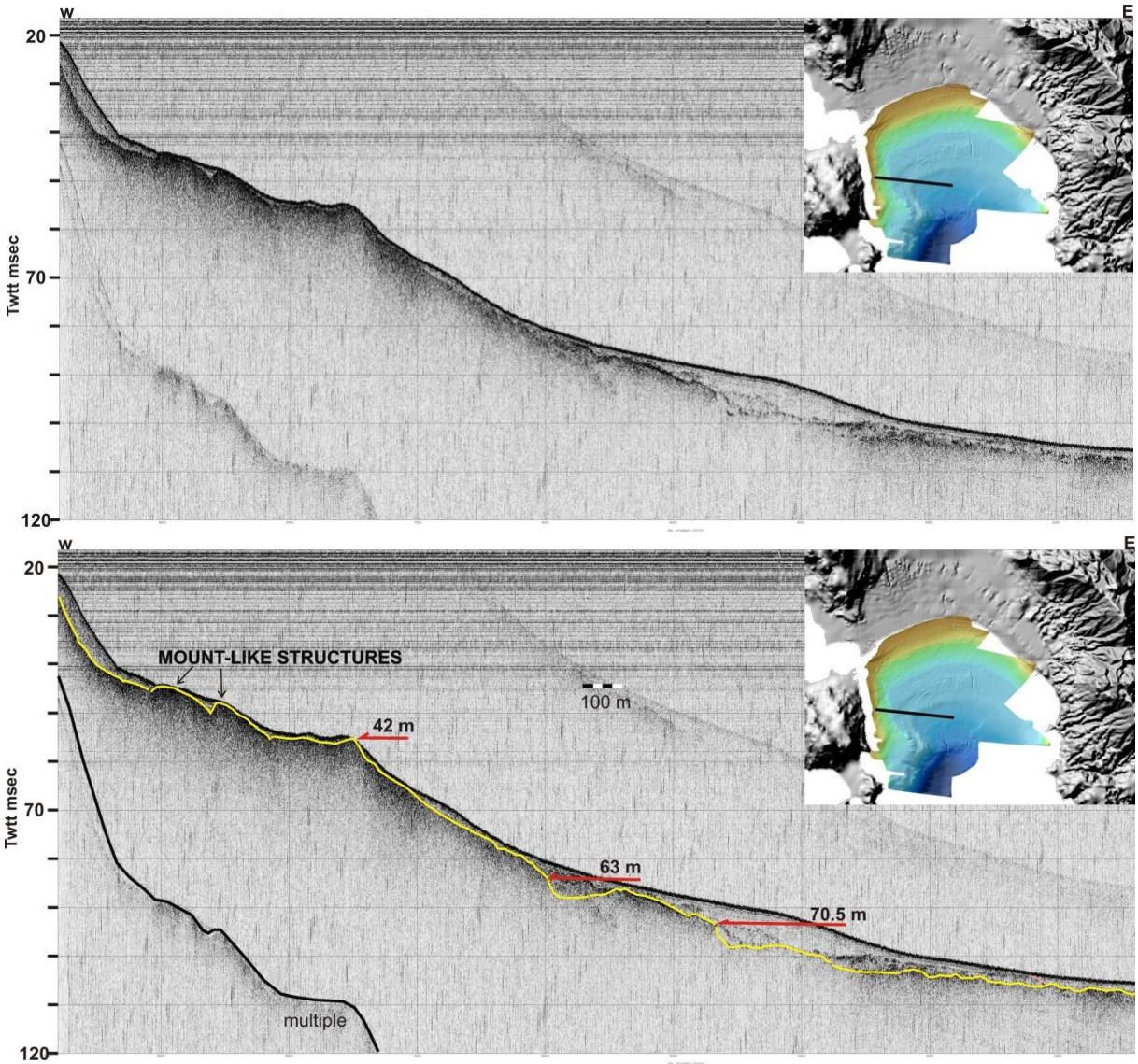

Fig.3.29: Profile 45, Pinger (3.5 kHz). Red arrows indicate terraces.

Profile 60 (Fig.3.30) is E-W directed and runs almost perpendicular in respect to the mean direction of slope off the eastern coast of Elaphonisos island. After a gently dipping upper slope, the seafloor displays steeper, staircase-like morphology. The uppermost, thin, seismically transparent layer occurs locally and covers the strongly reflecting top of the acoustic basement. The latter is marked with a yellow line and displays irregular relief. The

transparent layer is interpreted as the marine sediments deposited after the post-LGM sea-level rise. Consequently, the strongly reflecting top of the acoustic basement may represent the sub-aerially exposed landscape during the last low sea-level stage. Holocene sedimentation is very limited. It is about 1-2 ms thick along the profile. The staircase-like morphology derives from the presence of multiple terraces developed on the acoustic basement across the eastern slope of Pavlopetri. The most prominent occur at 76 ms (57 m), at 90.5 (67.8 m), at 122.4 ms (91.8 m) and at 138 ms (103.6 m) depth.

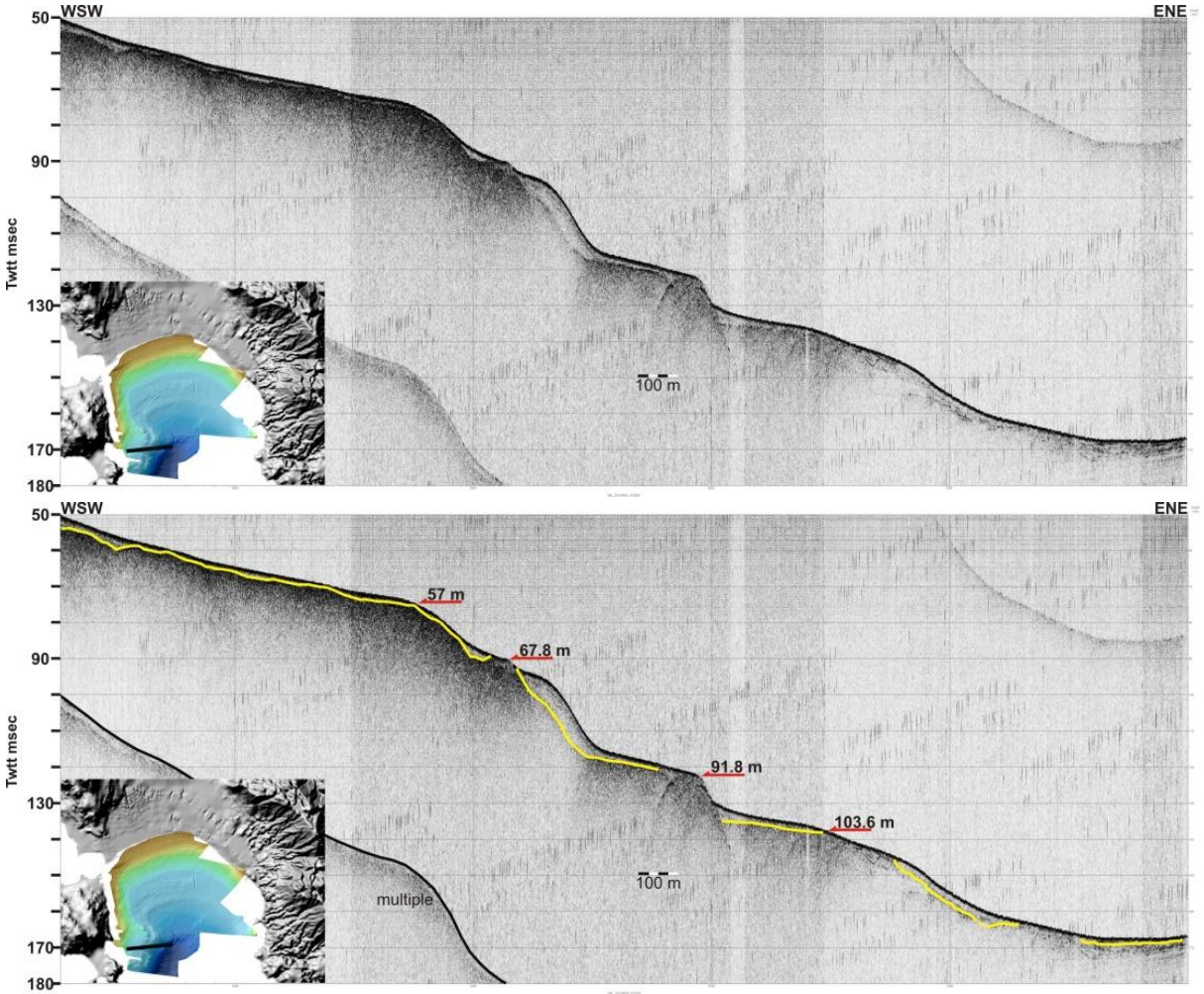

Fig.3.30: Profile 60, Pinger (3.5 kHz). Red arrows indicate terraces.

Profile 22 (Fig.3.31) runs perpendicular in respect to the mean direction of slope off the western slope of Vatika bay. After a gently dipping upper slope, the seafloor displays steeper, staircase-like morphology. In the uppermost part, a thin, seismically transparent layer occurs. It is separated from the acoustic basement with a continuous reflector, characterized by strong reflectivity at the western part of the profile. The latter reflector is marked with a yellow line and displays irregular relief. At the eastern part it is of medium amplitude and it is truncated at the seafloor. The transparent layer is interpreted as the marine sediments deposited after the post-LGM sea-level rise. Consequently, the strongly reflecting top of the acoustic basement may represent the sub-aerially exposed landscape during the last low sea-level stage. At the central part of the profile a mount-like structure of significant dimensions occur. It is about 66 m thick and 12 m long. Next to it, across the slope, a discontinuous reflector of medium amplitude marked with a pink line, possibly represents sediment deposition within Holocene. At the eastern part, erosion of the seafloor

is indicated by three faint reflectors truncated to it. The staircase-like morphology derives from the presence of multiple terraces developed on the acoustic basement. The most prominent occur at 41.5 ms (31.1 m) and at 57.3 ms (42.9 m) depth.

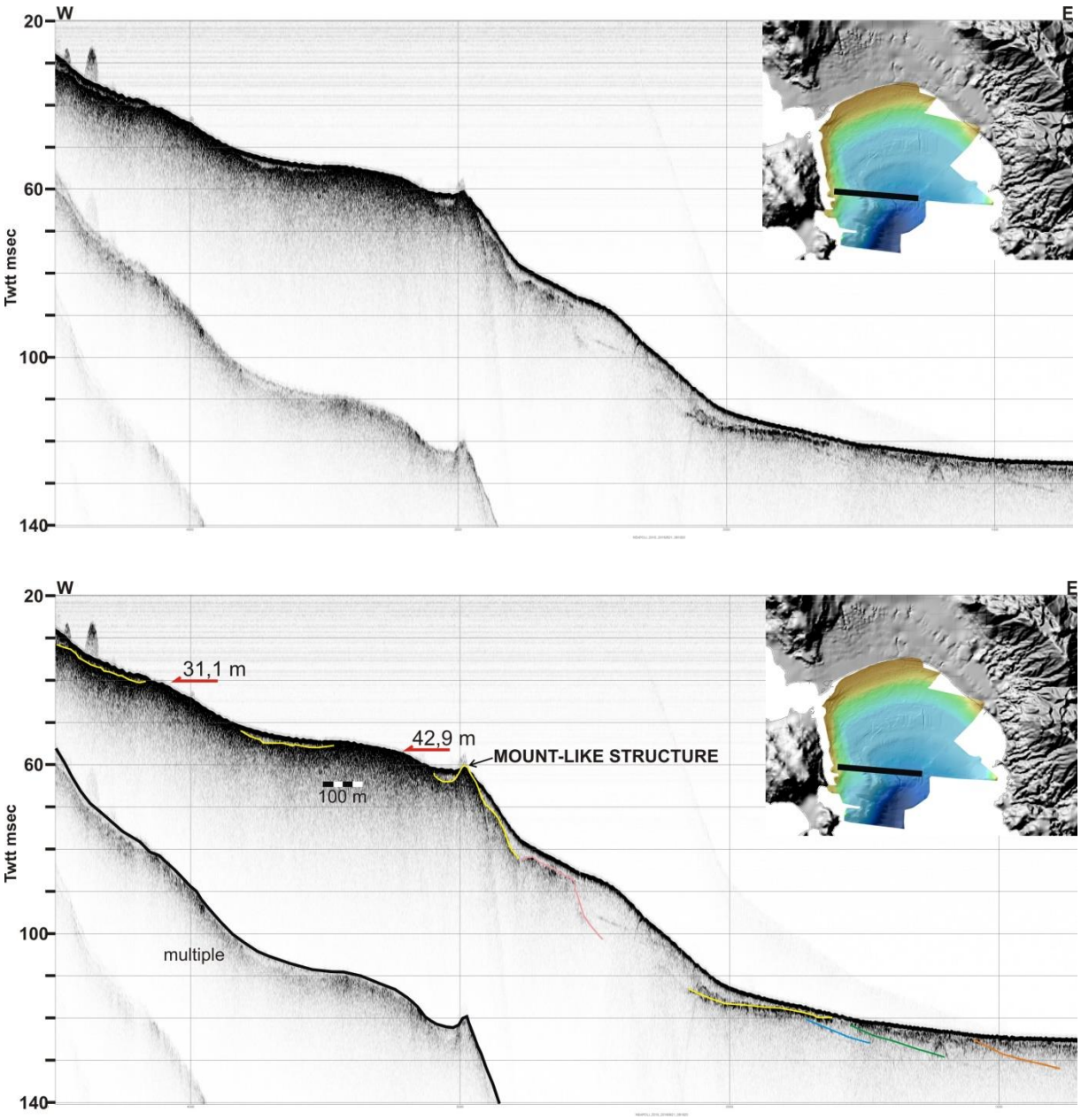

Fig.3.31: Profile 22, Chirp.

Profile 24 (Fig.3.32) runs perpendicular in respect to the mean direction of slope off the western slope of Vatika bay and displays similar seismic stratigraphy and morphology, as the previous profiles. The uppermost, thin, seismically transparent layer occurs locally and is separated from the acoustic basement with a morphologically irregular reflector of high amplitude. The latter, marked with a yellow line, represents the base of the Holocene. Sedimentation within Holocene is very limited across the profile. It is 1-2 ms up to 7 ms thick after the staircase-like morphology. At the eastern part of the profile, three reflectors of medium amplitude (colored in orange, blue and pink) are truncated to the seafloor and to the landscape surface. The staircase-like morphology indicates the presence of multiple terraces. Two prominent ones occur at 58.8 ms (44 m) and 85.4 ms (64 m) depth.

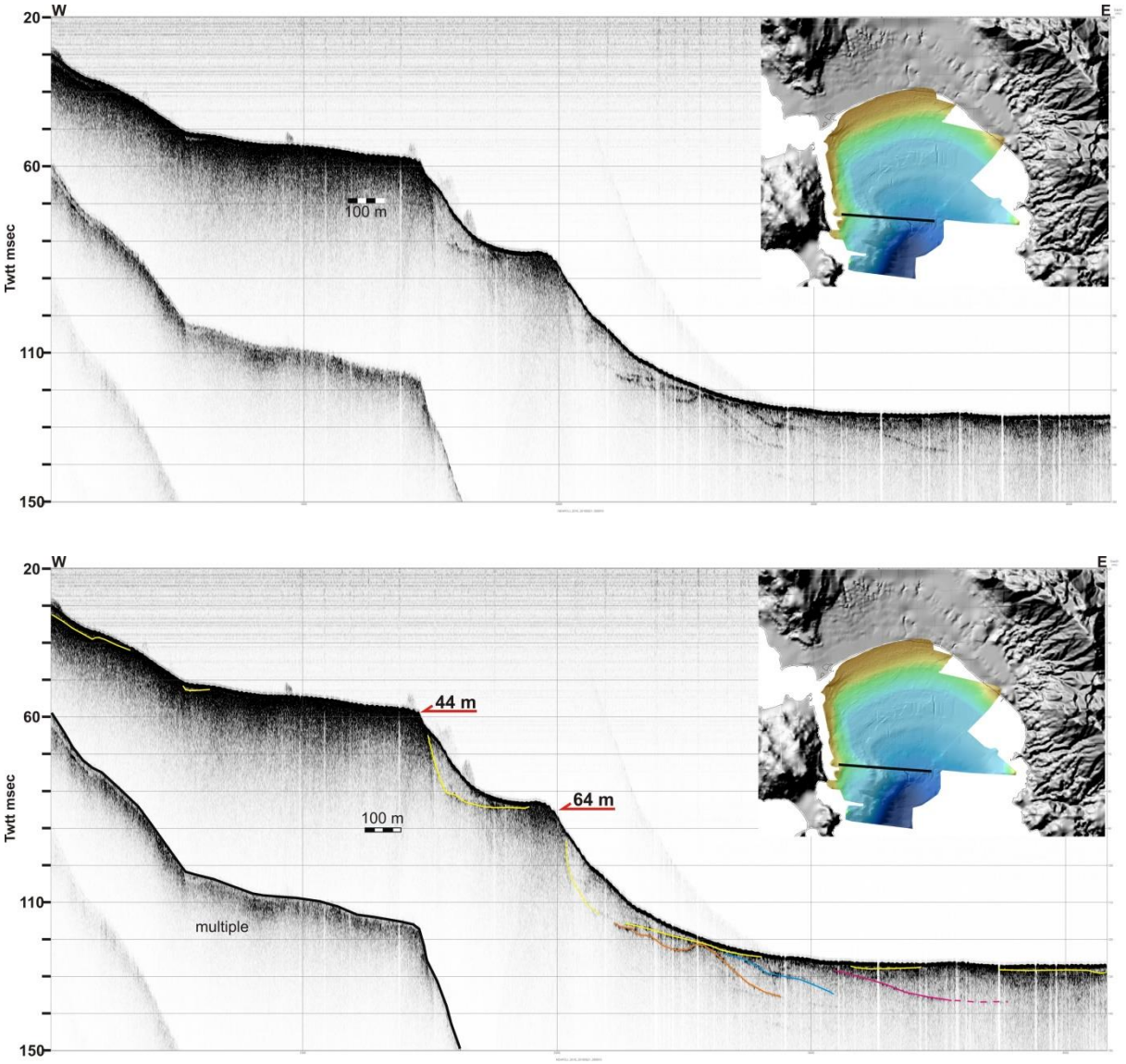

Fig.3.32: Profile 24, Chirp. Red arrows indicate terraces.

Profile 26 (Fig.3.33) runs perpendicular in respect to the mean direction of slope off the western slope of Vatika bay and displays similar seismic stratigraphy and morphology, as the previous profiles. In the uppermost part, a thin, seismically transparent layer occurs and covers the strongly reflecting top of the acoustic basement. The latter is marked with a yellow line and displays irregular relief. The transparent layer is interpreted as the marine sediments deposited after the post-LGM sea-level rise. Consequently, the top of the acoustic basement may represent the sub-aerially exposed landscape during the last low sea-level stage. The thickness of the Holocene deposits is very limited. It is about 1-2 ms of thickness across the profile. Along the slope at the central part of the profile, multiple mount-like structures occur. The staircase-like morphology derives from the presence of multiple terraces developed on the acoustic basement. Two prominent terraces occur at 62 ms (46.5 m) and 83 ms (62.2 m).

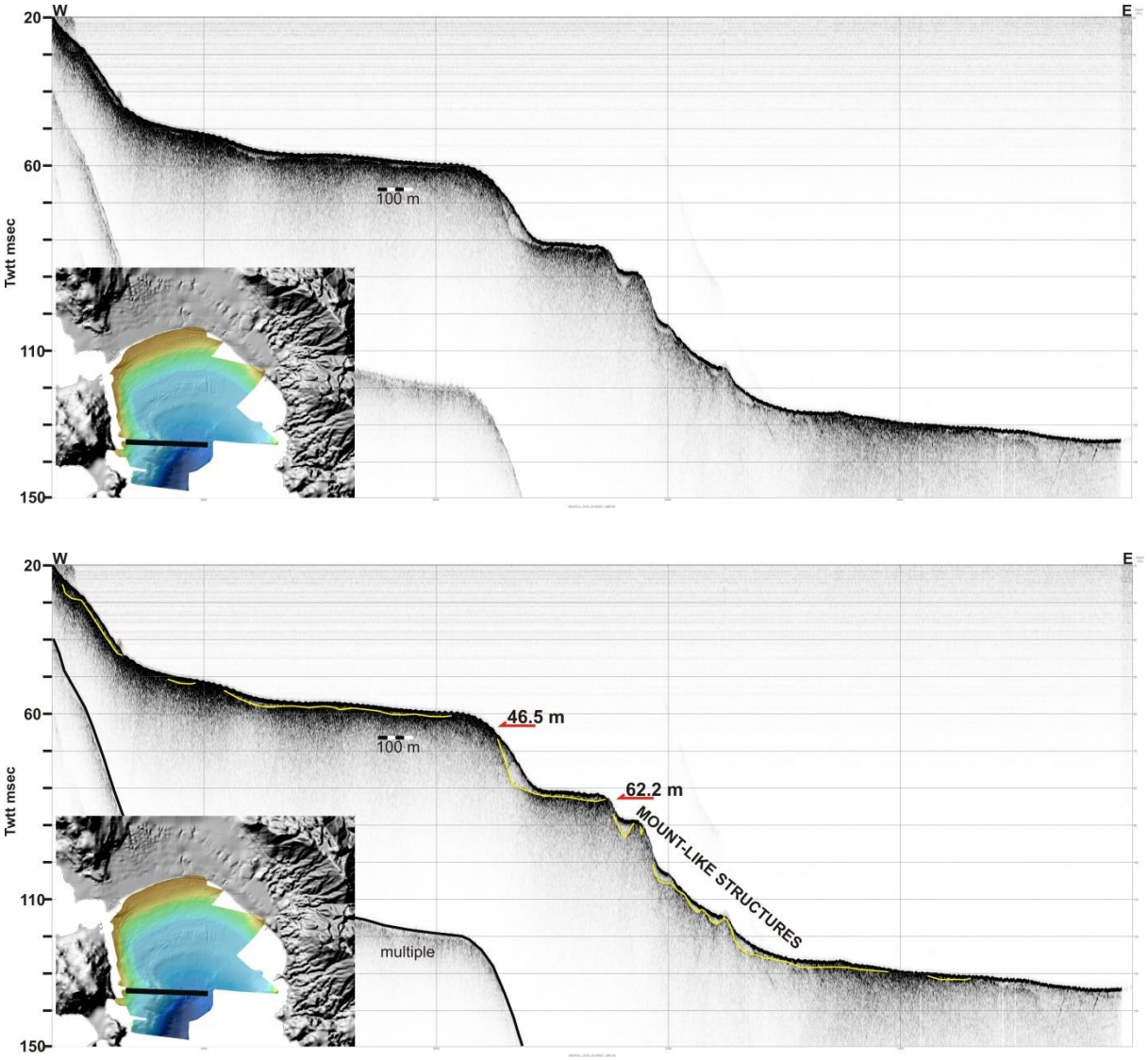

Fig.3.33: Profile 26, Chirp. Red arrows indicate terraces.

Profile 28 (Fig.3.34) runs perpendicular in respect to the mean direction of slope off the eastern slope of Elaphonisos island and displays similar seismic stratigraphy, as the previous profiles. In the uppermost part, a thin, seismically transparent layer occurs and covers the strongly reflecting top of the acoustic basement. The latter is marked with a yellow line and displays irregular relief. The transparent layer is interpreted as the marine sediments deposited after the post-LGM sea-level rise. Consequently, the top of the acoustic basement may represent the sub-aerially exposed landscape during the last low sea-level stage. The thickness of the Holocene deposits is very limited. It reaches about 1-2 ms of thickness across the profile. The staircase-like morphology derives from the presence of multiple terraces developed on the acoustic basement. The most prominent ones occur at 63.3 ms (47.5 m), at 81.7 ms (61.2 m), at 106 ms (79.5 m) and at 129 ms (96.7 m) depth.

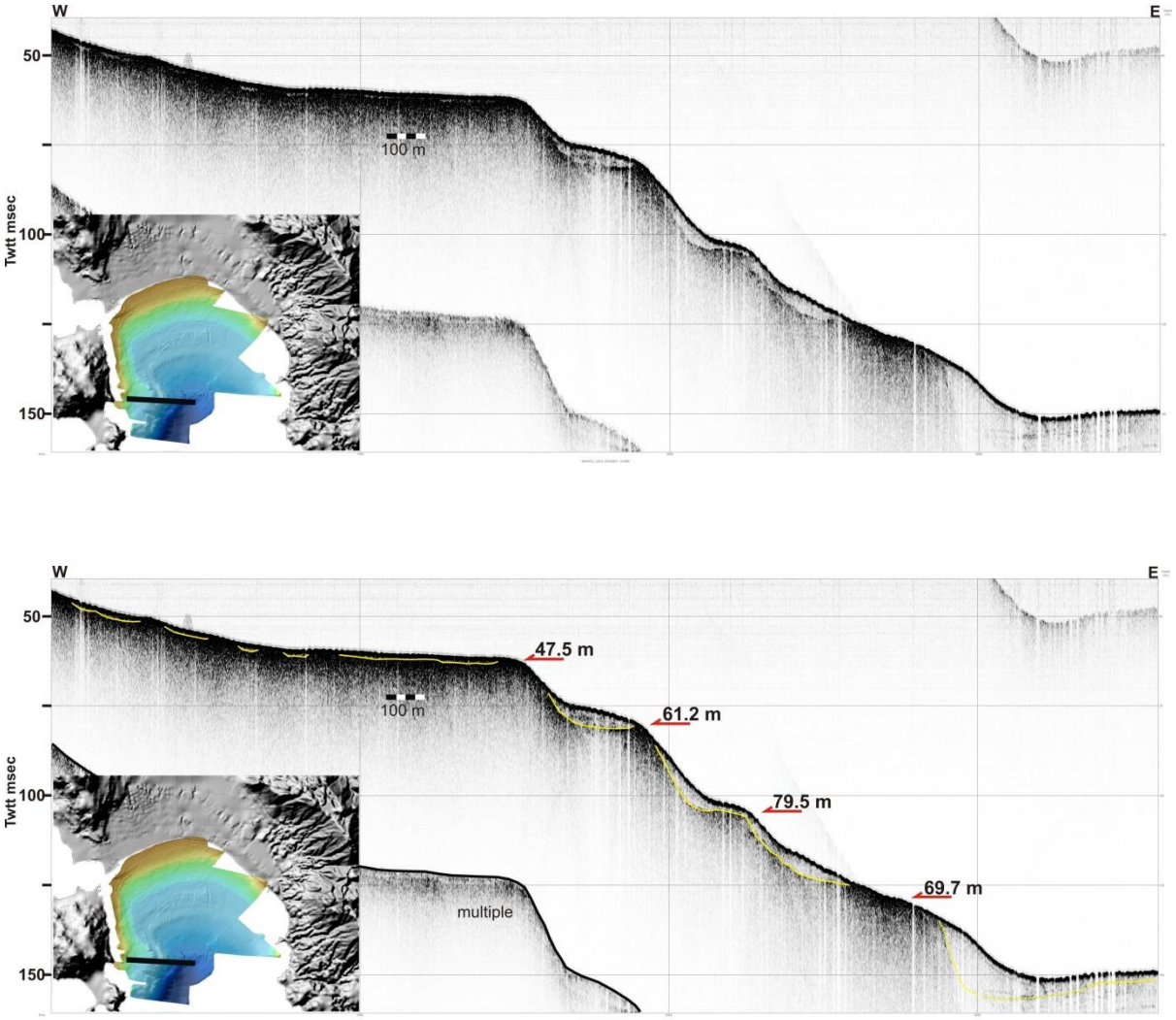

Fig.3.34: Profile 28, Chirp. Red arrows indicate terraces.

Profile 30 (Fig.3.35) runs perpendicular in respect to the mean direction of slope off the eastern slope of Elaphonisos island and displays similar seismic stratigraphy, as the abovementioned profiles. In the uppermost part, a thin, seismically transparent layer occurs and covers the strongly reflecting top of the acoustic basement. The latter is marked with a yellow line and displays irregular relief. The transparent layer is interpreted as the marine sediments deposited after the post-LGM sea-level rise. Consequently, the top of the acoustic basement may represent the sub-aerially exposed landscape during the last low sea-level stage. Holocene sedimentation thickness does not exceed 1-2 ms along most of the slope. Thicker deposits (up to 6 ms) are observed only in the central part of the profile, across the slope. The staircase-like morphology derives from the presence of multiple terraces, developed on the acoustic basement. The most prominent ones occur at 66.9 ms (50.1 m), at 81.5 ms (61.1 m), at 110 ms (82.5 m) and at 131 ms (98.2 m) depth.

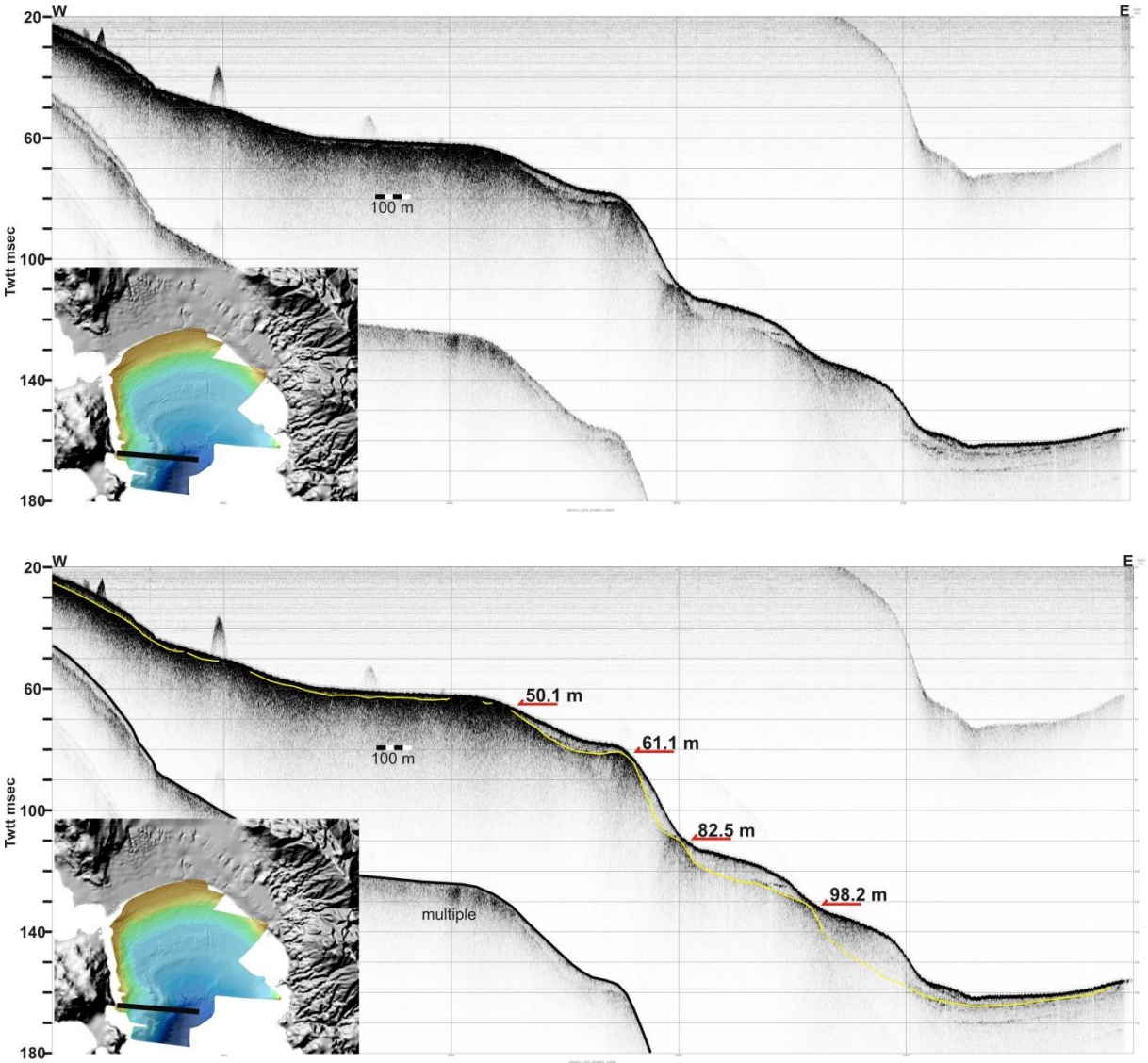

Fig.3.35: Profile 30, Chirp. Red arrows indicate terraces.

Profile 34 (Fig.3.36) runs perpendicular in respect to the mean direction of slope off the eastern slope of Elaphonisos island and displays similar seismic stratigraphy, as the abovementioned profiles. In the uppermost part, a thin, seismically transparent layer occurs and covers the strongly reflecting top of the acoustic basement. The latter is marked with a yellow line and displays irregular relief. The transparent layer is interpreted as the marine sediments deposited after the post-LGM sea-level rise. Consequently, the top of the acoustic basement may represent the sub-aerially exposed landscape during the last low sea-level stage. Holocene sedimentation thickness does not exceed 1-2 ms along most of the slope. Thicker deposits (up to 6 ms) are observed only in the central part of the profile, across the slope. The staircase-like morphology derives from the presence of multiple terraces developed on the acoustic basement. The most prominent ones occur at 75.7 ms (56.7 m), at 97.3 ms (72.9 m), at 122.4 ms (91.8 m) and at 137.7 ms (103.2 m) depth.

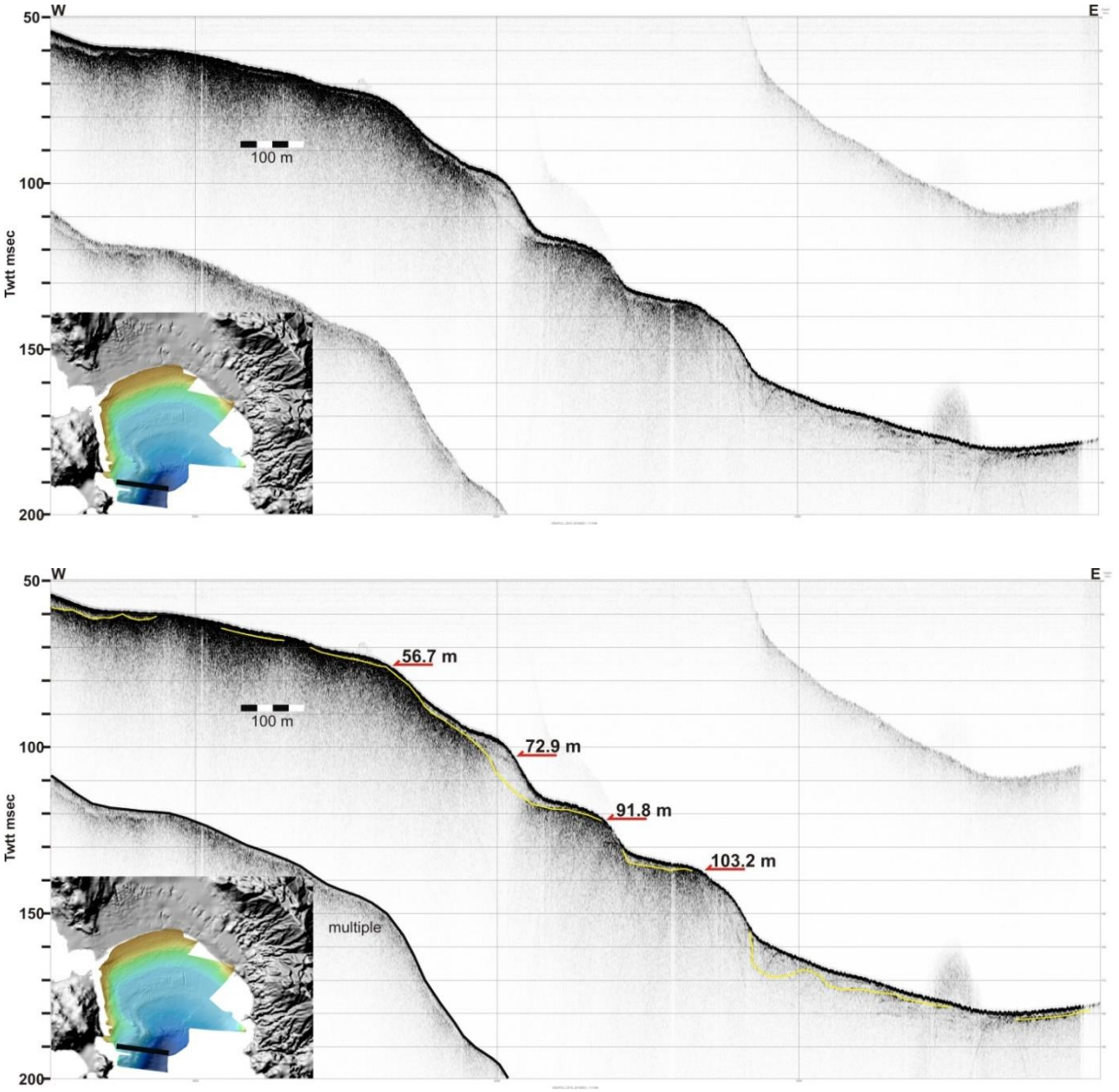

Fig.3.36: Profile 34, Chirp. Red arrows indicate terraces.

Profile 36 (Fig.3.37) runs perpendicular in respect to the mean direction of slope off the eastern slope of Elaphonisos island and displays similar seismic stratigraphy, as the abovementioned profiles. In the uppermost part, a thin, seismically transparent layer occurs and covers the strongly reflecting top of the acoustic basement. The latter is marked with a yellow line and displays irregular relief. The transparent layer is interpreted as the marine sediments deposited after the post-LGM sea-level rise. Consequently, the top of the acoustic basement may represent the sub-aerially exposed landscape during the last low sea-level stage. Holocene sedimentation thickness does not exceed 1-2 ms along most of the slope. Thicker deposits (up to 6 ms) are observed only in the central part of the profile, across the slope. The staircase-like morphology derives from the presence of multiple terraces developed on the acoustic basement. The most prominent ones occur at 75 ms (56.2 m), at 104.6 ms (78.4 m) and at 140 ms (105 m) depth.

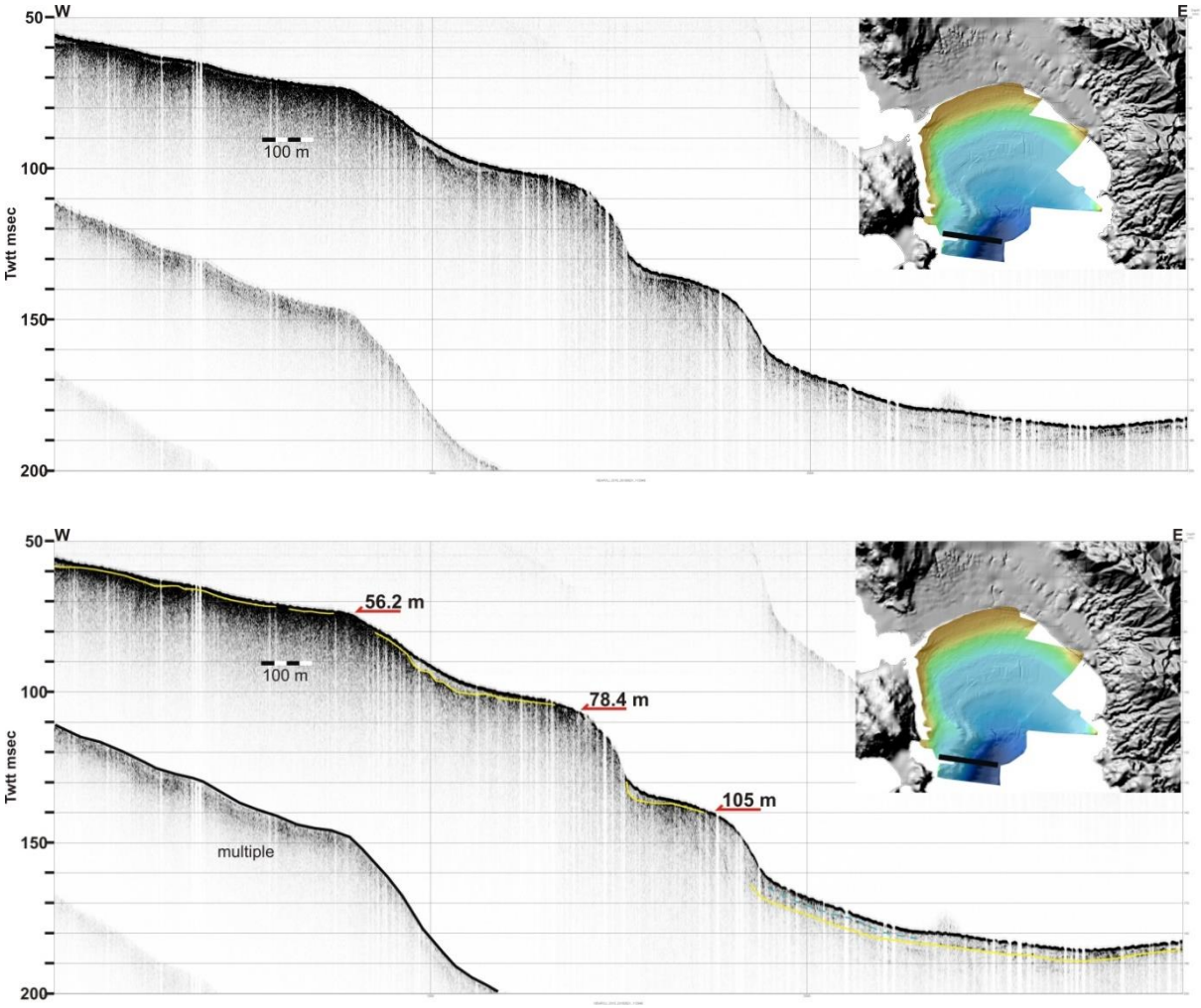

Fig.3.37: Profile 36, Chirp.

Profile 38 (Fig.3.38) runs perpendicular in respect to the mean direction of slope off the eastern slope of Elaphonisos island and displays similar seismic stratigraphy, as the abovementioned profiles. In the uppermost part, a thin, seismically transparent layer occurs and covers the strongly reflecting top of the acoustic basement. The latter is marked with a yellow line and displays irregular relief. The transparent layer is interpreted as the marine sediments deposited after the post-LGM sea-level rise. Consequently, the top of the acoustic basement may represent the sub-aerially exposed landscape during the last low sea-level stage. Holocene sedimentation thickness does not exceed 1-2 ms along most of the slope. Thicker deposits (up to 6 ms) are observed only in the central part of the profile, across the slope. The staircase-like morphology derives from the presence of multiple terraces developed on the acoustic basement. The most prominent ones occur at 69.6 ms (52.2 m), at 78.7 ms (59 m), at 102.3 ms (76.7 m), at 135.2 ms (101.4 m) and at 143.4 ms (107.5 m) depth.

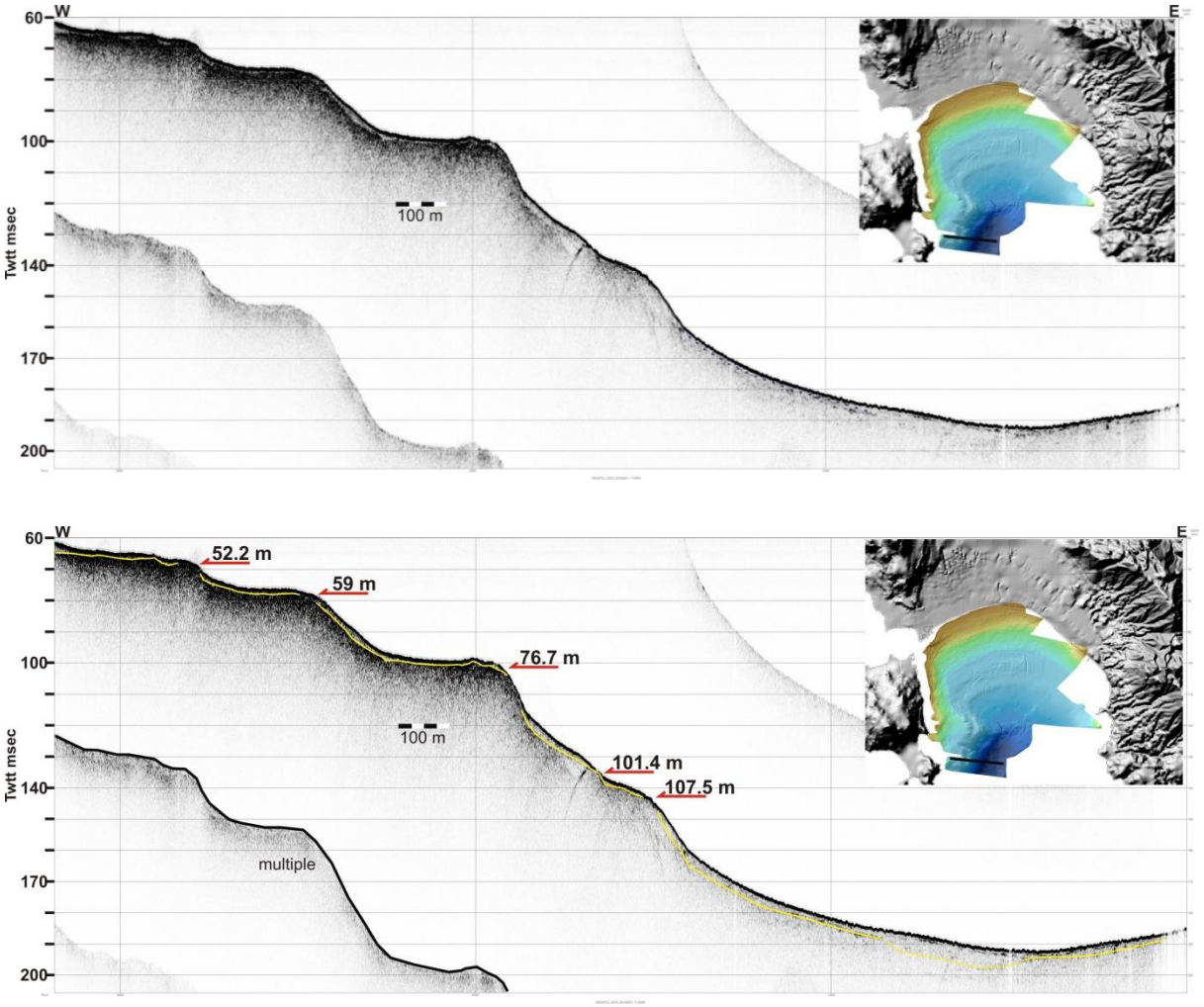

Fig.3.38: Profile 38, Chirp.

The chirp profile 43 (Fig.3.39) provides a complete cross section of the Vatika Bay in SW-NE direction, from the southern edge of Elaphonisos Island to the town of Neapolis. It records the valley-like morphology of the Bay and highlights the morphological differences between the western and the eastern slopes. The western slope is steep, compared to the eastern one, and displays staircase morphology, with evident terraces as described on the previous profiles. The seismic stratigraphy is rather simple: locally occurring, thin, transparent sediments have been deposited on the flat terraces of both slopes. They are underlain by the strongly reflective top of the acoustic basement of the profile.

The morphological terraces have been developed on the acoustic basement and display erosional character. It is worth noting that the terraces on the two slopes occur at different depths. Thus, the terraces on the western slope occur at the following depths: 66 ms (49.5 m), 75.8 ms (56.8 m), 78 ms (58.5 m), 104.2 ms (78.1 m), 123 ms (92.2 m), 138.3 ms (103.7 m) and 148 ms (111 m) depth. On the eastern slope the observed terraces occur at the following depths: 152 ms (114 m), 139.4 ms (104.5 m), 127.5 ms (95.8 m), 119 ms (89.2 m) and 109 ms (81.4 m). The different depths of the terraces on the two slopes are probably the result of vertical tectonic movements occurring at different rates on the western and eastern slopes.

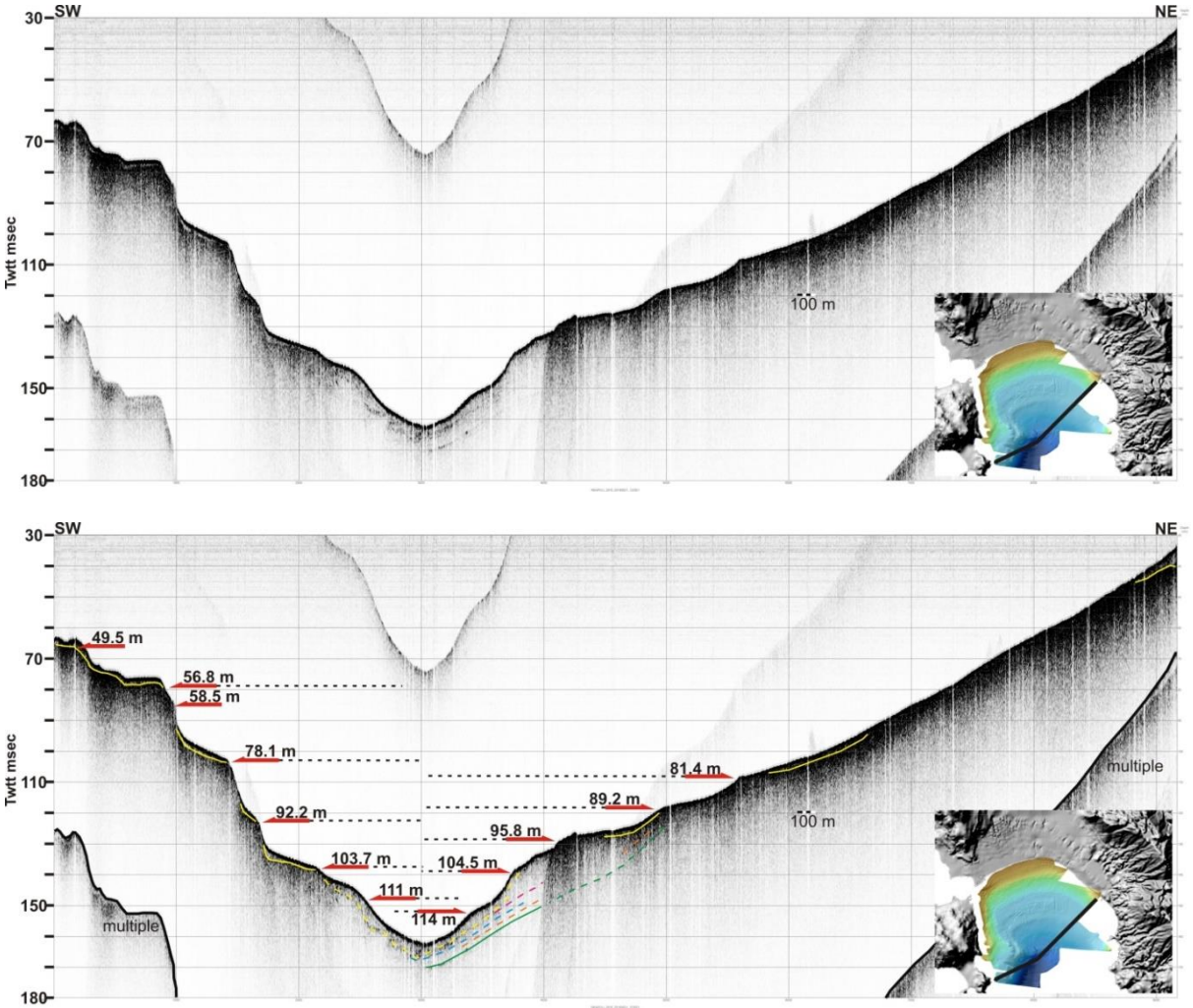

Fig.3.39: Profile 43, Chirp. Red arrows indicate terraces.

Profile 5 (Fig.3.40) provides a N-S view of the central, deeper part of Vatika Bay. A thin, seismically transparent layer is separated from the acoustic basement with a reflector of high amplitude and strong reflectivity. The latter reflector, marked with a yellow line, displays irregular relief. The transparent layer is interpreted as the marine sediments deposited after the post-LGM sea-level rise. Consequently, the top of the acoustic basement may represent the sub-aerially exposed landscape during the last low sea-level stage. Holocene sedimentation is very limited, and reaches up to 1-2 ms across the profile. The landscape surface shapes an unconformity with an older structure (reflectors marked with pink, blue, orange, green and purple). As a main feature in the present profile, there is a depositional terrace at its central part, at 126 ms (94.5 m) and 136.5 ms (102.3 m) depth. It separates the shallower part, where the morphologically irregular reflector indicates the presence of the acoustic basement, from the deeper part of the profile, where sediment deposition occurs.

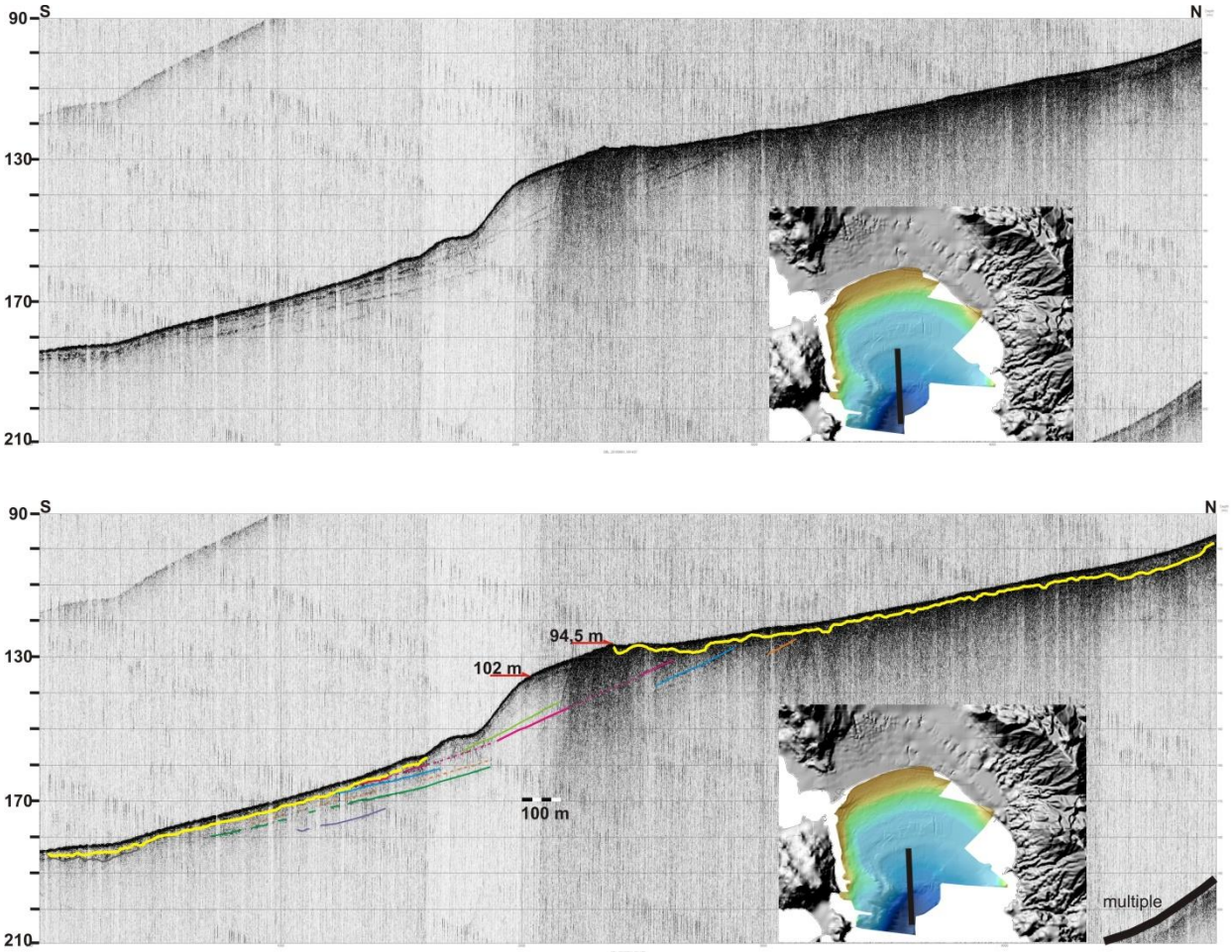

Fig.3.40: Profile 5, Pinger (3.5 kHz). Red arrows indicate terraces.

Profile 61 (Fig.3.41) is N-S directed and runs perpendicular in respect with the northern coast of the bay. A thin, seismically transparent layer occurs locally and covers the strongly reflecting top of the acoustic basement. The latter is marked with a yellow line and displays irregular relief. The transparent layer is interpreted as the marine sediments deposited after the post-LGM sea-level rise. Consequently, the top of the acoustic basement may represent the sub-aerially exposed landscape during the last low sea-level stage. Holocene sedimentation is very limited. It is about 2 ms thick and reaches up to 7 ms at the shallower part of the profile. The landscape reflector, which represents the base of the Holocene, truncates the reflectors marked with purple, orange, blue, pink and green lines. At the northern shallow part of the profile, a reflector of medium to low amplitude marked with a light blue line, highlight the sedimentary structure of the present littoral wedge. As seen in the previous profiles of the chapter, the seafloor displays a staircase-like morphology. It derives from the presence of multiple marine terraces developed on the acoustic basement. The deepest is the depositional terrace at 125.4 ms (94.05 m) depth, also seen in profile 5 (Fig.3.40). The rest of the terraces occur at 93.3 ms (70 m) and at 71 ms (53.2 m) depth.

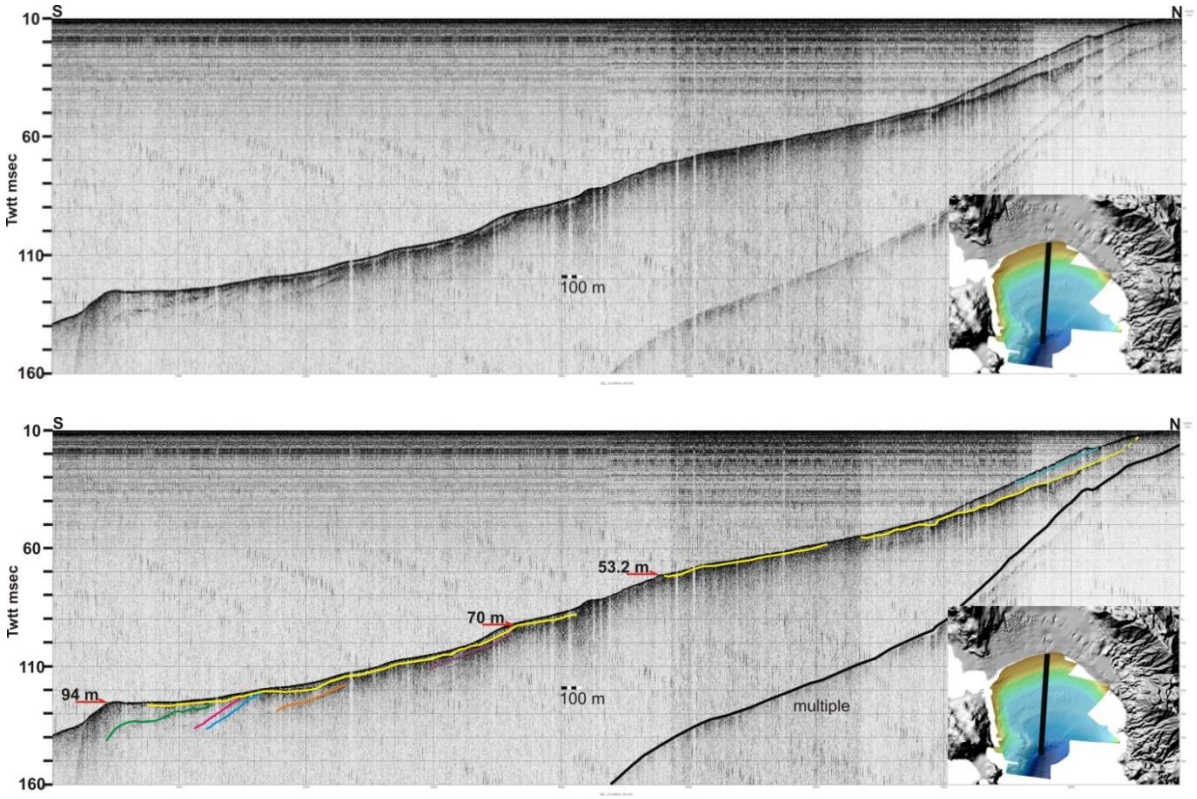

Fig.3.41: Profile 61, Pinger (3.5 kHz). Red arrows indicate terraces.

3.2.3 Seismic stratigraphy on Boomer profiles

The Boomer seismic profiles, due to the lower frequency in respect to the chirp and 3.5 kHz ones, they provide deeper penetration and yield information on the seismic stratigraphy of Vatika Bay at depths up to 50 m or more below the seafloor. The interpretation of the Boomer seismic profiles aims at providing a comprehensive understanding of the evolution of the Bay during the successive high- and low sea-level stages of Upper Quaternary.

Profile 32 (Fig.3.42) shows the valley-like morphology of Vatika Bay (chapter 3.1). A thin, seismically transparent layer occurs (U1) at the uppermost part of the profile. It is about 1-2 ms thick and reaches up to 9 ms at the eastern part of the profile. Unit 2 (U2) is chaotic and about 4 ms thick. Unit 3 (U3) is 10-13 ms thick and follows the morphology of the basin, shaping an unconformity with a continuous reflector of high amplitude. The latter reflector (R1), marked with a yellow line, is morphologically irregular and separates U3 from the uppermost unit U1. At the eastern part of the profile, it separates U1 from the acoustic basement (U6). Unit 4 (U4) is 15-25 ms thick and has 3 seismic facies. The uppermost part of it displays layers of low amplitude, truncated to a reflector of high amplitude, marked with an orange line (R2). The second facies is a mass with chaotic seismic character of significant dimensions (colored in brown). It truncates the reflections bellow and its upper boundary has an irregular character. Therefore, from the abovementioned, it is a mass transport deposit (MTD). It has changed the sedimentation pattern within U4. The lower part is subparallel to the upper unit and is shaping an unconformity with R2. Along with its strong reflectivity and irregular morphology, R2 is a landscape reflector. Unit 5 (U5) has similar seismic stratigraphy to U3. It has been deposited on the seafloor of that period, truncated by a reflector of irregular morphology, marked with a light blue line (R3). R3 is continuous and of high amplitude, it displays irregular morphology and separates U5 from U4. Therefore, it may represent a subaerially exposed surface, probably a landscape surface. Also, U5 is interrupted by a transparent dome-like body (deep purple). U5 is 11-22 ms thick and it is separated from the unit bellow with a continuous reflector of high amplitude (R4). The latter, along with its reflectivity and irregular morphology, may constitute a landscape surface. Bellow R4, the reflectivity of the layers is faint, so it is not possible to distinguish more packages. On either side of the basin, faults occur. The basin is bounded by a fault to the west and another to the east. They separate the basin from the acoustic basement (U6). The eastern fault is covered by U4.

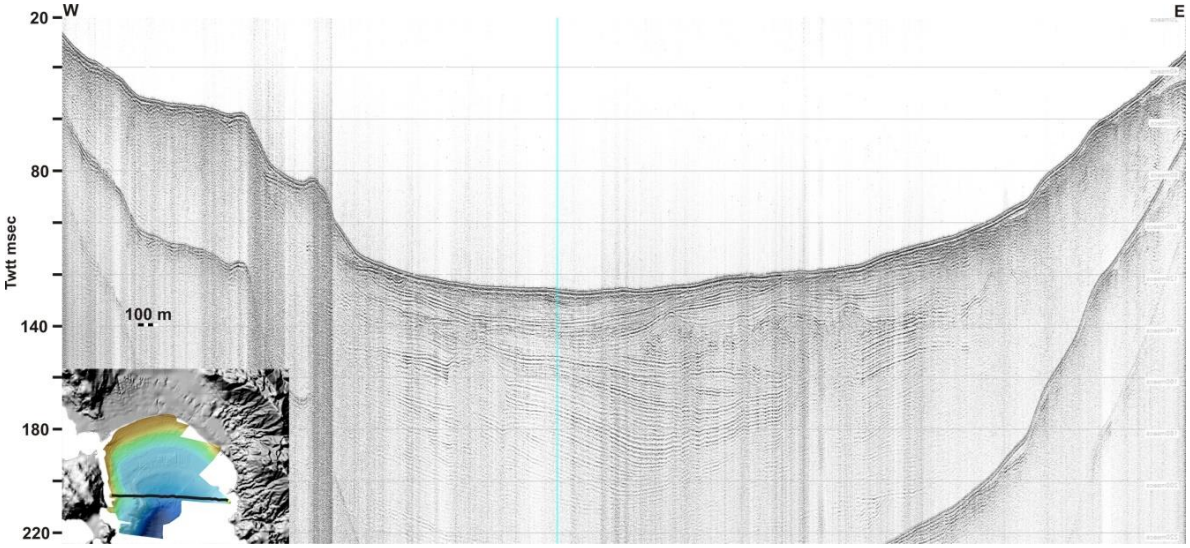

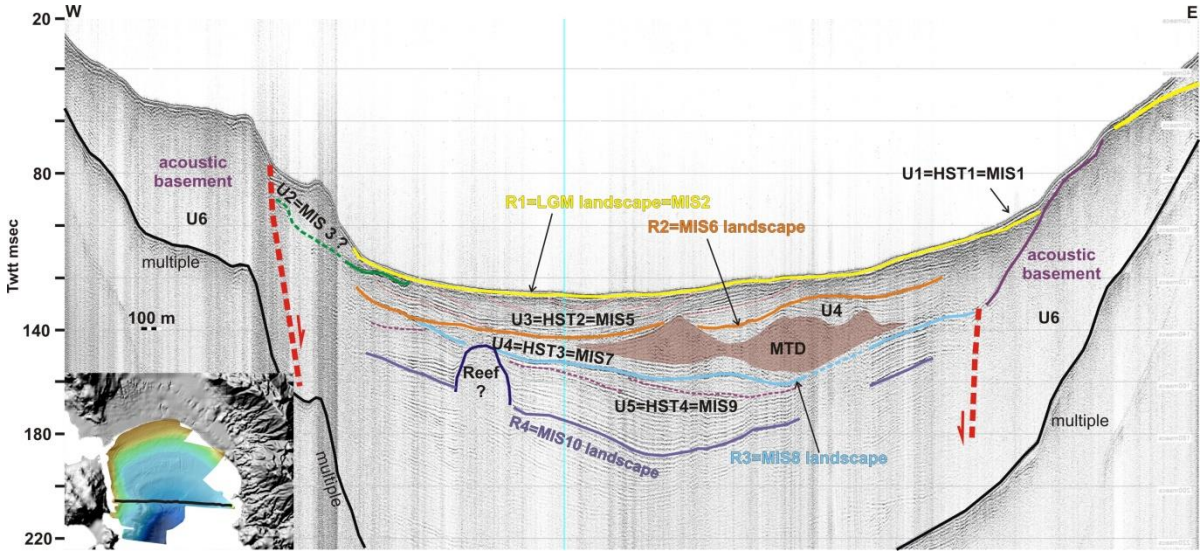

Fig.3.42: Profile 32, Boomer. R1, R2, R3, R4 are landscape surfaces. MIS= Marine isotopic stage. MTD= mass transport deposit. HST= Highstand system track. LST= Lowstand system track.

Seismic reflector packages have been correlated with marine isotopic stages (MIS). The uppermost transparent layer (U1) is interpreted as the marine sediments deposited after the post-LGM sea-level rise. Consequently, R1 may represent the sub-aerially exposed landscape during the last low sea-level stage (MIS 2). Therefore, the uppermost U1 corresponds to the MIS 1. U2 occurs bellow the LGM landscape surface. It represents sediment deposition within MIS 3. In a lower stratigraphic position, U3 is correlated with MIS 5. Embedded layers within it (pink dashed lines) indicate the present day center of the basin. Bellow that, the landscape reflector R2, which truncates U4, corresponds to the MIS 6 landscape. U4 represents MIS 7. Within the latter unit, an MTD is possibly related to a strong event that took place during this period. U4 is separated from U5 with an irregular reflector of high amplitude (R3), as abovementioned. Therefore, R3 represents MIS 8 landscape. U5 shapes an unconformity with R3. It represents sediment deposition within MIS 9. During MIS 9, thicker sediments have been deposited within the bay. Thick undisturbed sediment succession is interrupted by a transparent dome-shaped body, which has the morphology of a reef. The center of the basin is shifted westwards as seen in the stratigraphic levels of the different units within U5. R4 is a landscape reflector, as abovementioned and represents MIS 10 landscape surface. The basin is bounded by faults westwards and eastwards respectively. The fault at the eastern part of the profile, is buried under U4, thus, it must have been active during the interglacial MIS 8 and has not been reactivated since. The faults have contributed to the subsidence of the central part of Vatika Bay. Finally, Unit U6 represents the acoustic basement.

Profile 33 (Fig.3.43) is subparallel to the profile 32 and provides a cross section across the western half of Vatika Bay. In the uppermost part, a thin unit (U1) occurs parallel to the seafloor. It is about 2 ms thick and reaches 8 ms at the foot of the slope, where it onlaps a reflector of high amplitude and irregular morphology. Unit 2 (U2) is chaotic and about 4 ms thick. Unit 3 (U3) is 3-4 ms thick and it is wavy, truncated by R1, which is an erosional surface. Unit 4 (U4) is 15-20 ms thick (NE part is thicker). It has multiple lenticular-shaped masses with chaotic seismic character, emplaced between subparallel layers. The masses' lower boundaries either follow the stratigraphy, or truncate the reflections bellow, while their upper boundaries have an undulating character. From the above, arises that they possibly are MTDs. At the upper surface of the central MTD within U4, there is a channel (CH)-like

morphology with a divergent fill, as seen in Fig.3.43. U4 is truncated by a reflector of high amplitude and irregular morphology (R2). R2 separates U4 from U3 and along with its' geometry and reflectivity, it probably represents a subaerially exposed, landscape reflector. Thickness of Unit 5 (U5) varies across the profile. At the central part it is 17 ms, while on either side, 12-13 ms thick. At the NE part of the profile, it is about 6 ms thick. U5 has similar seismic stratigraphy with U4. It contains a lenticular-shaped mass with chaotic character, which possibly is an MTD of larger dimensions than the ones within U4. U5 is truncated by a reflector of high amplitude and irregular morphology (R3). So, R3 is probably a landscape reflector and separates U5 from U4. Bellow, R4 truncates both U5 and its underlying layers. It is a reflector of high amplitude and irregular morphology. On the basis of its geometry and reflectivity, it is probably a landscape surface. Bellow R4 it is not easy to distinguish specific features in the seismic stratigraphy, because of the low amplitude and reflectivity. Nevertheless, five reflectors of medium amplitude are marked with green dashed lines. Along with their relation with the layers above and below and their irregular morphology, they possibly are landscape surfaces. The stratified basin is bounded by a fault, as seen in the Fig.3.43. The fault controls the subsidence of the basin and the uplift of the western slope of Vatika Bay. U6 represents the acoustic basement.

Seismic reflector packages have been correlated with marine isotopic stages (MIS). The uppermost transparent layer (U1) is interpreted as the marine sediments deposited after the post-LGM sea-level rise. Consequently, R1 may represent the sub-aerially exposed landscape during the last low sea-level stage (MIS 2). Therefore, the uppermost U1 corresponds to the MIS 1. U2 occurs bellow the LGM landscape surface. It possibly represents sediment deposition within MIS 3. In a lower stratigraphic position, U3 is correlated with MIS 5. Bellow, the landscape reflector R2, which truncates U4, corresponds to the MIS 6 landscape. U4 represents MIS 7. Within it, multiple MTDs are possibly related to a strong instability event that took place during this period. U4 is separated from U5 with an irregular reflector of high amplitude (R3), as abovementioned. Therefore, R3 represents MIS 8 landscape. U5 shapes an unconformity with R3 and represents sediment deposition within MIS 9. Within MIS 9 (U5) an MTD of significant dimensions is possibly related to a strong event during this period. R4 truncates U5 and the layers bellow and it is a landscape surface, as abovementioned. It represents MIS 10 landscape.

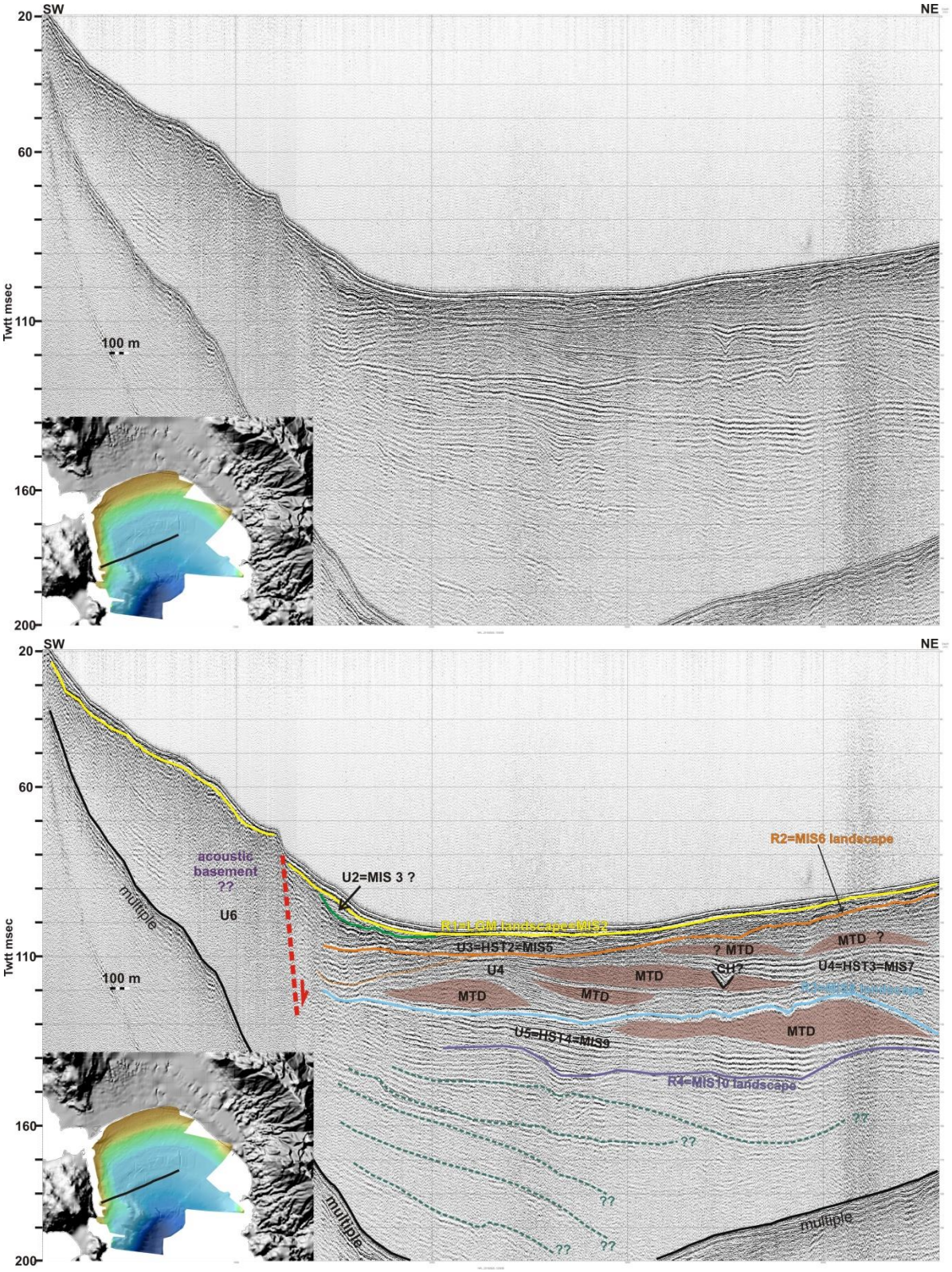

Fig.3.43: Profile 33, Boomer. R1, R2, R3, R4 are landscape surfaces. MIS= Marine isotopic stage. MTD= mass transport deposit. HST= Highstand system track. LST= Lowstand system track. CH= channel.

Profile 31 (Fig.3.44) runs NW-SE and provides a cross section along the eastern slope of Vatika Bay. Unit 1 (U1) is about 2-3 ms thick across the basin with layers parallel to the seafloor. Along the southern slope it contains two transparent bodies, 6 and 10 ms thick respectively, towards SE. The base of U1 represents an angular unconformity between U1

and the underlying unit 3 (U3). A strong high amplitude morphologically irregular reflector (R1) marks the base of U1 and truncates the internal reflectors of U2 indicating that erosion prevailed prior to the deposition of U1. U3 is 5-7 ms thick. It is locally observed at the central-NW part of the profile and has wavy layers truncated by R1, as aforementioned. Unit 4 (U4) is characterized by three large masses with chaotic seismic character embedded within undulating discontinuous layers of medium amplitude, locally truncated by R2. The masses' bases truncate the reflections bellow, while their upper boundaries are morphologically irregular. Therefore, from the abovementioned, they are mass transport deposits (MTDs). At the SE part of the profile, along the slope, U4 is undulating to chaotic. R2 is a strong reflector of high amplitude and irregular morphology. It separates U4 from U3 and therefore, represents a landscape surface. Unit 5 (U5) is discontinuous undulating to chaotic and contains two masses with similar seismic character with the ones within U4, but of smaller dimensions. So, the masses are also MTDs. The thickness of U5 varies across the profile. At the NW part it is 17-20 ms thick, while a few meters deeper than the masses 10-13 ms. According to seismic profiles perpendicular to the profile 31, R3 separates U5 from U4. It is continuous and of high amplitude in comparison to the layers above and below. So, R3 is a landscape surface. R4 separates U5 from the lower unit. At the NW part of the profile, layers bellow R4 are truncated by it. Therefore, R4 is a landscape surface. At the central and SE part of the profile, the borders of R3 and R4 are not well distinguished, due to the chaotic character of the reflections.

Seismic reflector packages have been correlated with marine isotopic stages (MIS). The uppermost layer (U1) is interpreted as the marine sediments deposited after the post-LGM sea-level rise. Consequently, R1 may represent the subaerially exposed landscape during the last low sea-level stage (MIS 2). Therefore, the uppermost U1 corresponds to the sedimentation within Holocene (MIS 1). During MIS 3 and MIS 4 the sea-level has fluctuated between roughly 70 and 90 m below the present sea-level. There is no clear evidence of sediment deposition during them on the studied seismic profiles. So, U3 is correlated with MIS 5. Below that, the landscape reflector R2, which truncates U4, corresponds to the MIS 6 landscape. U4 represents sedimentation during MIS 7. Within it, three MTDs of significant dimensions are possibly related to a strong event that took place during this period. U4 is separated from U5 with an irregular reflector of high amplitude (R3), as abovementioned. Therefore, R3 is interpreted as MIS 8 landscape. In a lower stratigraphic position, U5 represents sediment deposition during MIS 9. Within this period two MTDs of smaller dimensions than the ones within U4, occur. R4 truncates the layers bellow, at the NW part of the profile. Therefore, R4 is a landscape reflector, as abovementioned and represents MIS 10 landscape surface.

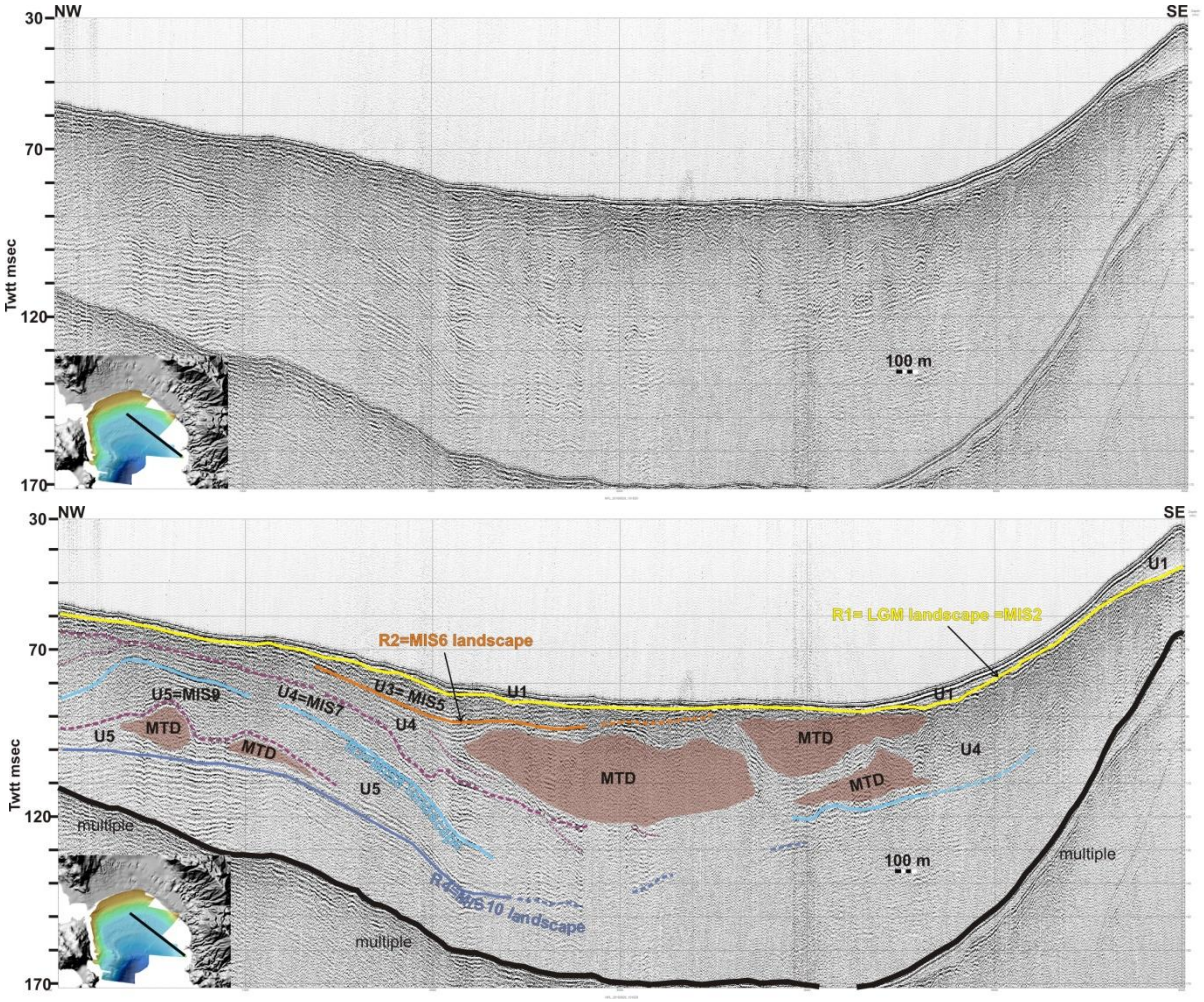

Fig.3.44: Profile 31, Boomer. R1, R2, R3, R4 are landscape surfaces. MIS= Marine isotopic stage. MTD= Mass transport deposit. HST= Highstand system track. LST= Lowstand system track.

The following profiles run roughly N-S and provide informative cross sections on the structural and sedimentological configuration of the Vatika Bay from the northern, shallow part to the southern, deeper area:

Profile 12 (Fig.3.45) is perpendicular to the profiles 32 and 33. A thin, seismically transparent layer occurs (U1) at the uppermost part of the profile, which is 1-2 ms thick. At the northern part of the profile it is 9-12 ms thick and characterized by continuous, undulating, medium amplitude reflectors. Its base is R1, which is an erosional surface and truncates Unit 3 (U3). R1 is a reflector of high amplitude and irregular morphology, displaying thus subaerial erosion. Unit 2 is chaotic and it is about 8-10 ms thick. U3 follows the morphology of the seafloor. U3 is about 7-13 ms thick. U3 is separated from Unit 4 (U4) with a reflector of high amplitude, strong reflectivity and irregular morphology (R2). It truncates both units. Therefore it is a landscape surface. U4 is characterized by a large lenticular-shaped mass with chaotic to undulating seismic character emplaced between parallel to undulating continuous layers. The lower boundary of the mass follows the stratigraphy, while the upper boundary is morphologically irregular. From the above arises that it is an MTD. U4 at the central and northern part of the profile is about 20-30 ms thick and at the southern part it is 6-10 ms thick. R3 truncates layers of the lower unit 5 (U5). It is a reflector of strong reflectivity and high amplitude. Along with its reflectivity and irregular morphology, R3 is a landscape reflector. U5 is interrupted by a transparent dome-like body (deep purple) with

isolated reflections. It is standing on a strong irregular reflector (R4) and it has the morphology of a reef. It is also seen in the intersected profile 32 (Fig.3.42). On the right side of the reef-like body, U5 is continuous parallel and about 10 ms thick. On the other side, it is parallel dipping southwards with 5 ms thickness. The lowermost part of the sedimentary sequence of U5, at the southern part of the profile, has been deformed by a fault, which uplifts the southern part of the profile. This part is about 13-15 ms thick. R4 is a strong reflector of irregular morphology, as aforementioned. It shapes an unconformity with the layers bellow U5, which are undulating of low amplitude and reflectivity (U7). Therefore, R4 is a landscape surface.

Seismic reflector packages have been correlated with marine isotopic stages (MIS). The uppermost transparent layer (U1) is interpreted as the marine sediments deposited after the post-LGM sea level rise. Consequently, R1 may represent the subaerially exposed landscape during the last low sea-level stage (MIS 2). Therefore, the uppermost U1 corresponds to the MIS 1. U2 occurs bellow the LGM landscape surface. It represents sediment deposition within MIS 3. In a lower stratigraphic position, U3 is correlated with MIS 5. The base of U3 is R2. It is a landscape reflector, as abovementioned and is correlated with MIS 6 landscape. U4 represents MIS 7. Within, an MTD is possibly related to a strong event that took place during this period. U4 is separated from U5 with an irregular reflector of high amplitude (R3). Therefore, R3 represents MIS 8 landscape. U5 shapes an unconformity with R3. It represents sediment deposition within MIS 9. Thick undisturbed sediment succession is interrupted by a transparent dome-shaped body, which has the morphology of a reef. R4 is a landscape reflector, as abovementioned and represents MIS 10 landscape surface. At the deepest part of the profile, R4 and the lowermost layers of U5 are interrupted by a fault, which is subsiding the northern part and uplifts the southern part of Vatika Bay. Across the profile four prominent terraces occur at 156 ms (117 m), at 127 ms (95.2 m), at 95 ms (71. 2 m) and at 73 ms (54.7 m).

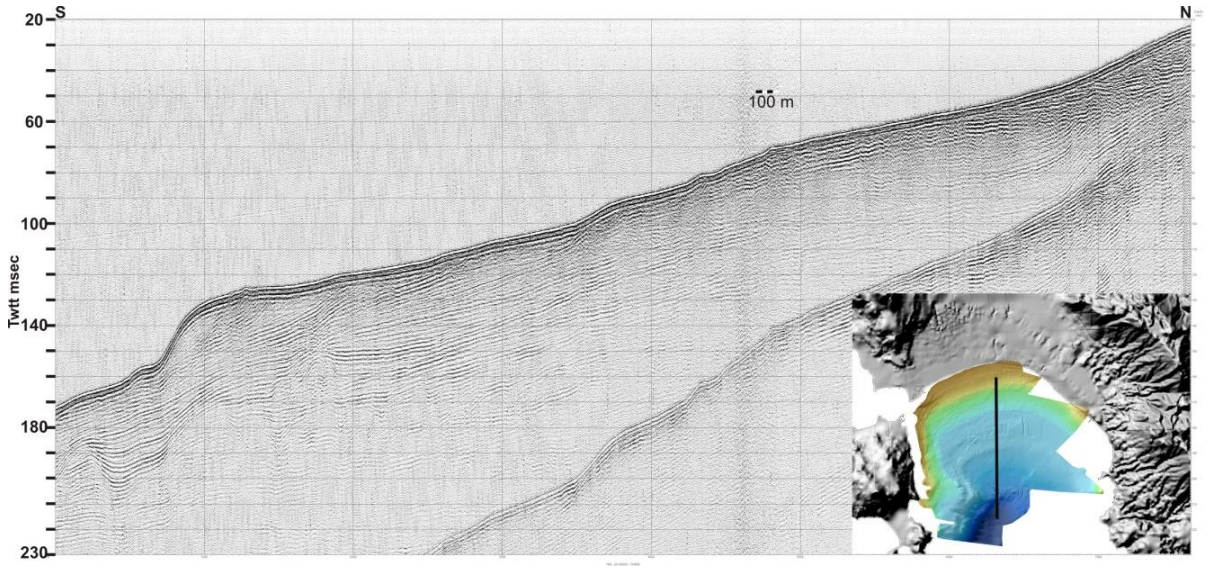

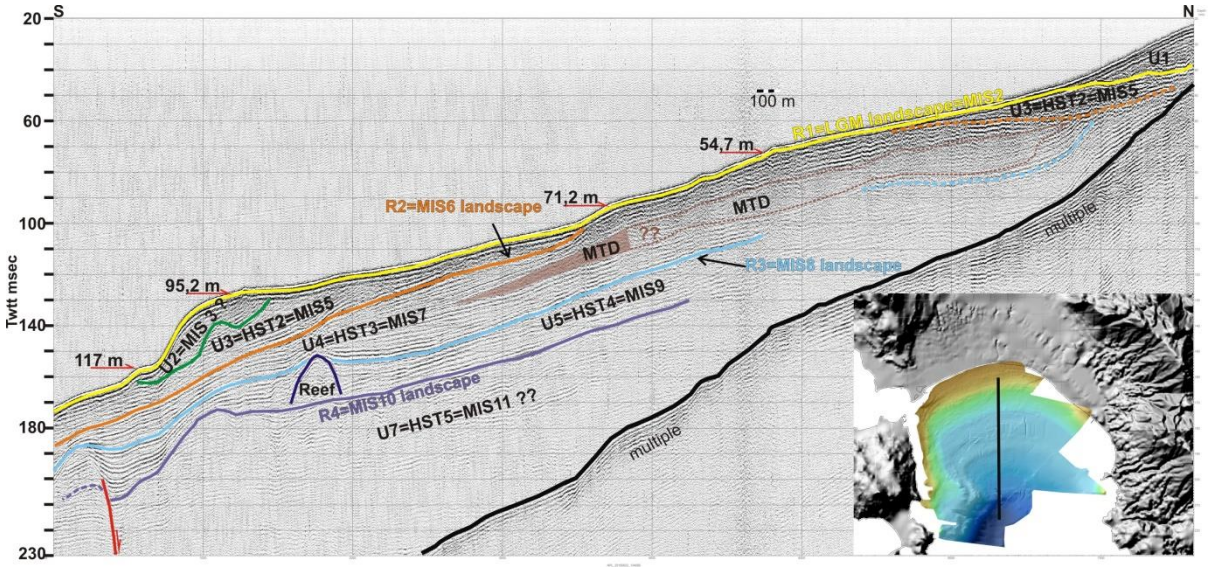

Fig.3.45: Profile 12, Boomer. R1, R2, R3, R4 are landscape surfaces. MIS= Marine isotopic stage. MTD= mass transport deposit. HST= Highstand system track. LST= Lowstand system track.

Profile 10 (Fig.3.46) is parallel to the profile 12 (Fig.3.45). The uppermost thin seismically transparent unit 1 (U1) is continuous and parallel to the seafloor. It is about 4 ms thick across the most part of the profile, while at the northern part it is about 9-11 ms thick. R1 is a continuous reflector of high amplitude, which truncates the stratigraphically lower unit 3 (U3). Unit 2 (U2) is chaotic and its thickness is about 8-15 ms. U3 is continuous and truncated to R1. It is about 4 ms thick. R2 is of high reflectivity, irregular morphology and truncates layers of the unit 4 (U4). Therefore, it is a landscape surface. U4 contains three lenticular-shaped masses with chaotic to undulating seismic character emplaced between parallel continuous layers. Some of them are truncated by R2, as abovementioned. The masses' lower boundaries either follow the stratigraphy, or truncate the reflections bellow, while their upper boundaries have an undulating character. Therefore, they are possibly mass transport deposits (MTDs). U4 is about 11 ms thick across the profile. Its southern part is about 4 ms thick while the thickest part of U4 between the MTDs reaches up to 26 ms. R4 shapes an unconformity with U5. It is of high amplitude and irregular morphology. So, it is a landscape reflector. U5 is interrupted by two dome-shaped bodies with isolated reflections. They have the morphology of a reef. The northern one is possibly identified with the reef-like feature seen in profiles 12 (Fig.3.45) and 32 (Fig.3.42). U5 is continuous parallel of medium amplitude and it is about 12 ms thick. Deeper than the southern reef-like feature, it is undulating of low amplitude (4 ms thick) interrupted by a channel-like morphology with mounded fill (up to 13 ms thick). The base of U5 is a continuous reflector of high amplitude and irregular morphology (R4). R4 shapes an unconformity with the lower stratigraphic unit and therefore it is a landscape reflector. Layers truncated by R4 are parallel to undulating and of low amplitude. Bellow the latter layers a morphologically irregular reflector in green dashed lines is probably another landscape reflector, but because of its low amplitude, it is not well distinguished.

Seismic reflector packages have been correlated with marine isotopic stages (MIS). The uppermost layer (U1) is interpreted as the marine sediments deposited after the post-LGM sea level rise. Consequently, R1 may represent the subaerially exposed landscape during the last low sea-level stage (MIS 2). Therefore, the uppermost U1 corresponds to the MIS 1. U2 occurs bellow the LGM landscape surface. It represents sediment deposition within MIS 3. In a lower stratigraphic position, U3 is correlated with MIS 5. The base of U3 is R2. It is a

landscape reflector, as abovementioned and is correlated with MIS 6 landscape. U4 represents MIS 7. Within, three MTDs are possibly related to a strong event that took place during this period. U4 is separated from U5 with an irregular reflector of high amplitude (R3). Therefore, R3 represents MIS 8 landscape. U5 shapes an unconformity with R3. It represents sediment deposition within MIS 9. Thick undisturbed sediment succession is interrupted by two transparent dome-shaped bodies, which have the morphology of a reef. R4 is a landscape reflector, as abovementioned and represents MIS 10 landscape surface. Four terraces occur at 145 ms (108.7 m), at 121 ms (90.7 m), at 92 ms (69 m) and at 61 ms (45.7 m).

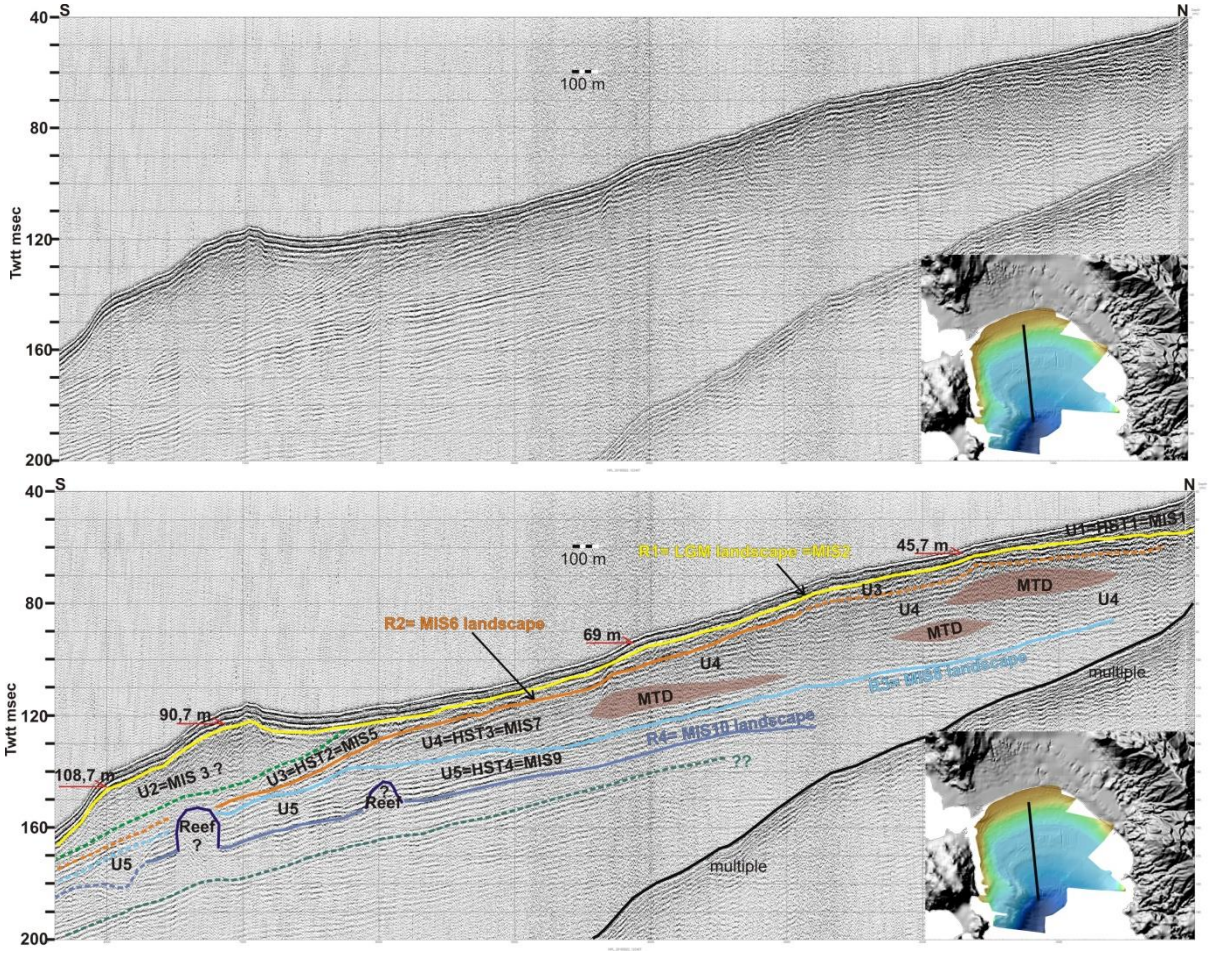

Fig.3.46: Profile 10, Boomer. R1, R2, R3, R4 are landscape surfaces. MIS= Marine isotopic stage. MTD= Mass transport deposit. HST= Highstand system track. LST= Lowstand system track.

Profile 8 (Fig.3.47) is parallel to profiles 12 (Fig.3.45) and 10 (Fig.3.46). After a gently dipping upper slope, the seafloor displays steeper, mount-like morphology. A thin, seismically transparent layer occurs at the uppermost part of the profile (U1). At the southern part of the profile, U1 covers the strongly reflecting top of the acoustic basement (U6). The latter is marked with a yellow line and displays irregular relief. Beneath it, the acoustic basement (U6) is seismically chaotic to undulating. U1 is about 4 ms thick across the most part of the profile. It reaches 8-10 ms at the northern, southern and at the central part of the profile, across the slope. At the southern part and across the slope it is chaotic to undulating of medium to low amplitude, while at the northern part it is undulating of high amplitude. Unit 2 (U2) is chaotic and it is about 5-10 ms thick. Unit 3 (U3) is undulating of medium amplitude and it is about 4 ms thick. It is truncated by R1, which is continuous and of high amplitude. Along with its reflectivity and irregular morphology, R1 should be considered as a landscape surface. R2

separates U3 from the lower unit 4 (U4) and shapes an unconformity with the latter. It is a strong reflector of high amplitude and irregular morphology. Therefore, R4 is a landscape reflector. U4 is characterized by a lenticular-shaped mass with chaotic seismic character emplaced between parallel undulating to chaotic layers of medium to low amplitude. The mass has a base that follows the stratigraphy of U4 and hummocky relief at the top. Therefore from the abovementioned arises that it is an MTD. U4 is thinner at the southern and northern part (11-13 ms) and at the part where the MTD occurs, it reaches 26 ms. Unit 5 (U5) is about 9 ms thick and it is undulating to chaotic of low amplitude. It is separated from U4 with a continuous reflector (R3) of high amplitude. Along with its reflectivity and irregular morphology, R3 is a landscape reflector. The base of U5 is a continuous reflector of high amplitude (R4) and irregular morphology. R4 has the morphology of a landscape reflector. The unit that occurs bellow R4 is parallel undulating to chaotic of low amplitude. Bellow the latter, a morphologically irregular reflector in green dashed lines is possibly another landscape reflector, but because of its low amplitude and reflectivity, it is not well distinguished.

Seismic reflector packages have been correlated with marine isotopic stages (MIS). The uppermost layer (U1) is interpreted as the marine sediments deposited after the post-LGM sea level rise. Consequently, R1 may represent the subaerially exposed landscape during the last low sea-level stage (MIS 2). Therefore, the uppermost U1 corresponds to the MIS 1. U2 occurs bellow the LGM landscape surface. It represents sediment deposition within MIS 3. In a lower stratigraphic position, U3 is correlated with MIS 5. The base of U3 is R2. It is a landscape reflector, as abovementioned and is correlated with MIS 6 landscape. U4 represents MIS 7. Within it, three MTDs are possibly related to a strong event that took place during this period. U4 is separated from U5 with an irregular reflector of high amplitude (R3). Therefore, R3 represents MIS 8 landscape. U5 represents sediment deposition within MIS 9. R4 is a landscape reflector, as abovementioned and represents MIS 10 landscape surface. At the southern part of the profile, a mount occurs. It is 28 m high and about 400 m wide. It is possibly uplifted by a fault occurring at its northern part. The fault uplifts the southern part (acoustic basement) and downthrows the northern part of Vatika Bay. Four terraces occur at 123 ms (92.2 m), at 92 ms (69 m), at 73 ms (54.7 m) and 62 ms (46.5 m).

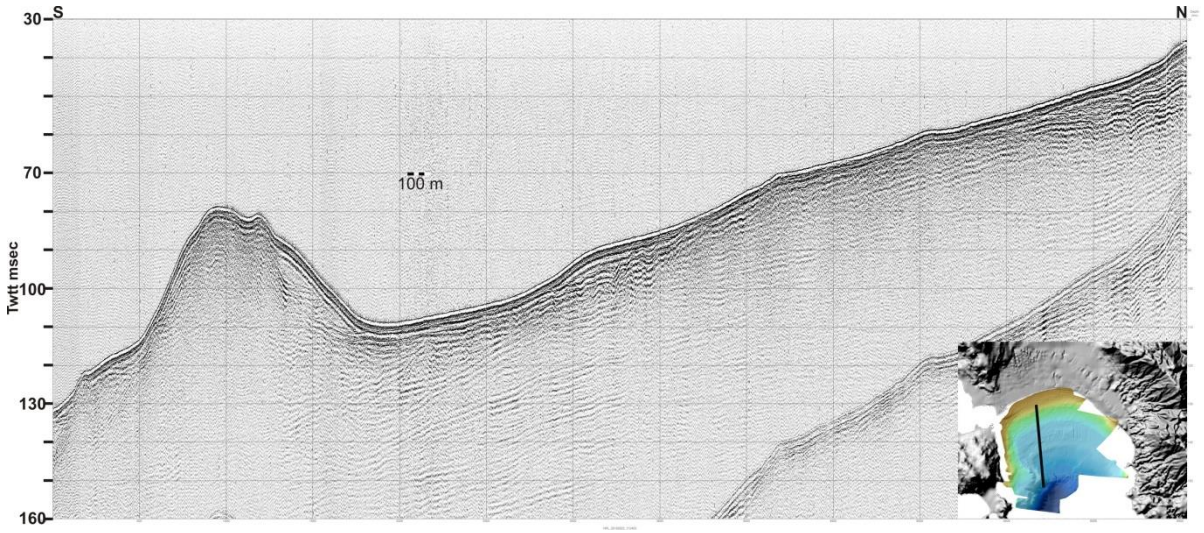

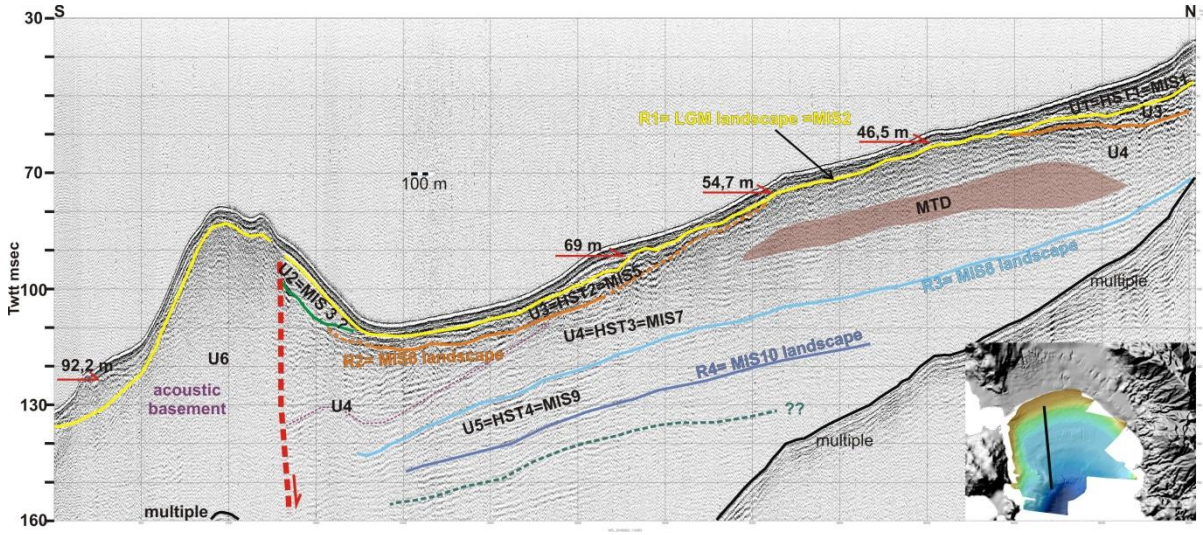

Fig.3.47: Profile 8, Boomer. R1, R2, R3, R4 are landscape surfaces. MIS= Marine isotopic stage. MTD= mass transport deposit. HST= Highstand system track. LST= Lowstand system track.

4. SYNTHESIS OF THE RESULTS & DISCUSSION

4.1. Map of faults of Vatika Bay

Onshore faults around the Vatika Bay have been studied and mapped by Lekkas et al (1995). According to them, a major, long, W-dipping, NNW-SSE trending normal fault runs along the base of the mountainous area to the east and separates it from the Vatika Bay to the west. At short distance north of Neapolis, in the area of Vourlopo, this fault has created a steep, 2-5 m high scarp within Plio-Pleistocene (?) sedimentary formations (Sakellariou et al., 2010).

NW-SE and NNE-SSW trending, probably active faults seem to control the eastern side of Elaphonisos Island (Lekkas et al., 1995). Similar fault directions have been mapped by these authors on the hilly area bounding the plain of Viglafia to the west.

The bathymetric and seismic profiling data presented in this study revealed the presence of two offshore faults in the surveyed area. A NW-SE trending, NE-dipping, apparently normal fault has been observed on three boomer profiles on the slope off the eastern shore of Elaphonisos Island. Its trace on the seafloor coincides with a 15 m high morphological scarp. This fault prolongs probably towards NW, but the available data do not provide clear evidence to confirm it. A second, probable fault has been inferred mostly on the bathymetric data and occurs in the southernmost part of the survey area. It runs NE-SW and marks the base of the parallel directed steep slope SE of Elaphonisos. No further information could be retrieved for this fault. Perpendicular to the latter, a NW-SE trending, SW-dipping fault has been observed on two boomer profiles (chapter 3.2-Fig.3.45). It offsets the MIS 10 landscape reflector and seems to have buried by the MIS 7 (?) and MIS 5 seismic units.

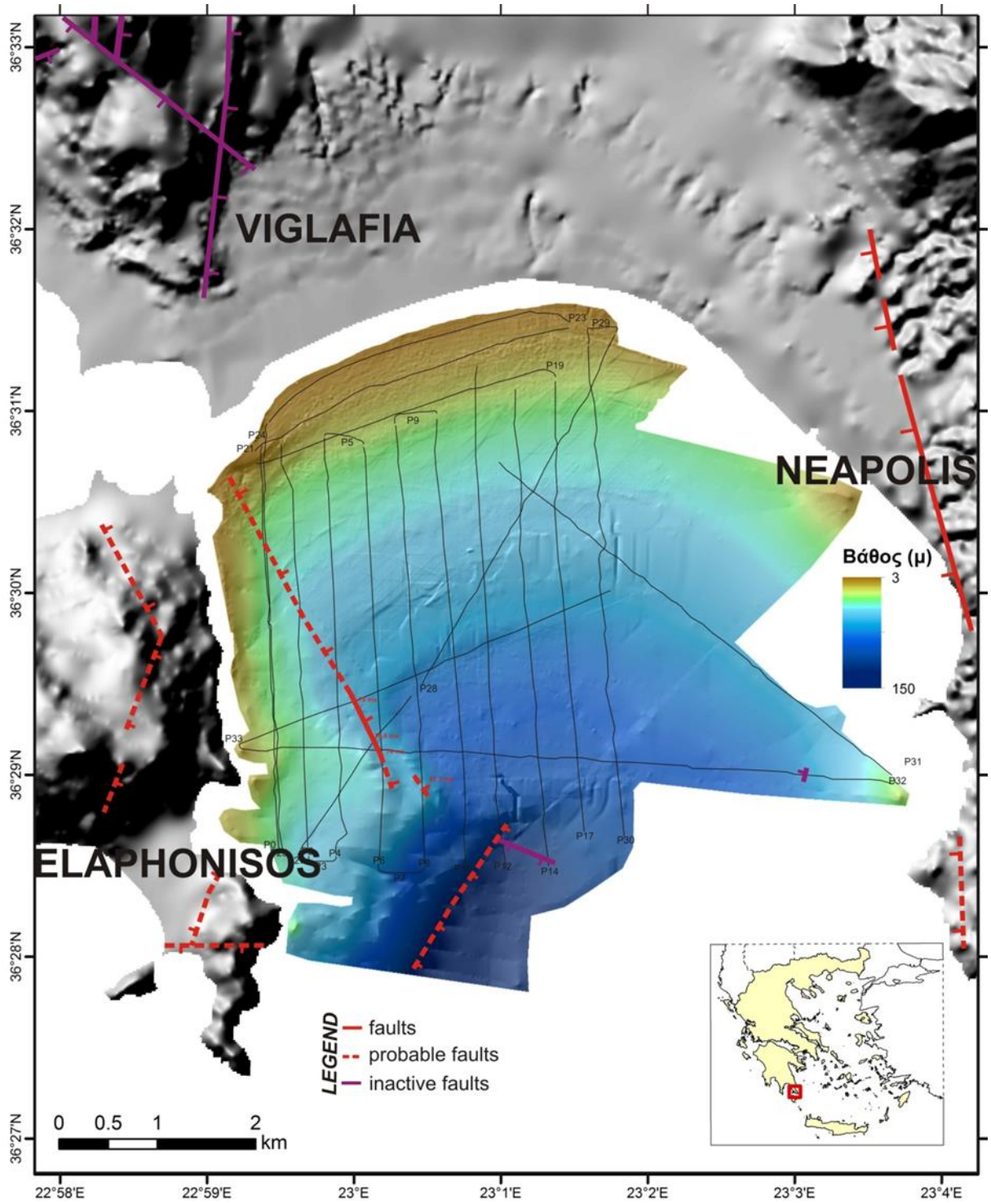

Fig.4.1: Map of onshore and offshore faults in the area of Vatika Bay. Black lines show the tracks of boomer sub-bottom profiles.

4.2. Map of terraces of Vatika Bay

The bathymetry map of Vatika Bay indicates a valley-like morphology with smoother relief at the eastern part, while the western part is characterized by steep slopes (chapter 3.1). Multiple terraces have been identified on the sub-bottom profiles (Boomer, Chirp and 3.5 kHz

sub-bottom profilers) (Fig.4.2). The majority of the observed and mapped terraces occur on the western, steep slope of the bay.

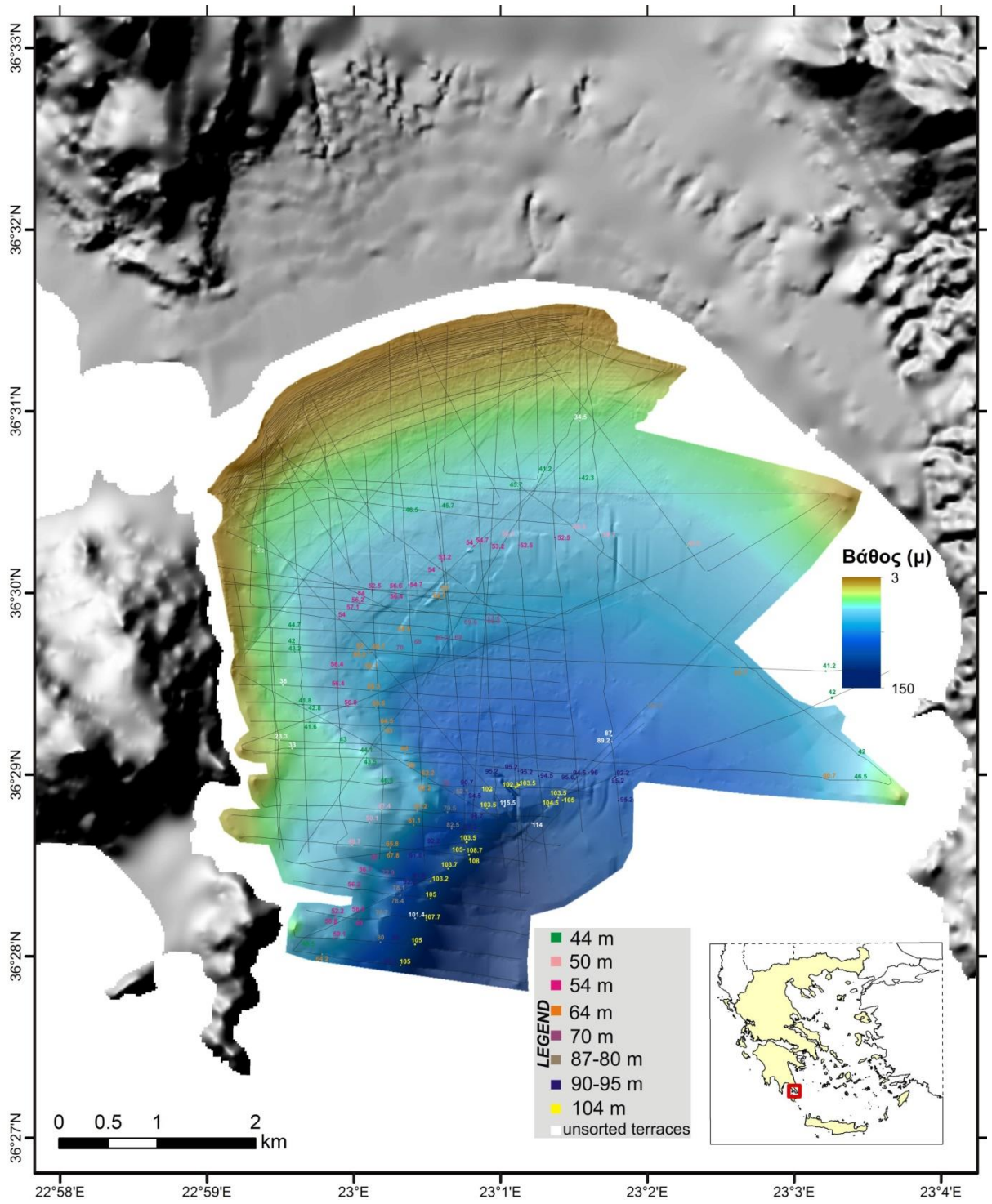

Fig.4.2: Map of the terraces indicating sea-level rise at Vatika Bay. Black lines are the tracks of Boomer, Chirp and 3.5 kHz sub-bottom profilers. Colorful spots are the terraces.

Systematic mapping of the location and depth of the outer edges of the observed terraces has been performed on the seismic profiles. The outcome of the mapping is presented on the map shown on Fig. 4.2. As expected, the distribution of the mapped points follows the general morphology of the area.

Evidence on morphological terraces has been found at several depths ranging roughly between 40 m and 104 m bsl. The measured points have been grouped according to their depth. Points of the same group have been connected with lines of different color for the different depths. The results are shown on the map of Fig. 4.3 and visualize the traces of the outer edges of the underwater terraces identified on the seafloor of the Bay of Vatika. The best preserved and most prominent terrace is the deepest one, which occurs at 104 m depth. It is a depositional terrace, as interpreted on the relevant seismic profiles. The next one at 90-95 m depth is a depositional terrace and is not preserved on the eastern steep part.

The 78-80 m terrace is characterized as depositional, while the one at 70 m depth as erosional. The terrace of 64 m depth is a depositional one and has developed both on the western-central part and the eastern part of the bay. The 54 m deep terrace is erosional and the one at 44 m depth is depositional. The latter occurs in different parts along the slopes of the bay, including the western steep slope and the northern and eastern smoother ones. Finally, a 50 m deep, depositional terrace occurs locally and only on the northeastern central part of the Bay. The latter is grouped with the one of 54 m.

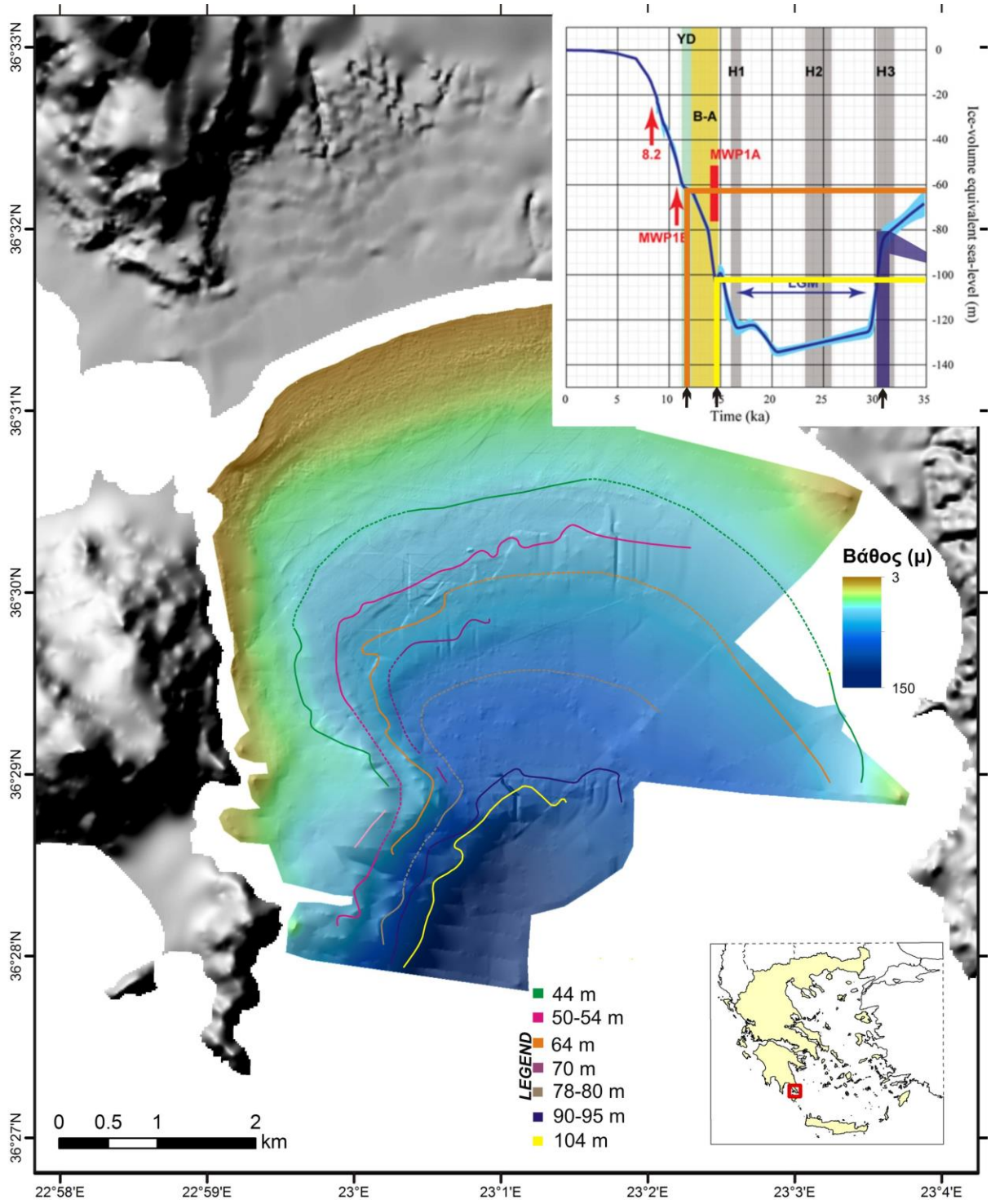

Fig.4.3: Map of the outer edges of the terraces in the bathymetry of Vatika Bay. The sea level curve is from *Lambeck et al., (2014)*.

In addition to the terraces observed and mapped on the seafloor of Bay of Vatika, a series of at least three, well developed, presumably marine terraces occur at various altitudes on the Island of Elaphonisos and on the hills west of the plain of Viglafia (Fig. 4.4). The occurrence of these terraces at altitudes several tens or hundreds of meters above the present sea level, indicates long term uplift.

Relicts of one more marine terrace occur on the plain of Viglafia and close to Neapolis, at altitudes of up to 10 meters above the sea-level. This latter terrace occurs next to the small, fishing port of Neapolis and at several places along the river valleys in the Viglafia plain. The sedimentary facies of this terrace, along with its altitude indicate probable age of formation during the Last Interglacial Stage (MIS 5.5), 125.000 ago. This hypothesis coincides with the observations of *Kelletat et al., (1976)* and *Van Andel, (1987),* who reports similar altitudes of occurrence of the MIS 5.5 terrace at many localities in South Peloponnese.

Mapping and study of the onshore terraces were beyond the scopes of this study. Still, the occurrence of high sea-level terraces on land indicates that some parts of the broader survey area undergo long term uplift. On the other side, the terrace observed at 5-10 m altitude in the plain of Viglafia, if it is correlated with MIS 5.5, indicates that this particular area has not been affected by significant vertical tectonic movements. Indeed, as *Lambeck, (1996)* has proposed, the altitude of the occurrence of the MIS 5.5 terrace, wherever preserved, provides a reliable indicator for the estimation of the rate of vertical tectonic movements during the last 125 kyrs.

Next to that, the submergence of the prehistoric settlement remains at Pavlopetri by at least 3-4 m can't be explained solely by the Late Holocene sea-level rise and requires at least some subsidence of tectonic origin. Similarly, the three bands of beachrocks, which are now submerged by 2.5 to 5 m below the present sea-level, constitute further evidence for subsidence along the northern shoreline of the Bay of Vatika.

Under the light of the above discussion and having in mind the variability of the rates and directions of tectonic movements (uplift and/or subsidence) as indicated by the onshore and nearshore observations we attempt to correlate the depths of the offshore terraces with the sea-level curve and indirectly provide a potential chronology for their formation.

Fig. 4.4: Uplifted marine terraces of unknown age, developed on the slopes of the mountains west of the plain of Viglafia.

By considering the subsidence at Pavlopetri and along the northern shoreline of the Bay, we assume that the seafloor of the Vatika Bay undergoes subsidence too, albeit of unknown rate.

Predicted sea levels for the Last Glacial Maximum (LGM), 20,000 years BP, in the Aegean region varies between -115 m and -135 m, compared to the eustatic value of about -125 m for this epoch *(Lambeck, 1996)*. The deepest observed submerged terrace on the seafloor of the Bay of Vatika is the one at 104 m depth. Despite the absence of reliable data on the sense and the rates of the vertical tectonic movements from within the Bay, it is reasonable to assume that this terrace has been developed at shallower position than the one expected for the Last Glacial Maximum. In addition, the stratigraphic position of this depositional terrace indicates that it is younger than the MIS 2 reflector. Consequently, and by taking into consideration the sea-level curve of *Lambeck et al., (2014)*, we propose here that the 104 m deep terrace can be associated with the short still-stand of the sea-level at about 14-15 ka BP, before the melt water pulse (MWP) 1A. Thus, the LGM shoreline must be located deeper and has not been imaged in the acquired data set.

The seismic stratigraphic structure of the 90-95 m deep terrace has been acquired and interpreted on the Boomer profiles. It indicates a relict form of progradational deposits formed very likely before the formation of the erosional, LGM, R1 reflector. If so, this terrace may be older than the LGM and may correspond to the final stage of the MIS 3 period, roughly 30-35 ka BP.

The terraces 64 m and 44 m depth occur systematically on the seafloor of the bay. If vertical tectonics in the area is not negligible, the age of the formation of the terrace can be estimated by comparing its depth with the predicted sea-level curve. The inset diagram at the Fig.4.3 shows part of the sea-level curve of *Lambeck et al., (2014).* The depth of the terrace of 64 m coincides possibly with the event of Younger Dryas ~12.5–11.5 ka BP.

4.3. Map of paleo-channels at the northern part of Vatika Bay

The northeastern part of Vatika Bay is characterized by the presence of multiple paleo-channels (Fig.4.5), as seen in the seismic profiles acquired in the area, especially in the 3.5 kHz profiles (chapter 3.2.1). The paleo-channels occur at the northeastern coastal zone of the area, at water depth between 8 and 18 m. The paleo-channels have been formed on the previously subaerially exposed and eroded landscape which is represented by the strong reflector at the top of the acoustic basement. They are filled and buried bellow about 5 m thick Holocene sediments (chapter 3.2.1).

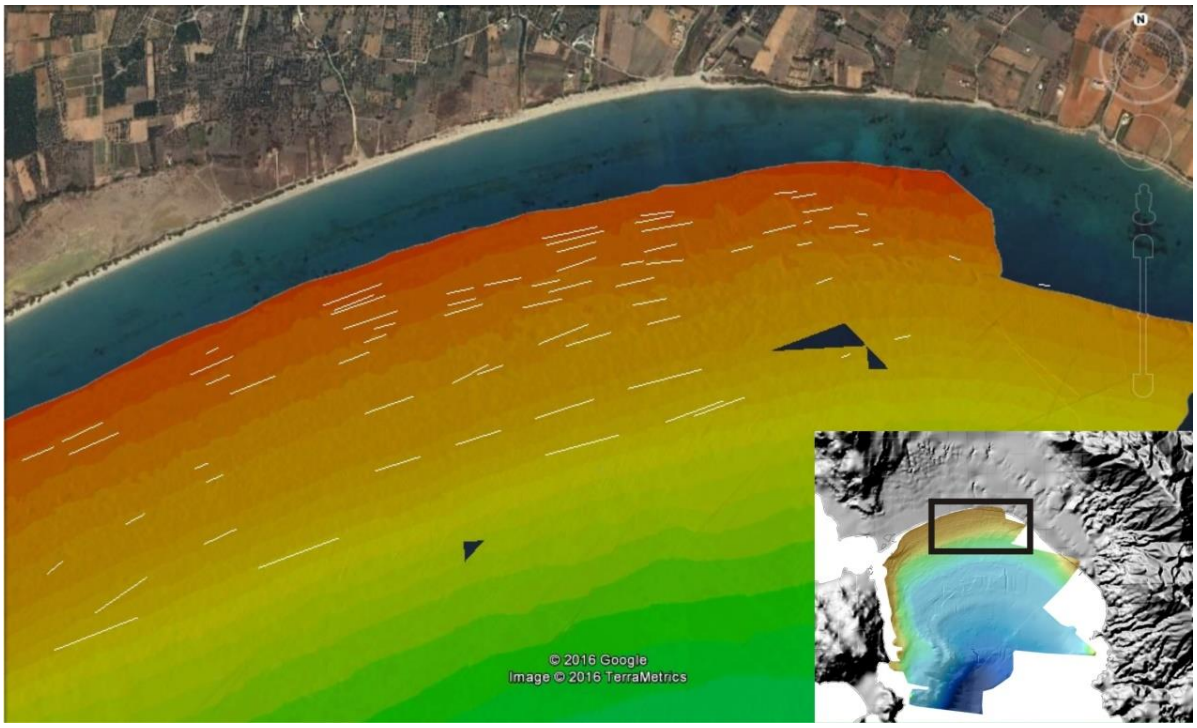

Fig.4.5: Swath bathymetry map of the northern shallow part of the Bay of Vatika. The white bars show the width of the paleo-channels as measured on the 3.5 kHz profiles.

The mapped paleo-channels may have acted as paleo-rivers. The tracks of the most prominent paleo-channels, as derived from the measurements on the profiles, are shown on the map of Fig.4.6: from west to east, G, M, C, D, B, A. The paleo-channels B and A are the most prominent ones and are probably related with the present rivers which outflow at the sites labelled with 2 and 3 respectively. Present rivermouth 1 is probably connected to the paleo-river C or to the D. The river outflowing at the site 4 does not seem to connect with any paleo-channel.

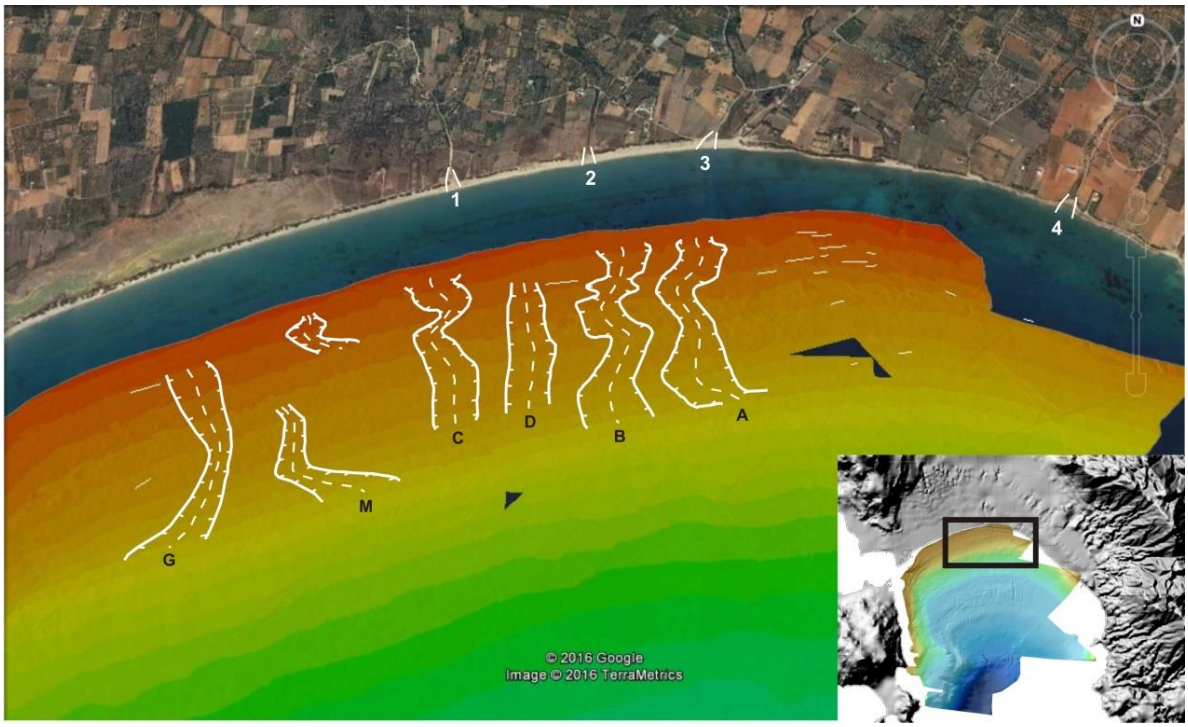

Fig.4.5: Map of the paleo-channels which occur below the Holocene drape at the northern shallow part of Vatika Bay. A, B, C, D, G and M, are paleo-channels. 1, 2, 3 and 4 show the mouths of the actual torrents/rivers. White lines are paleo-channels.

4.4. Mass Transport Deposits (MTD'S)

Mass-transport deposits (MTD'S) can comprise the stratigraphy of an area including sedimentary sheets, channel lobes, and channel fills, and can reach thickness in excess of 150 m. Greater thickness is observed where successive flows are amalgamated *(Posamentier and Martinsen, 2011)*. On seismic data, MTD'S can be recognized by certain geomorphologic as well as stratigraphic distinguishing characteristics: basal linear grooved and scoured surfaces, hummocky relief at the top and internal chaotic to transparent seismic facies, with common internal thrust faulting *(Posamentier and Martinsen, 2011*).

Where precise radiocarbon ages are available, major MTD episodes of deposition are correlated with the most rapid falls or rises of sea level. According to Posamentier & Kolla (2003), the occurrence of MTD'S has been traditionally associated with low-stand conditions, when sedimentation on the shelf edge is supposed to be at its peak and water overburden weight is being reduced over shelf regions. However, in the case of Vatika bay, MTD'S appear in the stratigraphic levels which have been associated with warm periods. The most prominent and frequent mass transport deposits occur within the units 4 and 5 which are correlated with the interglacial periods MIS 7 and MIS 9 (Fig.3.43).They have significantly large dimensions. Their occurrence at the eastern part has changed the axis of the valley westwards, which means that subsequent to their deposition, the eastern part tended to have a smoother relief.

4.5. Laconia Paradox: A submerged city within a long term uplifting area

At the southwestern part of the Hellenic Arc, the West Cretan Strait separates the island of Crete from SE Peloponnese. A NNW-SSE trending ridge bounded by steep scarps on both sides separates the 3000-5000 m deep Hellenic Trench to the west from the 1000-2000 m deep Cretan Sea basin to the east (*Lyberis et al., 1982*) and the islands of Kythera and Antikythera mark its summits. The shallowest parts of the ridge have been exposed during the major low-sea-level periods of the Middle and Late Pleistocene, when the islands Kythera and Antikythera were connected to the Peloponnese. The width of the sea strait separating them from Crete may have been only 2–3 nautical miles (*Sakellariou and Galanidou, 2015*).

The area is known for very high seismic potential and long-term vertical tectonic movements. Uplifted Late Pleistocene marine terraces and Holocene shorelines (Pirazzoli et al., 1982) are evident along the coastline of the southeastern Peloponnese indicating continuous tectonic uplift during the Quaternary as a response to the ongoing subduction of the Ionian lithosphere underneath the overriding Aegean microplate and the deformation of the latter. The continental shelf is very narrow and progresses very rapidly to steep submarine slopes leading to the deep basins of the Hellenic Trench to the SW, or to the deep Cretan Sea to the E (*Sakellariou et al., 2017*).

In southeast Peloponnese NW-SE faults are generally cut by NNW-SSE faults. On Kythera and Antikythera N-S to NNE-SSW striking faults are present. The active N-S normal fault system in Crete, since pre-Pliocene, progressively becomes NNE-SSW in southeast Peloponnesus and Kythera (*Lyberis et al., 1982*). As Crete has not undergone significant rotation since the Late Miocene (*Laj et al., 1982*), the clockwise rotation of Peloponnese may imply some equivalent counterclockwise rotation in the Kythera-Antikythera segment (*Lyberis et al., 1982*). Faults parallel to the axis of the arc corresponding to mainly oblique extension, but in addition, the presence of the en echelon normal fault system results in the dextral component of extensional motion parallel to the Kythera- Antikythera axis. It is very likely that the whole of the Kythera strait has undergone more extension than adjacent segments of the arc (Peloponnese and Crete). This, in turn, would easily explain its low altitude relative to other arc segments as extension induces subsidence (*Lyberis et al., 1982*).

Evidence of long-term tectonic uplift is known on the Lakonia peninsula at the SE Peloponnese. The area belongs to the seismically active Hellenic Arc and displays long term uplift, as indicated by the uplifted Late Quaternary marine terraces, and the short-term (historic) subsidence of the submerged cities of Pavlopetri and Plytra. In parallel to the prevailing long- and short-term tectonic uplift of the landmasses in this region, local tectonics and faulting result to the formation of deep basins and trenches and the rough seafloor morphology of the West Cretan Strait (*Sakellariou and Galanidou, 2015*). More precisely, in addition to the terraces observed and mapped on the seafloor of Vatika Bay (chapter 4.2), a sequence of at least three, well developed, presumably marine terraces occur at various altitudes on the Island of Elaphonisos and on the hills west of the plain of Viglafia. The occurrence of these terraces at altitudes of several tens or hundreds of meters above the present sea-level indicates long term uplift. Pleistocene marine terraces of Tyrrhenean age are preserved along the coast between Neapolis and Cape Maleas (*Theodoropoulos, 1973*) obtaining a vertical structure (*Lekkas et al., 1995*). The observed terrace occurs next to the small fishing port of Neapolis and at several places along the river valleys in the Viglafia plain, at altitudes of up to 10 m above the sea level. These observations coincide with the

ones of *Kelletat et al., (1976) and Van Andel, (1987)*, who report similar altitudes of occurrence of the MIS 5.5 terrace at many localities in South Peloponnese.

The presence of high sea-level terraces on land indicates long term uplift for some parts of the wider survey area. However vertical tectonic movements haven't affected the entire area. A terrace observed at 5-10 m altitude in the plain of Viglafia, if it is correlated with MIS 5.5, as aforementioned, suggests that this particular area has not been affected by significant vertical tectonic movements. Indeed, as *Lambeck (1996)* has proposed, its present position in southern Peloponnese provides a reliable indicator of long term tectonic stability, considering it occurs in many localities to within a few meters above present sea level. Limited vertical tectonic movement appears to have occurred in these localities during the past 125 yrs.

Furthermore the submerged prehistoric settlement remains of Pavlopetri (3-4 m during the last 5000 yrs) and the site of Plitra (located 26 km northern of Pavlopetri) can't be explained solely by the Late Holocene sea-level rise and requires at least some subsidence of tectonic origin (*Henderson et al., 2011, Flemming, 1973; Hadjidaki et al., 1980*). Similarly, the three bands of beach rocks, which are now submerged by 2.5 to 5 m below the present sea level, constitute more evidence for subsidence along the northern shoreline of the Bay of Vatika. The interpretation of high resolution seismic profiles has also shown that the differential subsidence rates across the Bay of Vatika have led to the formation of low sea-level terraces at different depths on the western and eastern slopes (chapter 3.2). The occurrence of the terraces has been mapped mainly on the western, steep part slope of the bay.

The interpretation of bathymetric and seismic profiling data in this work revealed the presence of a NW-SE trending, NE-dipping, apparently normal fault on the slope off the eastern shore of Elaphonisos. Its trace on the seafloor coincides very well with a 15 m high morphological scarp. Probably, it prolongs towards NW, but the available data do not provide clear evidence to confirm it. The fault is not connected to the mapped offshore faults, but has the same trending.

Having in mind the variability of the rates and directions of tectonic movements (uplift and/or subsidence) as indicated by the onshore and nearshore observations, there has been an attempt to solve the Laconia Paradox: a submerged city within a long-term uplifting area. It is thought that Pavlopetri is due largely to tectonic factors associated with the plate convergence and subduction in the Cretan Arc and the related local and regional faulting (*Marriner and Morhange 2007*).

The area is characterized by a valley-like morphology, as aforementioned in chapter 3.1 (Fig.4.6). In the western part of the map, uplifted terraces of the area of Viglafia and the island of Elaphonisos occur. The northern central part has not been affected by significant vertical tectonic movements and is characterized as relatively stable, as abovementioned. Furthermore, the NW-SE trending submarine fault combined with the uplifted terraces in the island of Elaphonisos, indicate relative subsidence of the bay. Pavlopetri (indicated with a star in the Fig.4.6) occurs very close to the intersection of two faults. Having in mind all the aforementioned data, the presence of the beachrock bands in the northern part of the bay and also the fact that the highest rate of subsidence is near the fault zone, it comes out that Pavlopetri is located in a regime of short-term fast subsidence.

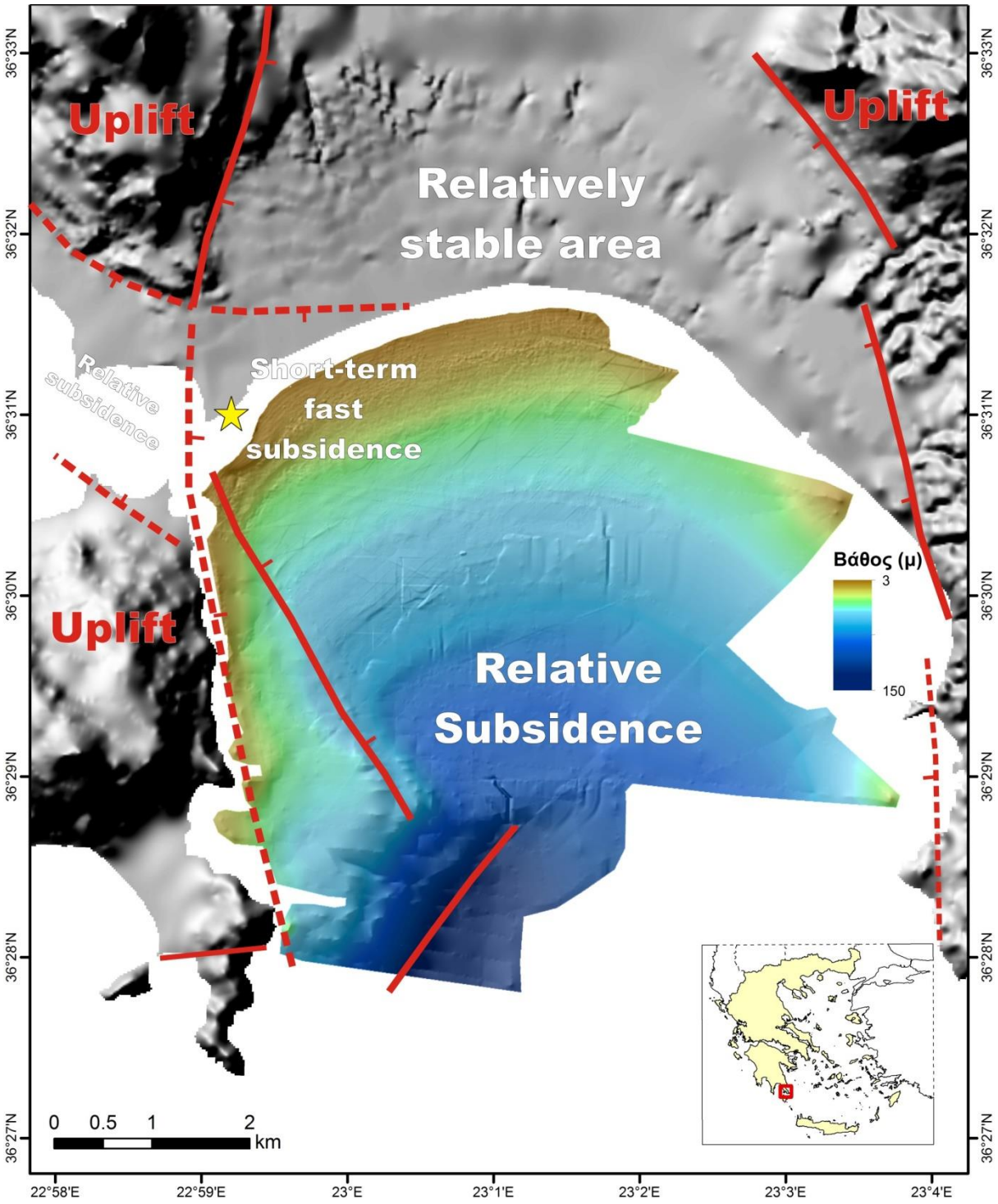

Fig.4.6: Structural map and tectonic movements in the area of Vatika Bay.

5. CONCLUSIONS

The bathymetric map of the study area, Vatika Bay, revealed a valley-like morphology with smooth relief in the northern and eastern part of the gulf, while the western part towards Elaphonisos Island is characterized by steep slopes and terraces. Numerous seafloor channels have been observed at the shallow northeastern part of the bay with a general direction NW-SE and some of them accord with present-day offshore rivers. Also, at the shallow northern part of Vatika bay multiple dinsict bands of submerged beachrock bands occur. The nearest bands are situated 150 m from shore, in depths of 3-4 m. Besides, Posidonia Oceanica meadows are clearly visible at the seafloor of Vatika Bay in depths up to 12-14 m. Trawler marks observed at the seafloor of Vatika Bay result from human activity and a shipwreck has been spotted at the western steeper part of Vatika Bay at the depth of 52 m.

High resolution seismic profiles revealed a valley like morphology due to N-S erosion of running water within the bay. Holocene sediment deposition on the shallow seafloor of the Bay is fairly limited, with sediment thickness not exceeding a few meters. More precisely, its thickness reaches up to 7.5 m with thicker deposits at the smoother eastern part and the northern shallower part of the bay. At the edge of both the western and the eastern slope of Vatika Bay thicker sedimentation, indicate recent sediment deposition related to the present littoral wedge. Moreover, at the shallow central part, at about 30-50 m depth, on the Holocene surface a series of transgressive deposits (TST) is locally observed. Seismic profiles parallel to the north coast indicate a series of submerged riverbeds running off the northern shore of the bay and buried below the recent sediments. Some of them are connected with present day offshore rivers.

Boomer seismic profiles reveal paleo-landscape reflectors which correspond to the marine isotopic stages 2, 6, 8 and 10. MTDs are widespread features during the warm interval MIS 7. Their presence at the eastern part mainly, has changed the relief of the bay. Prior to this event, the valley was symmetrical and the eastern slope was steeper than the present day. Moreover, multiple morphological terraces have been identified across the bay, mainly at the western steeper part at several depths ranging roughly between 40 m and 104 m bsl. Three prominent, erosional terraces have been mapped systematically on the seafloor of the Bay at depths of 104 m, 90-95 m and 65 m. According to the sea level curve of Lambeck et al., 2014, the 104 m deep terrace is associated with the short still-stand of the sea-level at about 14-15 ka BP, before the melt water pulse (MWP) 1A. Thus, the LGM shoreline must be located deeper and has not been imaged in the acquired data set. The terrace of 90-95 m depth may be older than the LGM and may correspond to the final stage of the MIS 3 period, roughly 30-35 kyrs BP, while the depth of the terrace of 64 m coincides possibly with the event of Younger Dryas ~12.5–11.5 ka BP. A few more morphological terraces, at depths of 78-80 m, 70 m, 64 m, 50-54 m are locally observed. In addition, a series of at least three, well developed, presumably marine terraces occur at various altitudes on the Island of Elaphonisos and on the hills west of the plain of Viglafia. The occurrence of these terraces at altitudes several tens or hundreds of meters above the present sea level, indicates long term uplift. Furthermore, relicts of one more marine terrace occur on the plain of Viglafia and close to Neapolis, at altitudes of up to 10 m above the sea-level corresponds to probable age of formation during the Last Interglacial Stage (MIS 5.5), 125.000 years ago (Tyrrhenian shoreline).

Interpretation of the obtained data, reveal a complicate regime of tectonic deformation.

It is observed that relative subsiding and uplifting areas, are controlled by active faulting. More precisely, high resolution seismic profiles across the western steep slope of the Bay provide evidence of NNW-SSE and NE-SW trending normal (?) faulting, separating the uplifted Elaphonisos Island from the subsiding Vatika Bay. Relevant features are being recognized on land and offshore. The eastern slope of the Bay displays marked differences: it dips smoothly westwards, while the observed submarine terraces do not match with the ones mapped along the western slope. The northern central part of the area is relatively stable. The submerged ancient city of Pavlopetri is located on the subsiding part of Vatika bay close to the intersection of two faults. The occurrence of three beachrock formations at different depths indicates rapid subsidence due to tectonic activity (earthquakes). Thus, it comes out that Pavlopetri is located in a regime of short-term fast subsidence.

Future work

It is proposed some future work to be done in order to gain evidence and the scenario to be integrated, thus, future work includes:

- Reconstruction of the shallow submerged near-coast area of the Vatika Bay with the aim to define palaeo-shorelines and river-valleys during Neolithic and Early Bronze age times.
- Validation and chronological constrains of the observed submerged and uplifted terraces with the aim to estimate rates of relative tectonic subsidence.
- Offshore geological mapping anew and investigation of the probable already mapped faults.

6. REFERENCES

1. Angelier, J. Tectonic evolution of the Hellenic arc since the late Miocene.*Tectonophysics* **49,** 23–36 (1978).

2. Angelier, J. & Pichon, X. Le. Neotectonique horizontale et verticale de l'Egée: subduction et expansion. *Aubouin, J. Debelmas M. Latreille (Coordinators),* (1980).

3. Angelier, J., Lybéris, N., Le Pichon, X., Barrier, E. & Huchon, P. The tectonic development of the hellenic arc and the sea of crete: A synthesis. *Tectonophysics* **86,** 159–196 (1982).

4. Bard, E., Fairbanks, R., Arnold, M., Maurice, P. & Duprat, J. Sea-level estimates during the last deglaciation based on δ 18 O and accelerator mass spectrometry 14 C ages measured in Globigerina bulloides. *Quat. Res.* **31,** 381–391 (1989).

5. Bard, E., Hamelin, B. & Fairbanks, R. U-Th ages obtained by mass spectrometry in corals from Barbados: sea level during the past 130, 000 years. *Nature* **346,** 456–458 (1990).

6. Benjamin, J. *et al.* Late Quaternary sea-level changes and early human societies in the central and eastern Mediterranean Basin : An interdisciplinary review. *Quat. Int.* 1–29 (2017). doi:10.1016/j.quaint.2017.06.025

7. Biju-Duval, B. *et al.* in *The Geology of Continental Margins* 695–721 (Springer Berlin Heidelberg, 1974). doi:10.1007/978-3-662-01141-6_52

8. Bohnhoff, M., Harjes, H.-P. & Meier, T. Deformation and stress regimes in the Hellenic subduction zone from focal Mechanisms. *J. Seismol.* **9,** 341–366 (2005).

9. Dewey, J. F., Pitman, W. C., Ryan, W. B. F. & Bonnin, J. Plate Tectonics and the Evolution of the Alpine System. *Geol. Soc. Am. Bull.* **84,** 3137–3180 (1973).

10. Fairbanks, R. A 17, 000-year glacio-eustatic sea level record: influence of glacial melting rates on the Younger Dryas event and deep-ocean circulation. *Nature* **342,** 637–641 (1989).

11. Flemming, N. C. Holocene Earth Movements and Eustatic Sea Level Change in the Peloponnese. *Nature* **217,** 1031–1032 (1968).

12. Flemming, N. C. Holocene Eustatic Changes and Coastal Tectonics in the Northeast Mediterranean: Implications for Models of Crustal Consumption. *Philos. Trans. R. Soc. A Math. Phys. Eng. Sci.* **289,** 405–458 (1978).

13. Flemming, N. & Czartoryska, N. Archaeological evidence for eustatic and tectonic components of relative sea level change in the South Aegean. *Marine* (1973).

14. Flemming, N. & Webb, C. Tectonic and eustatic coastal changes during the last 10,000 years derived from archaeological data. *Zeitschrift für Geomorphol.* (1986).

15. Galili, E. & Rosen, B. Submerged Neolithic settlements off the Carmel coast, Israel: cultural and environmental insights. *Submerg. prehistory* (2011).

16. Gallou, C. & Henderson, J. *Pavlopetri, an Early Bronze Age harbour town in south-east Laconia*. *Pharos* (2012).

17. Gautier, P. *et al.* Timing , kinematics and cause of Aegean extension : a scenario based on a comparison with simple analogue experiments . - Des ananlyses en tomographie sismique du manteau sous l β€^{TM} Egée révèlent la présence d β€^{TM} un slab froid penté vers le Nord et qui plong. *Tectonophysics* **315,** 31–72 (1999).

18. Gerolymatos, I. *Geological Map of Greece, scale 1: 50.000. Neapolis–Ag.Nikolaos Sheet IGME* (1999).

19. Hadjidaki, E., Lianos, N. & Edwards, M. A preliminary report on an underwater survey at Plitra, South Laconia, Greece: 1980. *Int. J. Naut. Archaeol.* **14,** 227–236 (1985).

20. Harding, A. PAVLOPETRI: A Mycenaean Town Underwater. *Archaeology* (1970).

21. Harding, A., Cadogan, G. & Howell, R. *Pavlopetri an Underwater Bronze Age Town in Laconia*. (1969).

22. Harff, J. *et al.* in *Submerged Landscapes of the European Continental Shelf: Quaternary Paleoenvironments* 11–49 (John Wiley & Sons Ltd., 2017).

23. Henderson, J. C., Gallou, C., Flemming, N. C. & Spondylis, E. in *Submerged Prehistory* 207–218 (2011).

24. Henderson, J., Pizarro, O., Johnson-Roberson, M. & Mahon, I. Mapping submerged archaeological sites using stereo-vision photogrammetry. *Int. J. Naut. Archaeol.* **42,** 243–256 (2013).

25. Huguen, C., Chamot-Rooke, N., Loubrieu, B. & Mascle, J. Morphology of a Pre-collisional, Salt-bearing, Accretionary Complex: The Mediterranean Ridge (Eastern Mediterranean). *Mar. Geophys. Res.* **27,** 61–75 (2006).

26. Jolivet, L., Brun, J. P., Gautier, P., Lallemant, S. & Patriat, M. 3D-kinematics of extension in the Aegean region from the early Miocene to the present; insights from the ductile crust. *Bull. la Société Géologique Fr.* **165,** 195–209 (1994).

27. Jolivet, L. A comparison of geodetic and finite strain pattern in the Aegean, geodynamic implications. *Earth Planet. Sci. Lett.* **187,** 95–104 (2001).

28. Jolivet, L. & Brun, J. P. Cenozoic geodynamic evolution of the Aegean. *Int. J. Earth Sci.* **99,** 109–138 (2010).

29. Jolivet, L. *et al.* Aegean tectonics: Strain localisation, slab tearing and trench retreat. *Tectonophysics* **597–598,** 1–33 (2013).

30. Kelletat, D., Kowalczyk, G., Schröder, B. & Winter, K.-P. A Synoptic View on the Neotectonic Development of the Peloponnesian Coastal Regions. *Zeitschrift der Dtsch. Geol. Gesellschaft* 447–465 (1976).

31. Kokinou, E., Tiago, A. & Evangelos, K. Structural decoupling in a convergent forearc setting (southern Crete, Eastern Mediterranean). *Geol. Soc. Am. Bull.* **124,** 1352–1364 (2012).

32. Laj, C., Jamet, M., Sorel, D. & Valente, J. P. First paleomagnetic results from Mio-Pliocene series of the hellenic sedimentary ARC. *Tectonophysics* **86,** 45–67 (1982).

33. Lambeck, K. Sea-level change and shore-line evolution in Aegean Greece since Upper Palaeolithic time. *Antiquity* **70,** 588–611 (1996).

34. Lambeck, K. Sea-level change through the last glacial cycle: geophysical, glaciological and palaeogeographic consequences. *Comptes Rendus Geosci.* **336,** 677–689 (2004).

35. Lambeck, K., Anzidei, M., Antonioli, F. & Benini, A. Sea level in Roman time in the Central Mediterranean and implications for recent change. *Earth Planet.* (2004).

36. Lambeck, K. & Chappell, J. Sea level change through the last glacial cycle. *Science (80-.).* **292,** 679–685 (2001).

37. Lambeck, K. Late Pleistocene and Holocene sea-level change in Greece and south-western Turkey: a separation of eustatic, isostatic and tectonic contributions. *Geophys. J. Int.* **122,** 1022–1044 (1995).

38. Lambeck, K. & Purcell, A. Sea-level change in the Mediterranean Sea since the LGM: Model predictions for tectonically stable areas. *Quat. Sci. Rev.* **24,** 1969–1988 (2005).

39. Le Bas, T. P. & Huvenne, V. A. I. Acquisition and processing of backscatter data for habitat mapping – Comparison of multibeam and sidescan systems. *Appl. Acoust.* **70,** 1248–1257 (2009).

40. Le Pichon, X. Land-locked oceanic basins and continental collision: the Eastern Mediterranean as a case example. *Mt. Build. Process.* (1982).

41. Le Pichon, X. & Angeliers, J. The Hellenic Arc and Trench system: A key to the Neotectonic evolution of the Eastern Mediterranean area. *Tectonophysics* **60,** 1–42 (1979).

42. Le Pichon, X., Lallemant, S. ., Chamot-Rooke, N., Lemeur, D. & Pascal, G. The Mediterranean Ridge backstop and the Hellenic nappes. *Mar. Geol.* **186,** 111–125 (2002).

43. Le Pichon, X., Chamot-Rooke, N., Lallemant, S., Noomen, R. & Veis, G. Geodetic determination of the kinematics of central Greece with respect to Europe: Implications for eastern Mediterranean tectonics. *J. Geophys. Res. Solid Earth* **100,** 12675–12690 (1995).

44. Leite, O. & Mascle, J. Geological structures on the South Cretan continental margin and Hellenic Trench (eastern Mediterranean). *Mar. Geol.* **49,** 199–223 (1982).

45. Lekkas, S., Alexopoulos, A. & Danamos, G. Neotectonic Map of Laconia. (1995).

46. Lobo, F. J. & Ridente, D. Stratigraphic architecture and spatio-temporal variability of high-frequency (Milankovitch) depositional cycles on modern continental margins: An overview. *Mar. Geol.* **352,** 215–247 (2014).

47. Lodolo, E. & Ben-avraham, Z. Journal of Archaeological Science : Reports A submerged monolith in the Sicilian Channel (central Mediterranean Sea): Evidence for Mesolithic human activity. *J. Archeol. Sci. Reports* **3,** 398–407 (2015).

48. Lyberis, N., Angelier, J., Barrier, E. & Lallemant, S. Active deformation of a segment of arc: the strait of Kythira, Hellenic arc, Greece. *Struct. Geol.* **4,** 229–311 (1982).

49. Marriner, N. & Morhange, C. Geoscience of ancient Mediterranean harbours. *Earth-Science Rev.* **80,** 137–194 (2007).

50. Marsellos, A. Mapping of a detachment fault in Kythera Island and study of the related structural shear sense indicators. *University at Albany, State University of New York Scholars Archive* (2006).

51. Mascle, J. *et al.* Images may show start of European-African plate collision. *Eos, Trans. Am. Geophys. Union* **80,** 421 (1999).

52. Mascle, J. & Mascle, G. Geological and morphotectonic map of the Mediterranean domain, 2012. Publication de la Commission de la Carte Géologique du Monde, CCGM. (2012).

53. Mascle, J. & Martin, L. Shallow structure and recent evolution of the Aegean Sea: A synthesis based on continuous reflection profiles. *Mar. Geol.* **94,** 271–299 (1990).

54. McClusky, S. *et al.* Global Positioning System constraints on plate kinematics and dynamics in the eastern Mediterranean and Caucasus. *J. Geophys. Res. Solid Earth* **105,** 5695–5719 (2000).

55. McClusky, S. *et al.* GPS constraints on Africa (Nubia) and Arabia plate motions. *Geophys. J. Int.* **155,** 126–138 (2003).

56. McKenzie, D. Active tectonics of the Alpine--Himalayan belt: the Aegean Sea and surrounding regions. *Geophys. J. Int.* **55,** 217–254 (1978).

57. McKenzie, D. P. Active Tectonics of the Mediterranean Region. *Geophys. J. Int.* **30,** 109–185 (1972).

58. Mentis, K. . Elaphonisos. Chapters on the geography and history of the region. (2007).

59. Meulenkamp, J. E., Wortel, M. J. R., van Wamel, W. A., Spakman, W. & Hoogerduyn Strating, E. On the Hellenic subduction zone and the geodynamic evolution of Crete since the late Middle Miocene. *Tectonophysics* **146,** 203–215 (1988).

60. Meulenkamp, J. & Hilgen, F. Event stratigraphy, basin evolution and tectonics of the Hellenic and Calabro-Sicilian arcs. *Orig. arcs* (1986).

61. Meyer, M. & Harff, J. Modelling Palaeo Coastline Changes of the Baltic Sea. *J. Coast. Res.* **213,** 598–609 (2005).

62. Mix, A. C. & Ruddiman, W. F. Oxygen-isotope analyses and Pleistocene ice volumes. *Quat. Res.* **21,** 1–20 (1984).

63. Morhange, C., Pirazzoli, P., Marriner, N., Montaggioni, L. & Nammour, T. Late Holocene relative sea-level changes in Lebanon, Eastern Mediterranean. *Mar. Geol.* **230,** 99–114 (2006).

64. Ninkovich, D. & D. Hays, J. Mediterranean island arcs and origin of high potash volcanoes. *Earth Planet. Sci. Lett.* **16,** 331–345 (1972).

65. Palla, M. P., Sakellariou, D. & Poulos, S. Reconstruction of the submerged landscape of Vatka Bay, Peloponnese, Grecce.

66. Papazachos, B. C., Karakostas, V. G., Papazachos, C. B. & Scordilis, E. M. The geometry of the Wadati–Benioff zone and lithospheric kinematics in the Hellenic arc. *Tectonophysics* **319,** 275–300 (2000).

67. Perissoratis, C. & Conispoliatis, N. The impacts of sea-level changes during latest Pleistocene and Holocene times on the morphology of the Ionian and Aegean seas (SE Alpine Europe). *Mar. Geol.* **196,** 145–156 (2003).

68. Pichon, X. Le, Angelier, J., Osmaston, M. F. & Stegena, L. The Aegean Sea [and Discussion]. *Philosophical Transactions of the Royal Society of London. Series A, Mathematical and Physical Sciences* **300,** 357–372

69. Pirazzoli, P. A., Thommeret, J., Thommeret, Y., Laborel, J. & Montaggioni, L. F. Crustal block movements from Holocene shorelines: Crete and Antikythira (Greece. *Tectonophysics* **86,** 27–43 (1982).

70. Pizarro, O. *et al.* AUV-assisted characterization of beachrock formations in Vatika Bay , Laconia , Peloponnese , Greece and their relevance to local sea level changes and Bronze Age settlements. in *Ocean Sciences 2012* 367 (2012).

71. Posamentier, H. W. & Kolla, V. Seismic Geomorphology and Stratigraphy of Depositional Elements in Deep-Water Settings. *J. Sediment. Res.* **73,** 367–388 (2003).

72. Posamentier, H. & Martinsen, O. in *Mass-transport deposits in deepwater settings:* (2011).

73. Rohling, E. J. *et al.* Sea-level and deep-sea-temperature variability over the past 5.3 million years. *Nature* **508,** 477–82 (2014).

74. Ryan, W. The stratigraphy of the Eastern Mediterranean, part II. (Columbia Univercity, New York, 1970).

75. Ryan, W., Stanley, D., Hersey, J. & Fahlquist, D. The tectonics and geology of the Mediterranean Sea. (1971).

76. Sakellariou D. & Tsampouraki-Kraounaki K. Offshore Faulting in the Aegean Sea: a Synthesis Based on Bathymetric and Seismic Profiling Data. *Bull. Geol. Soc. Greece* **L,** (2016).

77. Sakellariou, D. *Impact assessment of the conventional tankers anchory at Vatika Bay*. (2015).

78. Sakellariou, D., Fountoulis, I. & Lykousis, V. Evidence of Cold Seeping in Plio-Pleistocene Sediments of Se Peloponese : the Fossil Carbonate Chimneys of Neapolis Region. in *12th International Congress, Patras, May, 2010* 1046–1055 (2010).

79. Sakellariou, D. & Galanidou, N. Pleistocene submerged landscapes and Palaeolithic archaeology in the tectonically active Aegean region. (2015).

80. Sakellariou, D., Lykousis, V., Geraga, M., Rousakis, G. & Soukisian, T. in *Submerged Landscapes of the European Continental Shelf: Quaternary Paleoenvironments* 405–429 (Ltd., John Wiley & Sons, 2017).

81. Sakellariou, D., Rousakis, G., Maroulakis, S., Georgiou, P. & Hellenic, S. K. The submerged city of Pavlopetri , Greece : Innovative mapping techniques and reconstruction of the submerged landscape. in (2013).

82. Sakellariou, D. *et al.* The submerged city of Pavlopetri. in *Poseidons Reich XVI, (DEGUWA 2011)* (2011).

83. Sakellariou, D. Field trip guide. Active Faulting in Eastern Crete : Extension , transtension and uplift along the Hellenic Arc. 2–4 (2016).

84. Sakellariou, D., Mascle, J. & Lykousis, V. Strike Slip Tectonics and Transtensional Deformation in the Aegean Region and the Hellenic Arc : Preliminary Results. *Bull. Geol. Soc. Greece* **XLVII,** 647–656 (2013).

85. Scheffers, A., Kelletat, D., Vött, A., May, S. M. & Scheffers, S. Late Holocene tsunami traces on the western and southern coastlines of the Peloponnesus (Greece). *Earth Planet. Sci. Lett.* **269,** 271–279 (2008).

86. Shackleton, N. Oxygen isotopes, ice volume and sea level. *Quat. Sci. Rev.* **6,** 183–190 (1987).

87. Shaw, B. & Jackson, J. Earthquake mechanisms and active tectonics of the Hellenic subduction zone. *Geophys. J. Int.* **181,** 966–984 (2010).

88. Shipp, G., Weimer, P. & Posamentier, H. *Mass-Transport Deposits in Deepwater Settings*. **96,** (SEPM Society for Sedimentary Geology, 2011).

89. Stiros, S. The 8.5+ magnitude, AD365 earthquake in Crete: Coastal uplift, topography changes, archaeological and historical signature. *Quat. Int.* **216,** 54–63 (2010).

90. Taymaz, T. *et al.* Source parameters of large earthquakes in the East Anatolian Fault Zone (Turkey). *Geophys. J. Int.* **106,** 537–550 (1991).

91. Ten Veen, J. H. & Kleinspehn, K. L. Geodynamics along an increasingly curved convergent plate margin: Late Miocene-Pleistocene Rhodes, Greece. *Tectonics* **21,** 8-1-8–21 (2002).

92. Ten Veen, J. H. & Postma, G. Neogene tectonics and basin fill patterns in the Hellenic outer-arc (Crete, Greece). *Basin Res.* **11,** 223–241 (1999).

93. Van Andel, T. *The adjacent sea*. *Landscape and people of the Franchthi region. Indiana* (1987).

94. Vött, A. ; K. & Dieter. Editorial Holocene Palaeotsunami Landfalls and Neotectonic Dynamics in the Western and Southern Peloponnese (Greece). *Zeitschrift für Geomorphol.* **59,** 001–005 (2015).

95. Weiberg, E. *et al.* The socio-environmental history of the Peloponnese during the Holocene : Towards an integrated understanding of the past. *Quat. Sci. Rev.* **136,** 40–65 (2016).